Australian Government

Wine Australia

CSIRO

The yield:quality nexus: Substantiating similarity in the patterns of variation in grape yield/vine vigour and indices of fruit quality



FINAL REPORT TO WINE AUSTRALIA

Project Number: **CSL 1401**

Principal Investigator: **Rob Bramley**

Research Organisation: **CSIRO**

Date: **September 2018**

CSIRO Agriculture and Food, Waite Campus.

Citation

Bramley RGV, Mowat D, Ouzman J and Gobbett, DL (2018) The yield:quality nexus: Substantiating similarity in the patterns of variation in grape yield/vine vigour and indices of fruit quality. Wine Australia / CSIRO, Australia.

Copyright

© Commonwealth Scientific and Industrial Research Organisation 2018. To the extent permitted by law, all rights are reserved and no part of this publication covered by copyright may be reproduced or copied in any form or by any means except with the written permission of CSIRO.

Important disclaimer

CSIRO advises that the information contained in this publication comprises general statements based on scientific research. The reader is advised and needs to be aware that such information may be incomplete or unable to be used in any specific situation. No reliance or actions must therefore be made on that information without seeking prior expert professional, scientific and technical advice. To the extent permitted by law, CSIRO (including its employees and consultants) excludes all liability to any person for any consequences, including but not limited to all losses, damages, costs, expenses and any other compensation, arising directly or indirectly from using this publication (in part or in whole) and any information or material contained in it.

CSIRO is committed to providing web accessible content wherever possible. If you are having difficulties with accessing this document please contact csiroenquiries@csiro.au.

Abstract

This project sought to understand the 'yield:quality nexus' – the presumed link between fruit yield and quality such that higher yield means lower quality. It worked at the within-vineyard scale using the tools of precision viticulture (yield monitors, canopy sensors, GPS, etc). Albeit constrained by just two seasons of data collection, the evidence that yield and quality are inextricably linked was weak.

Developing a means of sensing fruit composition at harvest was an important part of the work. With much still to be done to deliver a commercial solution, the project established the potential of near-infrared (NIR) sensing as an on-the-go tool.

This page intentionally blank

Table of Contents

Abstract 2

Executive summary 6

1. Background 8

2. Project aims and the organisation of this report 9

3. Predicting fruit quality using an active proximal canopy sensor 12

3.1 Methods and materials 12

3.1.1 Site details 12

3.1.2 Pre-project data and high resolution soil survey 13

3.1.3 Vine sampling, canopy sensing in season and yield monitoring 13

3.1.4 Laboratory analysis 14

3.1.5 Spatial and statistical analysis 14

3.1.6 Relating berry chemistry to Crop Circle and other spatial data 15

3.2 Results and discussion 16

3.2.1 Pre-project data, identification of vineyard zones and establishment of a vine sampling strategy 16

3.2.2 Variation in vine vigour and yield during the project 24

3.2.3 Selection of an approach to modelling changes in fruit composition in the veraison to harvest period 26

3.2.4 Relating fruit composition to indices of vine vigour and yield 34

3.2.5 Discussion – the yield:quality nexus 37

4 Calibrating passive remote sensing against active proximal canopy sensing 42

4.1 Methods and materials 42

4.1.1 Remotely sensed imagery 42

4.1.2 Proximal canopy sensing 43

4.1.3 Image interpolation and spatial and statistical analysis 43

4.2 Results and discussion 45

5. Towards an on-the-go fruit quality sensing capability 53

5.1 Initial work using the Multiplex™ sensor 53

5.1 Methods and materials 57

5.1.1 Site details 57

5.1.2 Pre-project data 58

5.1.3 Vine sampling and NIR sensing. 58

5.1.4 On-the-go scanning 63

5.1.5 Laboratory analysis 65

5.1.6 Spectral analysis 65
5.1.7 Spatial analysis 66
5.2 Results and Discussion 66
5.3 Conclusions 77
6. Conclusions and recommendations 79
6.1 The yield:quality nexus 79
6.2 Calibration of remote and proximal sensing 80
6.3 On-the-go-sensing of fruit composition 80
6.4 Recommendations 81
7. Acknowledgements 83
Appendix 1: Communication 85
Appendix 2: Intellectual Property 87
Appendix 3: References 89
Appendix 4: Staff 93

Executive summary

Much decision making in wine production systems is governed by an assumed interaction between grape yield and quality – the yield:quality nexus - which can be summarised as an inference that higher yields mean lower quality. Interestingly, it is almost impossible to find definitions for 'higher' or 'lower' in reference to either yield or quality, yet this assumed interaction may lead to consequences for growers who might be paid a lower price for a parcel of fruit simply because its yield is deemed too high, or who might decide to crop thin in the expectation of an improvement in quality which may or may not actually be realised. In collaboration with Taylors Wines and Kingston Estate Wines, this project sought to understand the yield:quality nexus using detailed measurements made in contrasting vineyards in the Clare Valley and at Kingston-on-Murray in the Riverland. With a long history of work in vineyard variability and the knowledge that vineyards may be highly variable production systems, our approach was to use the tools of Precision Viticulture (yield monitoring, remote and proximal canopy sensing, the global positioning system (GPS), etc.) and methods of spatial analysis, to see whether links between fruit yield and quality could be established at the within-vineyard scale. Circumstances beyond the control of either the project team or vineyard management meant that, at both of the sites studied, our analysis was confined to just two seasons of data collection, albeit with underpinning access to several years of yield monitor and or remotely sensed imagery data obtained pre-project. In doing this work, we focussed on the 'standard' industry measures of quality – juice pH, titratable acidity, total soluble solids (TSS) and the concentrations of anthocyanins (colour) and total phenolics. The results suggest that the link between yield and quality at the within vineyard scale is, at best, a weak one. Certainly, they suggest that making targeted vineyard management decisions aimed at fruit quality improvement based on measures of yield or vine vigour is something that growers should treat with great caution. Our results are therefore consistent with other recent Wine Australia-funded work which draws a similar conclusion about the merits of manipulating vine balance in pursuit of improved quality (CSP 1202). On the other hand, they are in contrast to previous work conducted in vineyards where contrasting zones of characteristic performance were reflective of a '*terroir* effect'.

Two complications in this work arise in relation to the mode and timing of fruit quality assessment. First, while the concentrations of anthocyanins (colour) and total phenolics have been shown to relate to grape and wine quality, they are not widely adopted as quality measures in commercial winemaking. On the other hand, juice pH, titratable acidity and total soluble solids, which are used for this purpose, are much more indicators of fruit maturity, and whilst maturity is certainly a factor that interacts with fruit composition, whether these measures can be regarded as robust indicators of 'quality' is a moot point. This is important because we observed that measures of both components of yield and of fruit composition tended to reach a peak some time before the date of harvest, and to then either stabilise or decline. Thus, the time of harvest, which is generally the time at which both yield and quality are assessed for commercial purposes (i.e. payment to growers, allocation of fruit to target products streams, etc.) is not necessarily the most appropriate time to make measurements aimed at understanding the yield:quality nexus. As such, the date of harvest is somewhat arbitrary in the context of grape physiology or phenology. Resolution of this issue by, for example, making measurements at a standard maturity (i.e. fixed value of TSS) is not feasible at the within-vineyard scale given that TSS, and therefore the maturity status of the crop, can be markedly spatially variable. Overall, our work suggests that additional and on-going effort is needed, aimed at identification of robust and objective measures of fruit quality and a means of normalising these to the maturity of the crop at the time of measurement.

The aforementioned work relied on the collection of samples from a small number of 'target vines' and attempts to relate analysis of these samples to measures of vine vigour and yield collected at a much higher spatial intensity using yield mapping and remote and proximal canopy sensing. A key secondary component of the project therefore was to explore how information on fruit quality or composition might be obtained at a similar spatial resolution and intensity to the data on vine vigour or yield. Initial attempts to do this (in collaboration with Force-A, Paris, France) using a fluorescence sensor were not as successful as previous work suggested it might be. Instead, we sought to prove the concept of on-the-go sensing of fruit composition during harvest using an NIR sensor mounted above the yield monitor on the discharge chute of a harvester. The results obtained suggest that this technology has much promise, although it needs considerable further development, a key part of which would be the generation of calibrations between NIR spectra and objective measures of fruit quality (see above). Aside from promoting more robust understanding of yield:quality interactions (including whether these exist), being able to map fruit composition at high spatial resolution could prove highly commercially significant. Within-vineyard variation in yield and vine vigour has been shown to have patterns of variation that are temporally stable from year to year; that is, the lower and higher yielding parts of vineyards are generally always lower or higher yielding in the absence of targeted manipulation. If high resolution sensing could be used to demonstrate that certain parts of vineyards inherently produce fruit of either lower or higher quality, or are inherently suited to particular styles of wines, the commercial implications could be profound. Selective harvesting has already been shown to be potentially highly profitable, but an ability to robustly plan such a strategy well in advance of harvest would deliver significant benefit to both grapegrowers and winemakers. Of course, the data provided by such a sensor would, in concert with yield monitoring and remote sensing, promote better understanding of the yield:quality nexus on a site-specific basis.

1. Background

In the years prior to commencement of this project, the Australian wine industry was suffering a significant profit squeeze with winemakers, and especially grapegrowers, seeking opportunities to maximise vineyard profitability; under the somewhat improved market conditions of 2018, profit maximisation nevertheless remains a goal. In its 2012-17 Strategic Plan, the then Grape and Wine Research and Development Corporation (GWRDC) had a strategic objective (1.3) focussed on improved vineyard profitability, without compromise to sustainability, productivity or quality, and also sought to identify ways to improve vineyard efficiency though enhanced technology and altered (i.e. improved) processes (GWRDC, 2012). The associated gap analysis (GWRDC, 2013) focussed on the so-called yield:quality nexus and management practices to optimise yield and quality. Against a background of industry dogma which suggests that good quality and high yields are not simultaneously achievable, specific underlying drivers were the perception in some regions that profitability was dependent on yield optimisation, and grower distrust at perceived differences between fruit quality assessment in the vineyard and its quantification at the weighbridge, the point at which most payment decisions are made. No doubt, in some regions, both of these factors were in play.

One constraint to vineyard profitability is caused by the negative effects of implementing uniform management strategies in variable vineyards. Another is imperfect knowledge about the interactions between yield and quality. Precision Viticulture (PV) is intimately concerned with the optimisation of grapegrowing and winemaking through the use of spatial data at high resolution to better understand and take advantage of the inherent spatial variability present in all vineyards (Proffitt et al., 2006; Bramley, 2010, 2019 and references therein). Better understanding of yield:quality interactions at high spatial resolution would provide opportunities around more efficient, targeted use of management inputs (including labour) so that management actions targeted at yield-related objectives do not lead to negative consequences for fruit quality, and vice versa. In particular, such improved understanding would promote strategies such as selective harvesting and product streaming, which have been shown to be potentially highly profitable whether employed in situations where winery infrastructure permits small tonnage ferments (Bramley et al., 2005), or in production systems geared to large tonnage fermentation (Bramley et al., 2011c). Thus, a major intent of this project was to attempt to provide the information basis through which such practices may be implemented proactively and predictively, rather than purely reactively.

Vineyard variability research conducted prior to the present project demonstrated that for typical Australian spur pruned and hedge pruned vineyards, within-vineyard zones delineated on the basis of yield monitoring and/or remotely sensed imagery are stable in time (i.e. between seasons, when assessed at the same stage of the season – typically veraison) and generally relate to variation in the land (soil, topography) underlying the vineyard. However, zone delineation on the basis of grape compositional attributes has been less certain because it has relied on hand sampling and thus, a much lower data density - typically 26 samples/ha as in Bramley and Hamilton (2004) and Bramley (2005) - than that provided by remote sensing (40,000 pixels/ha for 50 cm imagery). Nonetheless, in almost all of the published examples, commercially important differences in fruit quality exist between zones delineated using yield and/or imagery (e.g. Bramley and Hamilton, 2004, 2007; Bramley et al., 2005, 2011b,c); cane-pruned vineyards are a possible exception where yield maps may not offer commercially useful assistance (Bramley et al., 2011d).

With the exception of the study of Bramley et al. (2011a), which used an on-the-go modification to the Multiplex™ sensor (Force-A, Paris, France) mounted on a harvester, no-one has yet collected fruit quality data at a spatial density comparable to that underpinning yield maps or imagery, a fact that contributes to the uncertainty of fruit quality zone delineation. Whilst it is thought that fruit quality zones follow the same spatial pattern as yield-imagery zones, their rank order may not be constant, in contrast to yield-imagery zones which do show constant rank order (i.e. high to low; Bramley and Hamilton, 2004). However, with appropriate targeted sampling pre-harvest, this should not present a constraint to realising the benefits of selective harvesting. The reliance on hand sampling is, however, a constraint and also limits better understanding of the yield:quality nexus given the resolution at which information about vine vigour and grape yield may be acquired. This project therefore sought to move towards realising the potential to enhance production efficiency and profitability through generating data streams that promote better decision making. Included among these may be predictions of objective quality measures derived from remote and proximal canopy sensing, in addition to more direct measures, such as from fruit quality sensors. One reason for pursuing this line of work was that a 2013 survey of wine industry attitudes to PV and its adoption (Bramley, 2013) indicated that, across a broad spectrum of industry involvement (grapegrowing, winemaking, etc...), business sizes and extent of PV adoption, 66% of respondents believed that PV was already delivering or would deliver a benefit to their business. The survey also suggested that greater adoption of such approaches to winegrowing would accrue through additional demonstration of the robustness of the information provided by PV.

This project was therefore conceived to facilitate adoption of practices that enhance vineyard profitability through the combined use of passive airborne remote sensing of the canopy, active proximal sensing of the canopy (using Crop Circle™ ACS-470; Holland Scientific, Lincoln, Nebraska, USA), hand sampling and lab analysis of fruit and on-the-go sensing of fruit quality indicators at harvest, in the first instance using the Multiplex sensor (Bramley et al., 2011a). A particular aim was to seek a means by which the delineation of vineyard zones could be done with increased confidence from a fruit quality perspective, an important element in realising the opportunity presented by selective harvesting for enhanced vineyard profitability. Of course, we also sought to be better understand the yield:quality nexus and test the merit of prevailing industry dogma.

2. Project aims and the organisation of this report

The objectives of this project were to:

1. Examine and quantify the coincidence (or otherwise) between patterns of within-block spatial variation in grape yield/vine vigour and fruit quality and their temporal stability when both are sensed at high spatial resolution and high data density. This aim was specifically targeted at assisting with understanding the yield:quality nexus.
2. Investigate the utility of an active canopy sensor (Crop Circle) as a predictor of indices of fruit quality.
3. Evaluate the Crop Circle sensor as a means of calibrating passive remotely sensed imagery (thereby enabling such remote sensing to be used quantitatively as opposed to qualitatively as it is at present).

4. Pending the results obtained in 2 and 3, examine the use of remote and proximal canopy sensing in combination as a means of predicting fruit quality at high spatial resolution.

The initial intent was to address these aims through collaborations with, and using field sites owned by, Taylors Wines (Auburn, Clare Valley) and Kingston Vineyards (Kingston-on-Murray, Riverland); we were also reliant on a collaboration with Force-A, the manufacturers of the Multiplex sensor. Originally funded as a three year project commencing in the season which ended with vintage 2015, the project proceeded as planned until vintage 2016. However, during the 2017 season, the Kingston site was very seriously affected by both frost and hail events and had to be abandoned by the project. At the same time, the Taylors site was affected by spray drift and also had to be abandoned. With only two seasons of data collected, our ability to properly examine whether patterns of variation in fruit quality were temporally stable was compromised, as was our work on the prediction of fruit quality using the Crop Circle sensor (or by remote sensing). Meanwhile, we discovered during vintage 2015, that our use of the 'on-the-go' version of the Multiplex, which was produced following the work of Bramley et al. (2011a), did not deliver data of sufficient quality to meet the needs of the project. For various reasons, Force-A was unable to modify it for the 2016 vintage when we felt obliged to revert to the hand-held version, and thus, low sampling densities. Subsequently, and with regret, it was agreed with Force-A, that the collaboration was no-longer working and it was therefore terminated.

In light of the above, and further to negotiation with Wine Australia, in an attempt to realise the investment made in the project to that point, the project was given a one-year extension with the intent of better enabling analysis of data collected to that point, and significantly shifting the focus of the project to:

5. Explore the proof of concept of using near-infrared (NIR) sensing as a tool for fruit quality assessment *in vivo* and 'on-the-go' during harvest.

This aim was tackled using a different field site at Taylors Wines and by accessing a site at The Lane Vineyard (Adelaide Hills) in collaboration Wine Australia project AWR 1503.

The project was always designed on the basis of that Aim 3 was a small, albeit enabling component of the project, with Aim 2 essentially a subset of Aim 4. Along with Aim 4, Aim 5 was the other major area of endeavour with the work conducted through Aims 2-5 collectively enabling Aim 1 to be addressed, at least in part. Given our inability to do justice to the temporal stability element of Aim 1, in this report, the work is organised into three sections describing our research aimed at:

- Predicting fruit quality/composition (and its phenology) using the active proximal Crop Circle sensor (Section 3);
- Calibrating passive remote sensing against Crop Circle sensing (Section 4); and
- Developing an on-the-go NIR fruit sensing capability (Section 5).

Note that throughout, the term 'fruit quality' is used euphemistically to refer to commonly measured elements of fruit composition – juice pH and titratable acidity, total soluble solids and the content of anthocyanins (colour) and total phenolics. Note also that, the project relied on the assumption, well established from previous work (see Bramley 2010, 2019 for a review), that variation in vine vigour is a reasonable surrogate measure of yield variation.

By its nature, this project involved the collection of a lot of data. To keep this report to a manageable size, we have confined the figures and analyses reported to those required to make a particular point or describe a particular approach to analysis.

3. Predicting fruit quality using an active proximal canopy sensor

Trought and Bramley (2011) demonstrated the concept of using proximal canopy sensing as a means of predicting juice quality, and the date on which this reached an optimum, in a Marlborough (NZ) vineyard planted to Sauvignon Blanc. They predicted juice pH, titratable acidity and soluble solids as a function of time in the veraison to harvest period and related these predicted values to the canopy sensor data. They coupled this with an evaluation of winemaker preferences for particular values for these attributes at harvest, to construct a juice quality index (JQI) which, in turn, could be predicted using the canopy data. Thus, they were able to track spatial variation in crop maturation and changes in the JQI in the veraison to harvest period. In the present study we sought to follow a similar approach, knowing that previous research had demonstrated strong similarities in the patterns of spatial variation in vine vigour and yield, on the basis that the success of such an approach was dependent on yield and fruit quality being related. Note however, that we did not attempt to construct a JQI (the then GWRDC quite explicitly did not fund us to do this). A key difference to the Trought and Bramley work, which was a single season study, was that here, we sought to develop generic (i.e. season independent) predictions of fruit quality based on canopy sensing (and yield) data. The reasoning behind this was that, in contrast to remote sensing from a satellite or aircraft which is 'passive' in that it relies on reflectance of sunlight, in the present work we used the Crop Circle sensor. Because this is an 'active' sensor that is able to compensate for variable background illumination, any given value of a canopy index (e.g. PCD – the ratio of infrared:red reflectance) obtained under different sensing conditions, on any given occasion or in any given location, should have the same meaning as that same value obtained on another occasion or at another location. Thus, the thinking was that a relationship between a vegetation index generated using Crop Circle and indices of fruit quality ought to be independent of season or, at least, would need to be, in order to be of value to grapegrowers and winemakers. It was also considered that if the approach proved successful, it would amount to a substantive demonstration of fruit quality and vine vigour / yield being related.

3.1 Methods and materials

3.1.1 Site details

The first site used for this work was an 8.2 ha block of Shiraz at Taylors Wines near Auburn in the Clare Valley. This vineyard was planted in 2004 on own roots (clone 1654) with row and vine spacings of 3.3 and 1.8 m; rows run approximately WSW to ENE. The block is spur pruned (2 bud spurs @ 30 buds/vine) to a ballerina canopy such that half the shoots sprawl whilst the other half are vertically shoot positioned using permanent foliage wires. The block is drip irrigated, receiving approximately 0.6 ML/ha supplementary irrigation during the late spring to early autumn period. Production is targeted at Taylors Clare Estate Shiraz, a premium table wine, the current vintage of which retails for $19/bottle at cellar door. This vineyard is the same one as that used by Bramley et al. (2011a) in their initial exploration of the Multiplex sensor.

The second site was a 19.6 ha block of Petit Verdot at Kingston Estate Wines near Kingston-on-Murray in the Riverland. This vineyard was planted in 1998 on its own roots (clone G7V1) with row and vine spacings of 3.3 and 1.5 m. Rows run approximately NW to SE. The block is minimally pruned to a

double cordon with a sprawling canopy. It is drip irrigated and receives approximately 8.5 ML/ha/y. Production is targeted at bulk wine for export and subsequent blending.

3.1.2 Pre-project data and high resolution soil survey

Taylors Wines has a history of engagement in PV; they have been using both yield monitoring/mapping and remotely sensed imagery for many years. Similarly, Kingston Estate Wines has used yield monitoring for several years, but had not acquired remotely sensed imagery prior to this project. At both sites, these available pre-project data were supplemented by two high resolution soil surveys, conducted simultaneously. The first measured bulk electrical soil conductivity using a dual dipole EM38 MK2 sensor (Geonics, Mississauga, ON, Canada) towed on a polypropylene sled behind an ATV, and allowed simultaneous measuring of conductivity in the 0–0.75 and 0–1.5 m range; here, we consider the 0–0.75 m data only. The second measured gamma radiometric counts derived from the natural decay of ^{238}U, ^{232}Th and ^{40}K which are contained in trace amounts in the soils' clay minerals. A 'Mole' gamma radiometer (The Soil Company, Groningen, The Netherlands) was used for this survey; this sensor uses a CsI crystal coupled to a photomultiplier unit and a 512 channel multi-channel analyser (Loonstra and van Egmond, 2009) to predict the concentrations of the radioactive elements; it also reports the total radiometric count. For both surveys, a real time kinematic global position system (RTKGPS—accurate to approximately 2 cm in the horizontal planes and to 3-4 cm in the vertical) was used to record position, with the EM38, gamma and GPS data logged simultaneously at 1 Hz to a ruggedised tablet PC. Proffitt et al. (2006) and Rodrigues et al. (2015) provide further description of the use of these sensors and, in the latter case, also outline the methods of data processing used. Suffice to say here that both soil sensors provide information at high spatial resolution about soil variation and have been shown in previous viticultural work (e.g. Bramley et al., 2002, 2011b,d) to be useful in understanding the drivers of spatial variation in vineyard performance. The RTK data were used to generate a digital elevation model (DEM - see below); both vineyards are located on undulating country.

3.1.3 Vine sampling, canopy sensing in season and yield monitoring

Spatial analysis and clustering of the pre-project data (see section 3.2.1) enabled identification of 30 sampling locations in each vineyard which covered the range of vineyard variation. At both sites, these sampling locations were located on three transects (i.e. three vineyard rows). The 30 sampling locations were approximately evenly divided amongst the three transects and were geo-referenced using a differentially correctly GPS[1] (dGPS – accurate to approximately +/- 50 cm in the horizontal plane).

At intervals of approximately one week during the veraison to harvest period, and at each sampling location, bunches were sampled randomly from a 1 m section centred on the trunk of each 'target' vine. At Taylors, five bunches were sampled, whilst eight bunches were sampled at Kingston - a reflection of the different typical bunch sizes at the two sites. At each sampling location, the sampled

[1] Note that here and throughout, we refer to 'GPS' in the general sense of using a satellite-based positioning system. More correctly, given present free access to autonomous geo-spatial positioning through satellites other than the American GPS system, it is the Global Navigation Satellite System (GNSS) that we used in this work.

bunches were placed in a plastic bag which, in turn, was placed in a chilled esky for transfer back to the laboratory. Note that to avoid the impact of one sampling event on our ability to sample on subsequent occasions, the actual vine sampled was moved either one or two vines along the row in either direction from the initially sampled vine, or to a vine opposite to this original target vine in an adjacent row; the actual vine sampled was geo-referenced on each sampling occasion and no vine was sampled more than once. All vines were sampled on the northern side of the row.

As described in Section 4.1.2, proximal sensing of the vine canopy was carried out using the Crop Circle sensor close to veraison in both 2015 and 2016 on a date as close as possible to the date of acquisition of airborne remotely sensed imagery which was purchased from a commercial provider (Specterra Services, Leederville, WA). In addition, on each sampling occasion in 2015, the sampled transects were re-scanned with the Crop Circle. Further information is provided in Section 4.1.2. Suffice to say here that both the proximally (Crop Circle) and remotely (airborne) sensed canopy data were expressed in terms of the so-called 'plant cell density' index (PCD), otherwise known as the 'simple ratio' (e.g. Dobrowski et al., 2003), the ratio of infrared: red reflectance.

At harvest, yield monitoring was carried out at both sites using commercially available yield monitors (Advanced Technology Viticulture, Joslin, SA) that were already in use at the collaborating vineyards. Harvest at Taylors occurred on 23 February in 2015 and 1 March in 2016. At Kingston, harvest occurred on 7 April in 2015 and 11 April in 2016.

3.1.4 Laboratory analysis

Sample pre-processing was carried out on the same day as sampling; sample analysis occurred the following day. On return to the laboratory the samples were weighed and an average bunch mass calculated. Berries were then randomly and equally stripped from each of the sampled bunches onto a plastic plate until approximately 250 berries had been picked. These were then mixed and three subsamples, each of 50 berries, were counted into plastic vials. These were weighed and the mean berry weight determined. From the mean bunch and berry mass, the mean number of berries per bunch was also determined. The plastic vials were then stored in a standard domestic freezer for later analysis of anthocyanin and phenolic content. The remainder of the sample was stored overnight in a refrigerator.

The following day, the remainder of each sample was crushed in a bag press and total soluble solids (TSS; °Brix; by digital refractometer with temperature compensation – Atago, Tokyo, Japan), juice pH and titratable acidity (TA; by autotitration) were measured. Subsequently, the concentrations of anthocyanins (colour) and phenolics were analysed spectrophotometrically on homogenised subsamples of the 150 berries that were stored frozen following berry mass determination (see above). All of these analyses were carried out using standard Australian methods (Iland et al. 2004).

3.1.5 Spatial and statistical analysis

Yield monitor, Crop Circle and soil survey data were mapped onto a 2 m grid using what have been standard procedures for several years; Proffitt et al. (2006) and Bramley et al. (2011b) provide details.

In brief, the protocol of Bramley and Williams (2001 with later published amendments) was followed. This involves local block kriging (data cloud of 100 points, 10 m blocks, exponential variogram) using VESPER (Minasny et al. 2005). Prior to mapping, yield data were trimmed so that all data values fell within ± 3 standard deviations (sd) of the mean. Remotely sensed imagery provided at 40 cm resolution was smoothed to the same 2 m grid as used for the other mapping using the focal statistics function available in ArcGIS (see Section 4).

Similarity in patterns of spatial variation in the mapped data (whether pre-project or collected during our field campaign) was examined using *k*-means clustering in JMP (v.11.0.0, SAS Institute, Cary, NC, USA) with the optimal number of clusters selected on the basis of the cubic clustering criterion (SAS, 1983). Map production and display was done using the ArcGIS software suite (v10.4.1; ESRI, Redlands, CA, USA) including the Spatial Analyst and 3-d Analyst extensions. The significance of differences between cluster mean kriged map values was tested on the basis of the median kriging standard error (Taylor et al. 2007). All other statistical analysis was done using either JMP or, in the case of some of the phenological curve fitting, using Sigmaplot (v. 14.0; Systat Software Inc, San Jose, CA, USA).

3.1.6 Relating berry chemistry to Crop Circle and other spatial data

The analytical approach followed here closely followed that used by Trought and Bramley (2011) with the important modification that because our analysis was over more than one season, we sought an approach that was independent of seasonal effects, in particular based on thermal time.

Trought and Bramley (2011) fitted regressions to mean values of the juice compositional aspects of interest (pH, TA, TSS) as a function of days after 1 February in order to identify appropriate functions to fit to location-specific data (they had 24 sampling locations within a 5.9 ha block). The location specific functions were then used to generate estimated values for the juice compositional attributes for each date of interest and these were then regressed, on a per date basis, against PCD data. The use of estimated/modelled juice compositional data rather than the raw data was done to remove the effects of sampling and laboratory errors. These may include the effects of within vine, bunch to bunch variation, and/or difficulty in taking a five (Taylors) or eight bunch sample (Kingston) that was truly representative of the entire vine, and effects of analytical errors in the laboratory.

In the present study, and conscious of inter-seasonal differences, we tried various approaches to the initial model fitting stage, trialling various dependent variables: days after 1 September, days after budburst, days after flowering, degree days after budburst and degree days after flowering. In the cases of the two variants of thermal time, they were calculated using a minimum floor temperature of 10 °C and both with and without a daily maximum temperature cap of 36 °C. At Taylors, data from the vineyard weather station were used for this, while at Kingston, data from a local weather station (Moorook) maintained by the South Australian NRM Weather Network (www.awsnetwork.com.au/) were used; this station is also used by Kingston Estate Wines in lieu of a weather station on site. While each of the dependent variables enabled good descriptions of changes in pH, TA and TSS in the veraison to harvest period for data from a single season, none of them was satisfactory when data were combined for two seasons; that is, we could not fit common equations to describe the phenology of these attributes as a function of either time or thermal time (see section 3.2.2). At Kingston, this was made especially difficult by uncertainty over the dates of budburst and flowering. Discussion on

this issue with Peter Clingeleffer (CSIRO) and Mike Trought (NZ Plant and Food Research) led to an alternative approach being evaluated:

Thermal time was defined on the basis of the 'Grapevine Flowering and Veraison' (GFV) model of Parker et al. (2011). In this model, 'GFV time' in the northern hemisphere is estimated on the basis of a cumulative mean daily temperature calculated with a start date on the 60th day of the year; in the southern hemisphere, this start date corresponds to 29 August. Regression models were fitted to the season-specific field data for TSS with GFV time as the independent variable. From these models, we calculated the GFV time when TSS was equal to 8 °Brix and used the corresponding date to define the date of veraison (Parker et al., 2014). It was then assumed that berry ripening post veraison was a part of the vine senescence process and so was independent of thermal time (Peter Clingeleffer, CSIRO – pers. comm.). Thus, we then generated regressions describing changes in pH, TA, TSS, colour and phenolics as a function of time after veraison – both on a vineyard mean and location specific basis, and for vintage 2015 and 2016 separately and for both vintages combined. From these, the modelled values of these fruit compositional attributes on the dates of our field sampling were calculated on a location-specific basis. These were then used in an analysis of their relationships with Crop Circle PCD and yield, using values of these yield/vigour indices extracted from the relevant map layers based on the GPS coordinates of the vines sampled on each sampling date. Using a similar approach, and a definition of harvest as being when TSS reached a particular winery target value, we were also able to calculate the duration of the veraison to harvest period.

3.2 Results and discussion

3.2.1 Pre-project data, identification of vineyard zones and establishment of a vine sampling strategy

At Taylors Wines, pre-project PCD imagery obtained at veraison using airborne digital multispectral video (Specterra Service, Leederville, WA) was available annually from 2008-2014 (Figure 3.1). With the arguable exception of 2010 and 2012, the patterns of variation in vine vigour, as measured by PCD, were consistent from year to year such that when the PCD values were normalised (μ=0, σ=1) on a per year basis, the map of average PCD over the seven years of imagery (bottom row, centre map in Figure 3.1) showed a similar pattern to that seen in any individual year; *k*-means clustering of these images (Figure 3.1 bottom right map) gave a similar result.

Yield maps were available from 2008-2012 (Figure 3.2). Each of these illustrate artefacts of either a yield monitor or harvester error (striping along the direction of row orientation), and/or a problem in some aspect of management during the season (e.g. rows which missed sprays or in which irrigation lines may have been blocked). Nonetheless, the patterns of variation were broadly consistent from year to year and were similar to the pattern seen in the average image, as indicated by the map of average yield and the results of clustering this average yield map with the average PCD image.

High resolution soil survey indicated a marked area of contrast running NE-SW through the vineyard with the elevation model and derivative map of slope strongly suggesting that the region of higher bulk soil electrical conductivity (EC_a) was an area of moist soil (i.e. poor drainage) associated with a drainage line (Figure 3.3). The effects of this are apparent in terms of both reduced vine vigour (Figure

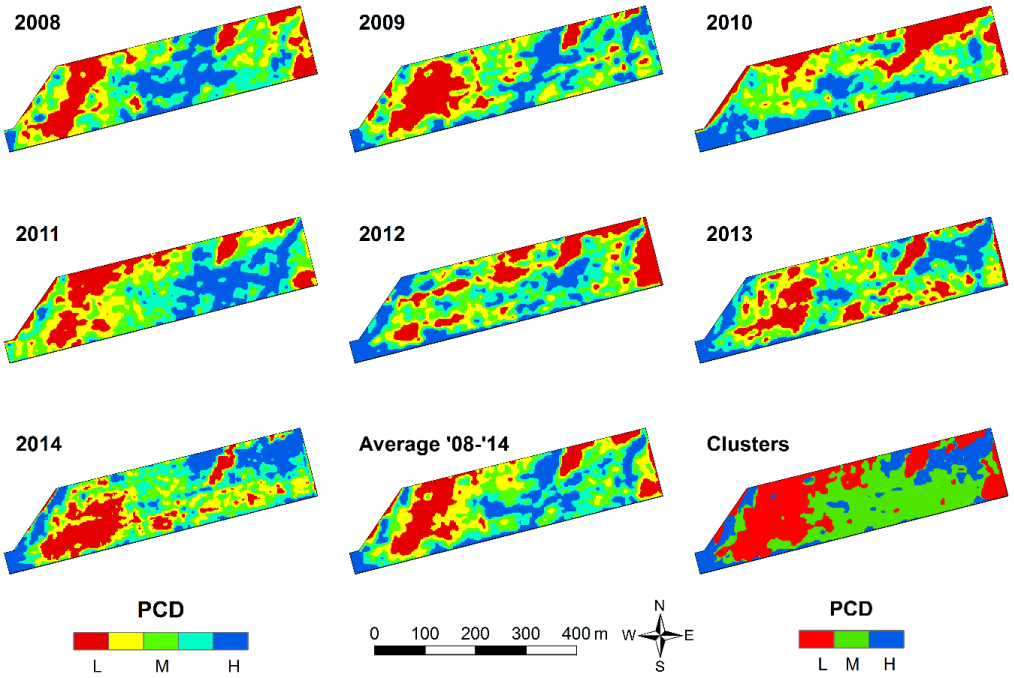


Figure 3.1 Variation in vine vigour at the Taylors site, measured as PCD at veraison using commercially available airborne multispectral digital video, 2008-2014. Note that in each image, the data have been classified into 20th percentiles. Also shown (bottom centre) is an average PCD map calculated from normalised (μ=0, σ=1) PCD values (per year) and the results of clustering the imagery using *k*-means (3 cluster solution – bottom right).

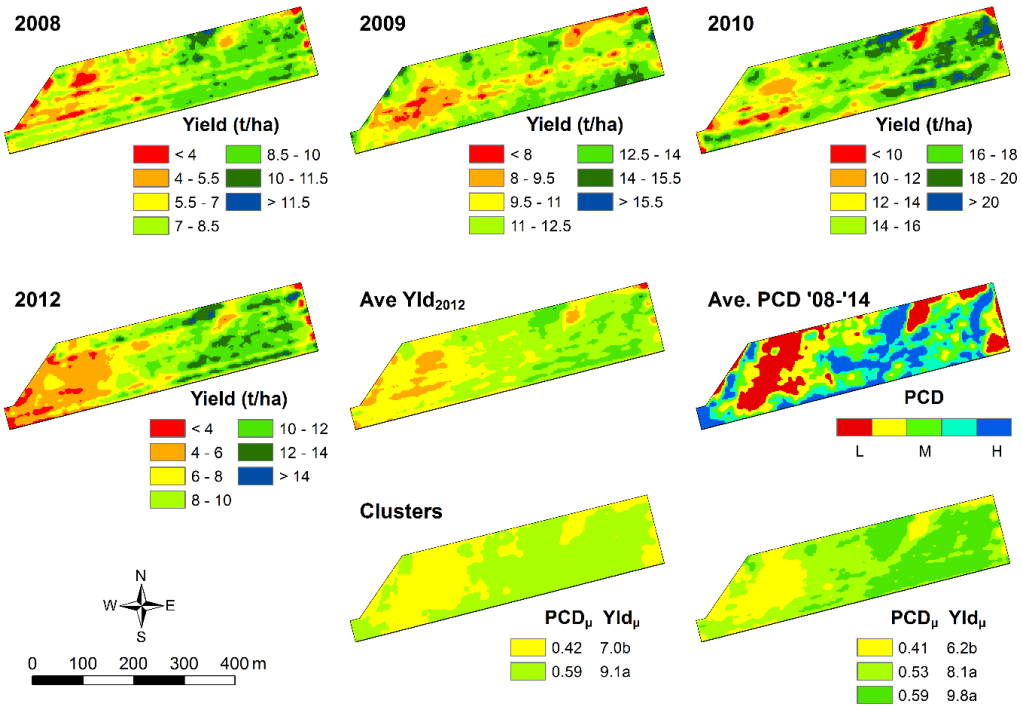


Figure 3.2 Variation in yield at the Taylors site, 2008-2012. Also shown (centre) is an average yield map calculated after the values underpinning each map had been adjusted to an equivalent 2012 basis, and the results of clustering this map with the average PCD image (2008-2014) – 2 and 3 cluster solutions shown. Note that the mean yield in each year falls in the legend category denoted by pale green.

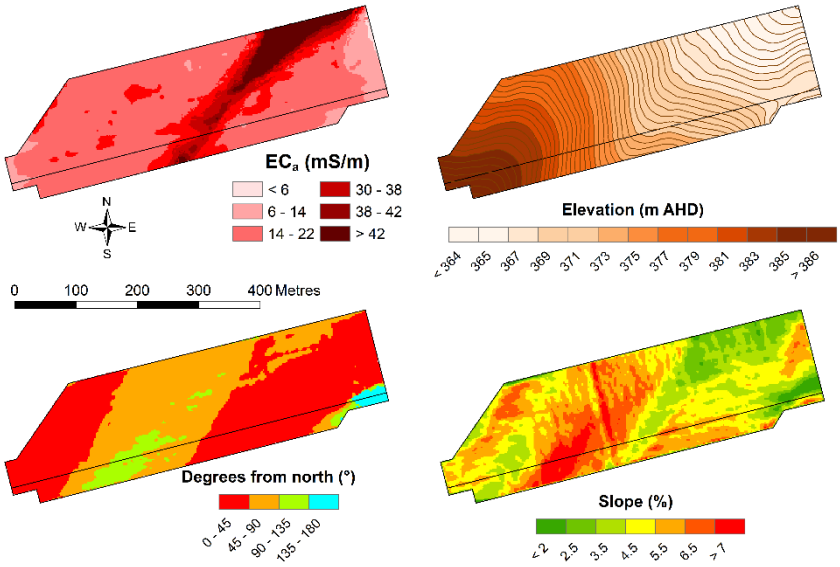


Figure 3.3 Soil and topographic variation at the Taylors site expressed in terms of bulk electrical soil conductivity (EC_a – 0-75 cm depth) measured using a dual dipole EM38MK2 in vertical mode (top left) and a digital elevation model (DEM; top right). The maps of aspect (bottom left) expressed in terms of degrees from north and of slope (bottom right) were derived from the DEM using functions available in ArcGIS.

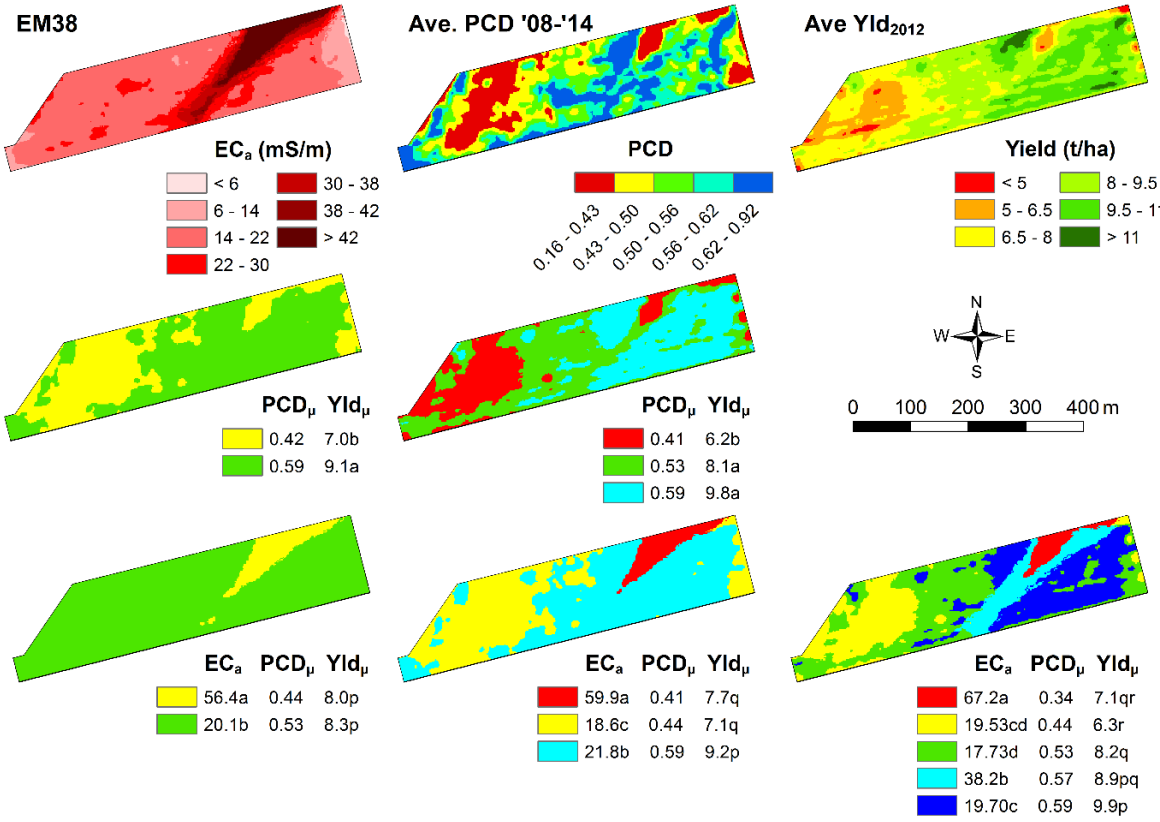


Figure 3.4 Variation in vine vigour and yield and their relationship to soil variation at the Taylors site assessed using *k*-means clustering. Cluster means labelled with different letters are significantly different (P<0.05). Note that as PCD is not kriged, the significance of differences cannot be tested using the median kriging variance (Taylor et al., 2007).

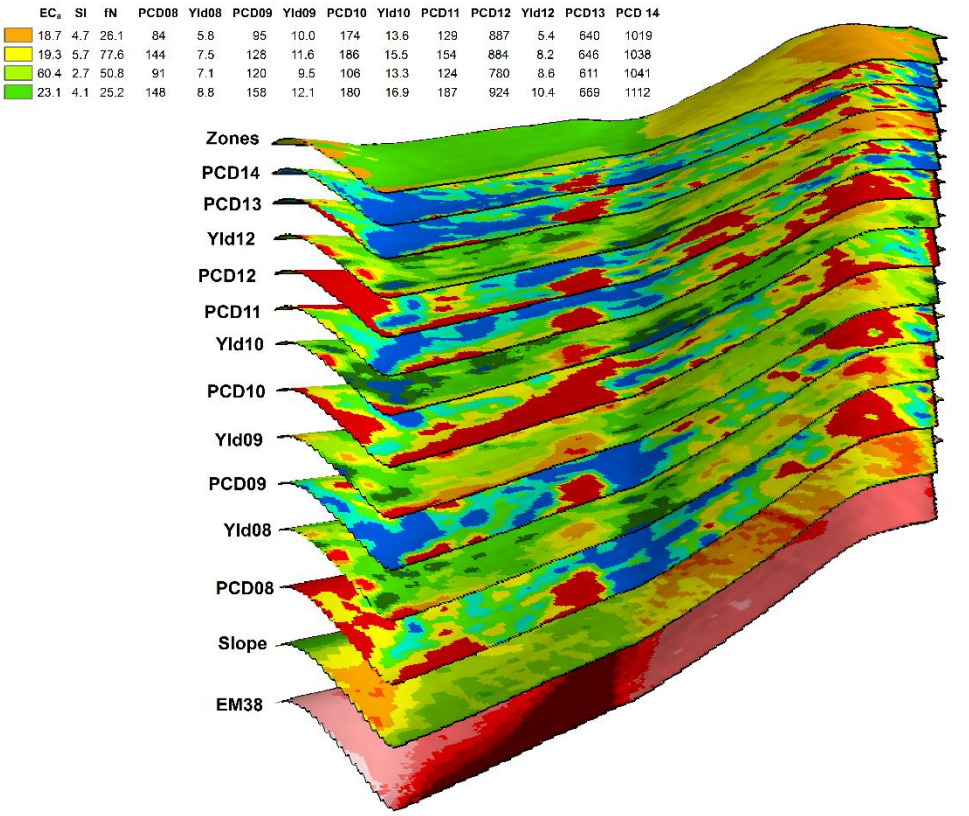


Figure 3.5 Variation in vine vigour and yield and their relationship to soil and topographic variation at the Taylors site. In the table of cluster means, slope is denoted by 'Sl' and aspect, measured in terms of orientation from north (°), by 'fN'. Note that the orientation of the map layers in this figure is approximately 180° from true north (e.g. Figure 3.4) to emphasise the effect of the zone of moist soil on the northern side of the block (bottom of figure as shown here).

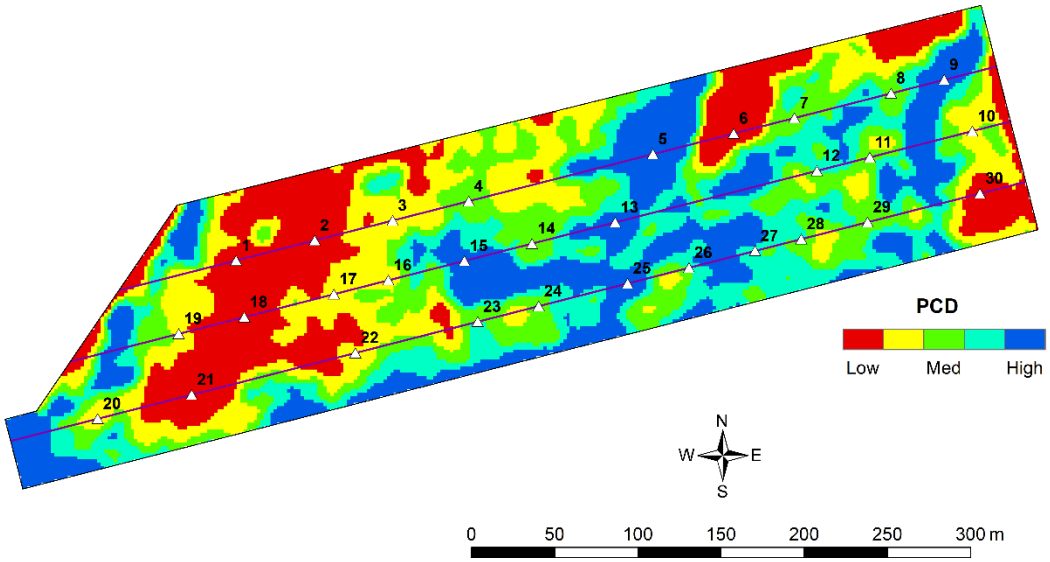


Figure 3.6 Location of sampling transects and 'target vines' selected for assessing relationships between vine vigour and yield and fruit quality at the Taylors site.

3.1) and yield (Figure 3.2) and are also reflected in the results of clustering the vine and soil data using *k*-means (Figures 3.4 and 3.5). Note that this area of apparently moist soil was also reflected in terms of the total gamma radiometric count (not shown); the radiometric soil survey did not otherwise add to the information provided by the EC_a map (Figure 3.3).

Based on the foregoing and the observation (Figures 3.1-3.5) that the major patterns of vineyard variation were crossed by the direction of the row orientation, three transects (i.e. vineyard rows) were selected for vine sampling, and target sampling locations chosen to evenly cover the range of within-vineyard variation; variation in vine vigour was used as the surrogate measure of variation for locating samples (Figure 3.6).

In contrast to Taylors, where the decision as to which block to focus on was made prior to commencing analysis, at the Kingston site, analysis of pre-project data was a key element of block selection for the project. Reliable pre-project remotely sensed imagery was only available for 2008 (Figure 3.7) and leaving aside the effects of between-block varietal differences (Petit Verdot vs Merlot), the imagery contained some striking artefacts which, based on discussion with vineyard management, were most likely associated with the aging, non-pressure compensating irrigation system and its management; this system has recently been significantly upgraded.

Yield maps were available for Kingston from 2009-2014. However, close inspection of these maps suggested numerous artefacts, again possibly associated with yield monitor or harvester errors, and likely also impacted by the design and segmentation of the irrigation system in these very large (ca. 20 ha) blocks. An additional significant problem was presented by the fact that, due to their size, these vineyard blocks tend to be harvested in several harvest 'events' – either over several days and/or using more than one harvester, as illustrated for 2013 in Figure 3.8. The effects of this issue were potentially amplified by the fact that calibration of the yield recorded by the yield monitor against the tonnage recorded as delivered to the winery was done on a whole block basis rather than a per-harvest event basis. Accordingly, an approach developed for sugarcane yield mapping (Bramley et al., 2018) was followed here whereby yield maps were produced using data that were normalised ($\mu=0$, $\sigma=1$) on a per-event basis and then back-adjusted to the block mean based on the total block tonnage delivered to the winery. Data from harvest events that were clearly divergent from neighbouring events were excluded, as were other areas of yield maps which still appeared to be compromised by artefacts. Finally, the remaining maps were adjusted so that the mean yield in any year was equal to the mean yield obtained in the central Petit Verdot block (Figures 3.7 and 3.8) in 2014 and an average yield map across all years calculated for the three blocks under consideration (Figure 3.9). Given that the coefficient of variation in yield across years was lowest in the Petit Verdot block to the northwest (Figure 3.9) and that this block displayed the greatest topographic variation (Figure 3.10), it was selected as the study location. This decision was also taken because, unlike the situation at Taylors, *k*-means clustering of soil survey data with the average yield map (not shown) did not present strong evidence of soil variation driving variation in yield (or vine vigour). Indeed, as Figure 3.11 illustrates, while higher ground and ridges were characterised by soils of low EC_a, these low values also occurred in lower lying areas and hollows. It was considered beyond the scope and resources of the present project to carefully ground truth the map shown in Figure 3.11 in terms of specific soil properties; the EC_a values do not infer, for example, an influence of soil salinity or sodicity and discussions with vineyard management did not indicate that such issues or other possible soil constraints were present.

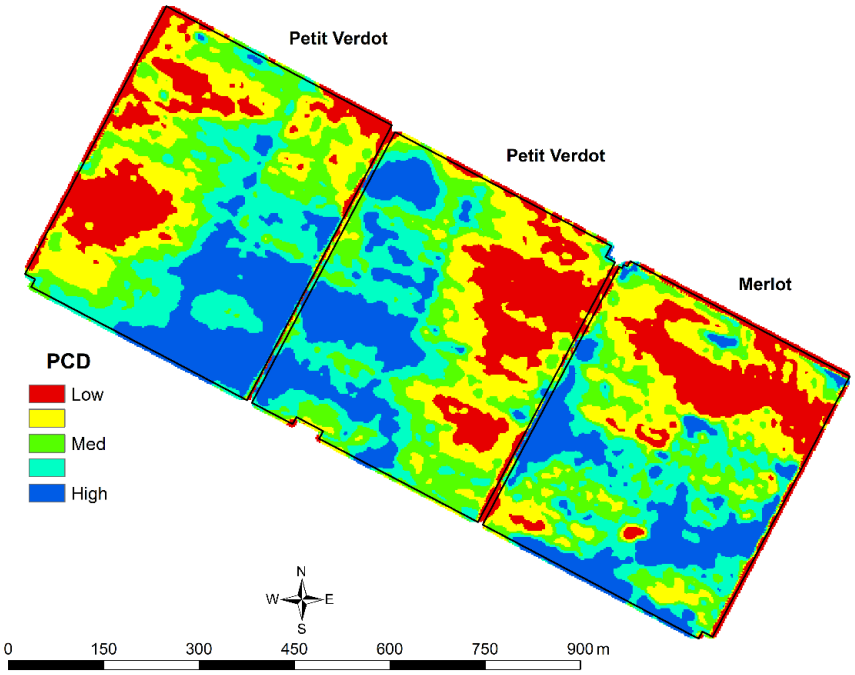


Figure 3.7 Remotely sensed imagery obtained at veraison in 2008 over a part of the Kingston Estate Wines property at Kingston-on-Murray. The block ultimately selected for the project is the one to the northwest planted to Petit Verdot.

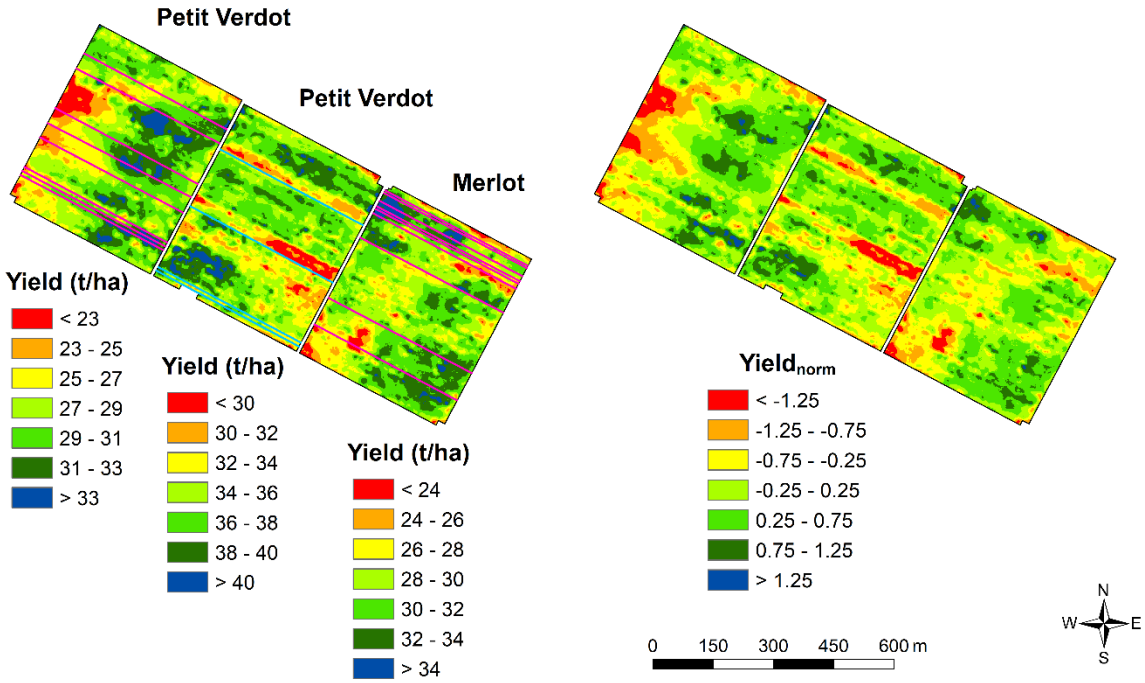


Figure 3.8 Yield maps for three blocks at Kingston Estate Wines, vintage 2013. In the maps on the left, each block has been mapped separately; note the different legend for each block, and that the mean block yield lies within the pale green legend category. Also shown (coloured lines) are the boundaries between different harvest events. In the maps on the right, the data have been normalised (μ=0, σ=1) on a per block basis prior to interpolation. The maps to the right therefore have units of standard deviations.

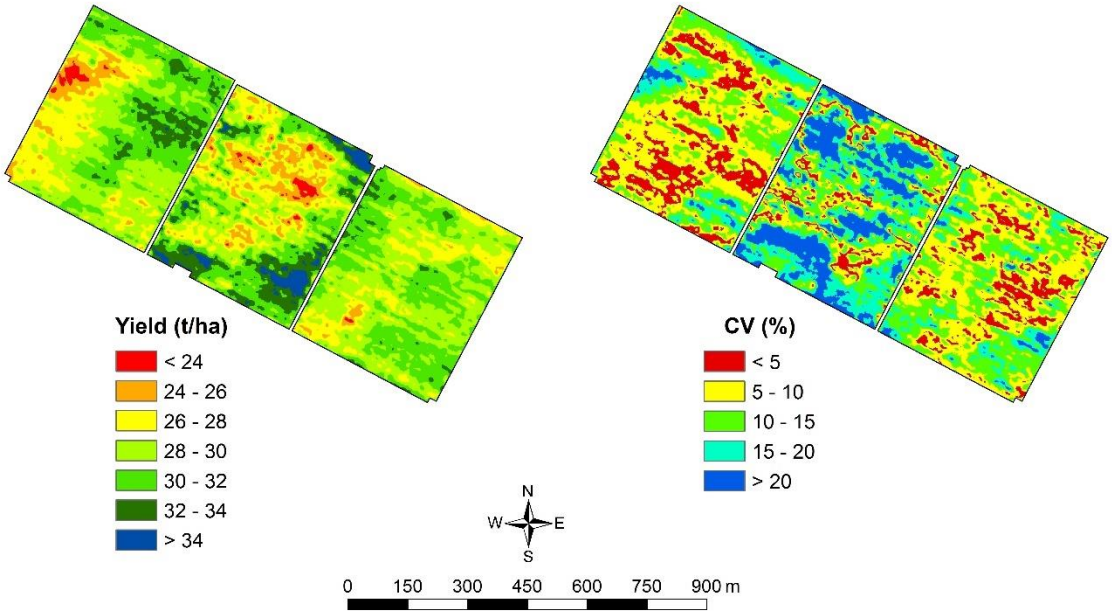


Figure 3.9 Average yield and coefficient of variation (CV) maps for three blocks at Kingston Estate Wines, 2009-2014 after adjustment of the mean yield obtained in each block and each year to that obtained in the central block in 2014.

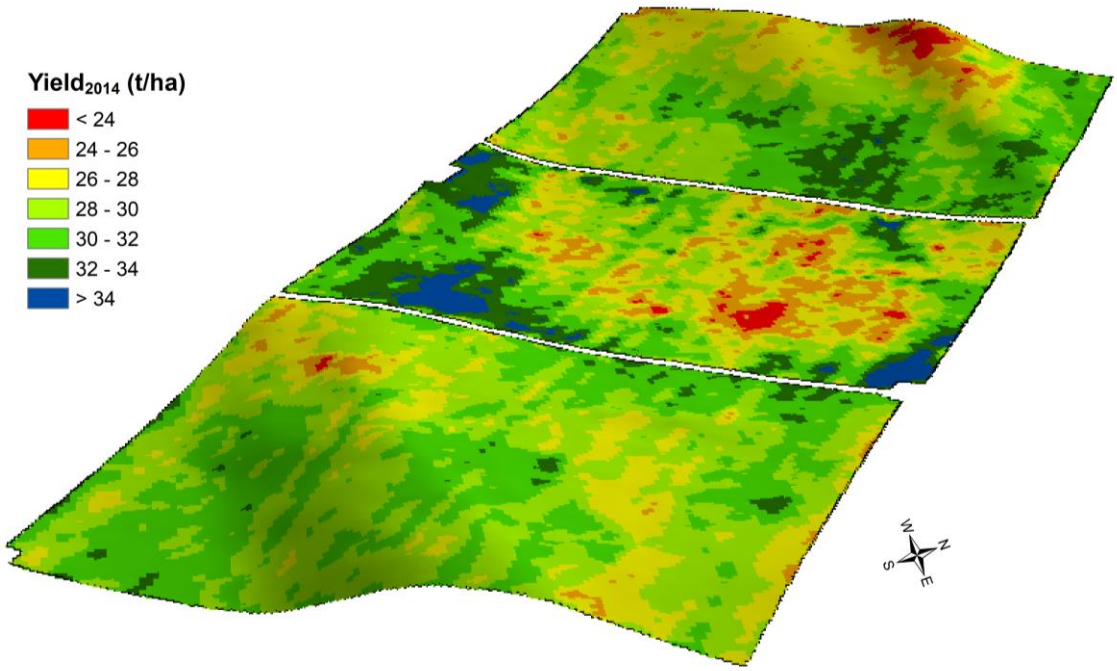


Figure 3.10 Variation in average yield and topography for three blocks at Kingston Estate Wines, 2009-2014, after adjustment of the mean yield obtained in each block and each year to that obtained in the central block in 2014. Note that the orientation of the north arrow is approximate only. The chosen study block is at the top of the figure.

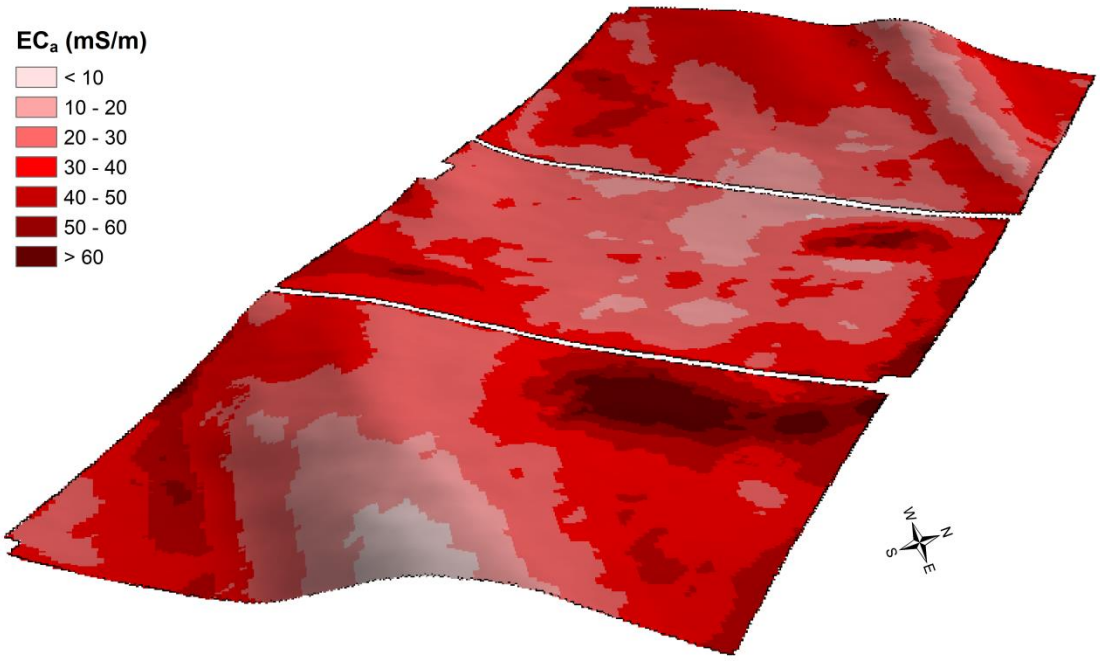


Figure 3.11 Soil and topographic variation in three blocks at Kingston Estate Wines. Note that the orientation of the north arrow is approximate only. The chosen study block is at the top of the figure.

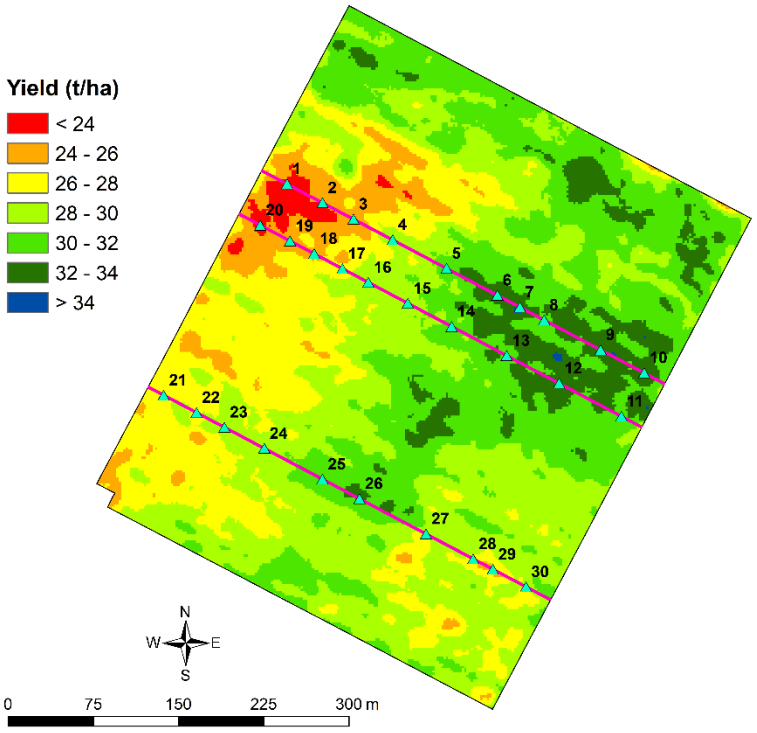


Figure 3.12 Location of sampling transects and 'target vines' selected for assessing relationships between yield and fruit quality at the Kingston site.

3.2.2 Variation in vine vigour and yield during the project

Remote and proximally sensed imagery for the Taylors site is shown in Figures 3.13 and 3.14; yield maps are also shown. Comparison of Figure 3.13 with Figure 3.1, 3.2 and 3.4 suggests that patterns of variation in vine vigour in 2015 and 2016 were broadly similar to the patterns seen in pre-project measures of vigour, albeit with some variation between the two project years. These were especially evident in the north-western part of the block and along the southern boundary. As expected, and as discussed further in Section 4, remote and proximal sensing gave a very similar representation of variation in PCD across the two project years. In contrast, and in both 2015 and 2016, initial inspection of the yield maps did not suggest a close alignment with the imagery (Figure 3.13). Both yield maps are also reflective of a lower range of variation (approximately four-fold) than in many other blocks used in PV research (approximately ten-fold; e.g. Bramley and Hamilton, 2004). Discussion with vineyard management did not indicate any obvious explanation for this in terms of targeted strategies aimed at reducing the within-block variation; the site was uniformly managed in both seasons. However, the Taylors vintage reports (pers. comm.) note that both 2015 and 2016 were unusually dry years, which likely explains the lower range of yield variation. 2015 was also affected by a hot spring, along with three significant frosts in October 2014. With seasonal rainfall only approximately half of the long-term average, yield was significantly impacted. 2016 was cooler and, notwithstanding the low seasonal rainfall, nevertheless experienced large rainfall events at the end of January and beginning of March which lifted berry size and raised yields well above the early season estimates. Of note in Figure 3.13 is that whereas PCD imagery is classified on the basis of 20th percentiles, the yield maps are classified on the basis of the measured variation. When yield is re-classified into 20th percentiles (Figure 3.14), a much closer alignment is seen in 2016 between areas of lower vigour and yield. In the very dry 2015, there is less alignment, with the low yielding area in the drainage line especially pronounced suggesting a strong soil effect. Careful examination of these issues and their likely soil-based interactions was beyond the scope of the present project.

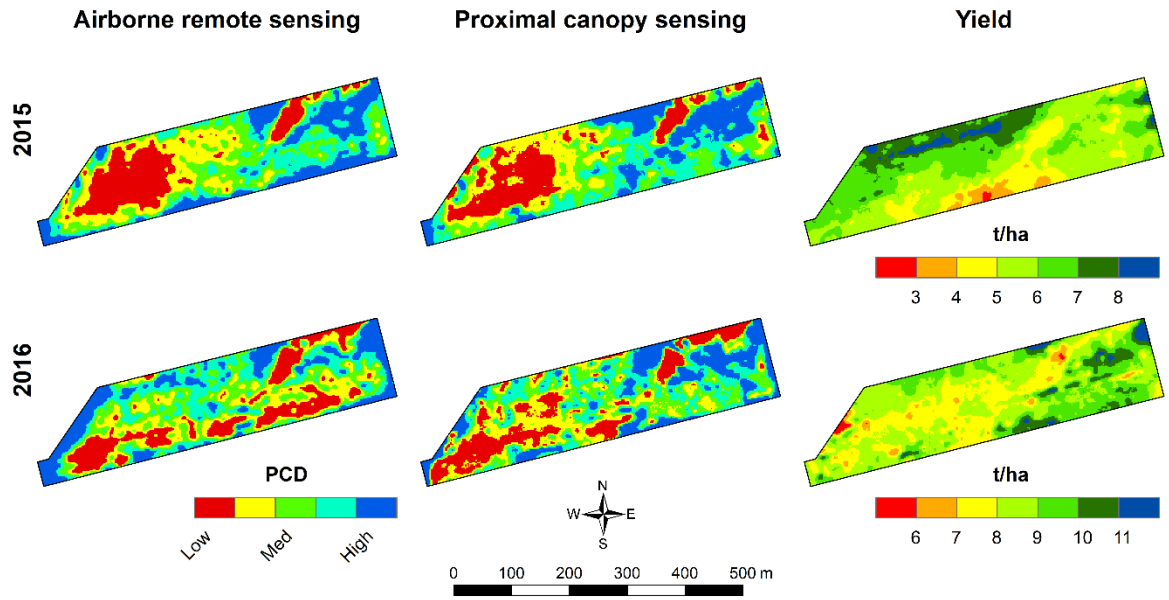


Figure 3.13 Variation in vine vigour and yield at the Taylors site in 2015 and 2016. Note that variation in PCD has been classified on the basis of 20th percentiles. The proximal canopy data were obtained using a Crop Circle sensor positioned above the canopy.

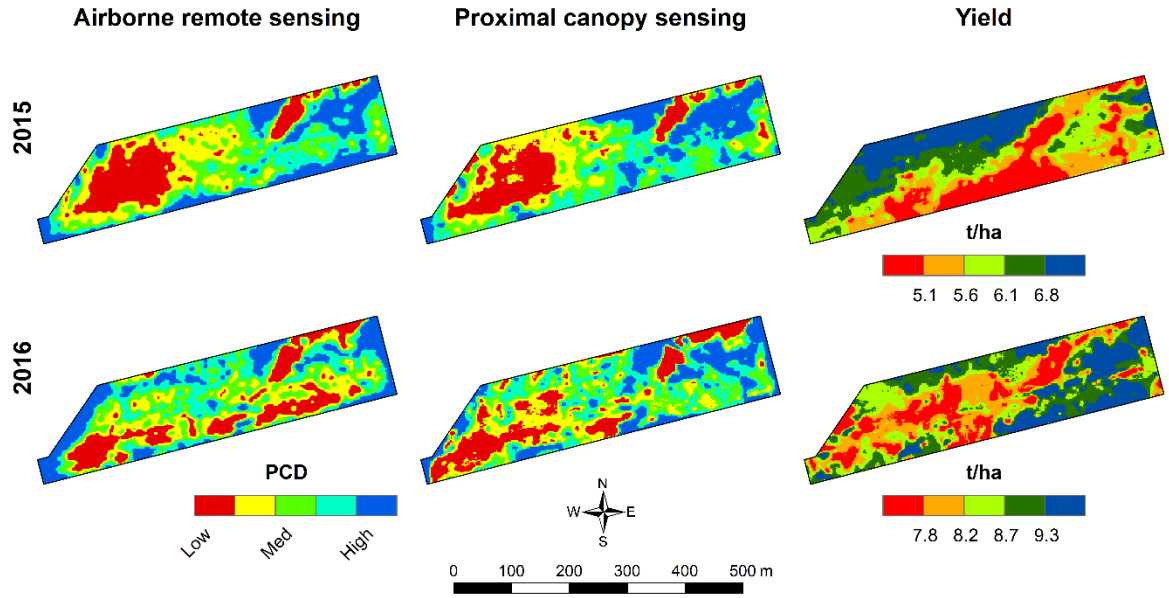


Figure 3.14 Variation in vine vigour and yield at the Taylors site in 2015 and 2016. Note that here, all variation has been classified on the basis of 20th percentiles.

At Kingston, there was a similar inconsistency between pre-project yield variation and that observed during the project (Figure 3.15). To some extent, this was not unexpected given uncertainty over the pre-project data (Section 3.2.1). However, of note is the close alignment of variation in vine vigour in 2015 and pre-project yield, especially in respect of the proximally sensed PCD data. Indeed, we believe there may be an error in the remotely sensed image given that the one initially delivered contained a clear artefact as a consequence of interaction between reflection from the highway which runs adjacent to the northern side of the block and the direction of flight. (When we raised concerns about this initially delivered image with the provider, this was the explanation offered and they instead moved to an adjacent frame in the video stream; whether this removed the artefact entirely is uncertain, but the similarity between the 2015 proximally sensed image and the pre-project yield data suggests perhaps not).

Given our confidence in the proximally sensed imagery, the mis-alignment between this and the 2015 yield map was unexpected. However, the manager at Kingston offered what he believed was a ready explanation. The start to the 2015 season was cool. The cold start meant that early season vigour was considered poor and accordingly, an additional application of fertiliser was made in an attempt to invigorate the vines. However, the flowering period was also cold which impacted on both flowering and the amount of fruitset with the impacts especially noticed in the lower lying parts of the block, especially the north east quarter. Accordingly, while this area was showing strong vigour by veraison, when the imagery was acquired, yields in this area were low due to the poor fruitset. Meanwhile, the north-western side of the block, which has good cold air drainage, was less affected by the cool conditions at flowering with fruitset consequently less impacted, and yields relatively enhanced through the additional early season fertilisation. Classification of the yield maps in terms of 20th percentiles (cf. Figure 3.14) lends weight to this explanation with the 2015 yield map presenting as essentially the inverse of the PCD image. Note that yield in 2015 was generally down on pre-project yields.

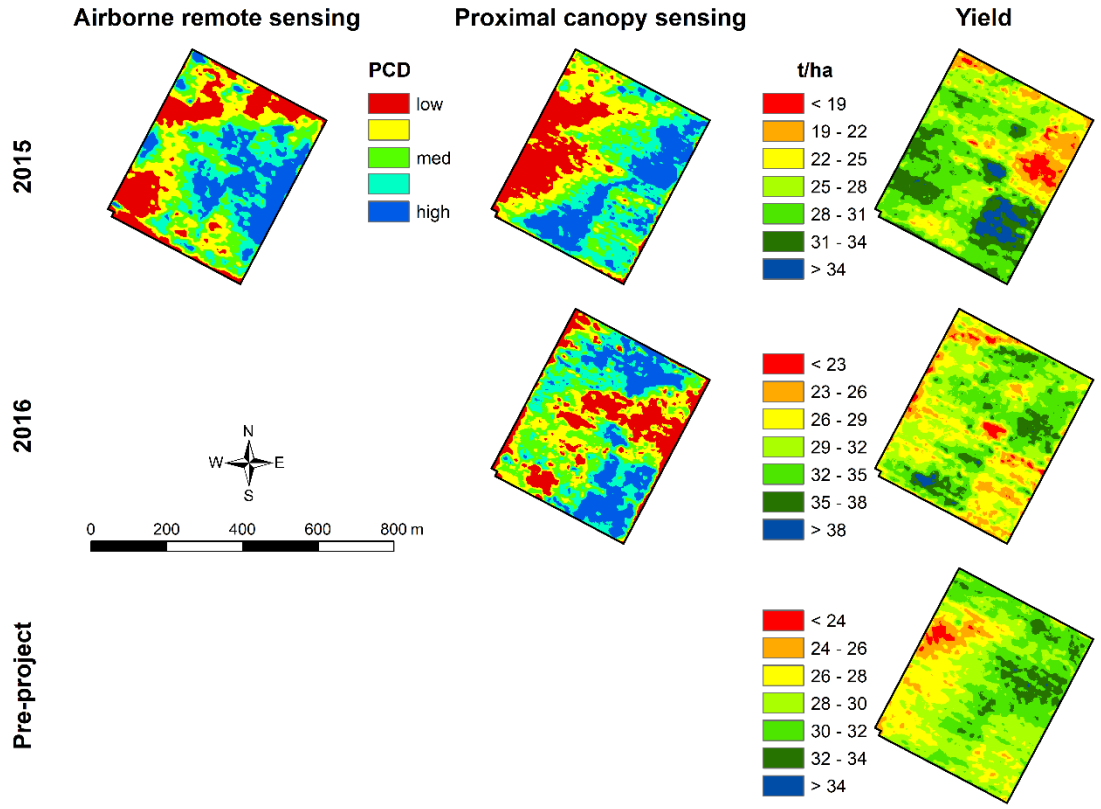


Figure 3.15 Variation in vine vigour and yield at the Kingston site in 2015 and 2016. Note that the pre-project yield is the average of that obtained in 2009-2014 adjusted to the 2014 mean.

The pattern of yield variation at Kingston in 2016 was somewhat similar to the pre-project years, although again, there was a poor and similarly unexpected lack of agreement between the yield map and imagery, especially in the lowest lying parts of the block to the east which show relatively low vine vigour but higher yields. Again, exploration of these interactions was beyond the scope of the present project. One possible contributor to the somewhat confused results is the fact that vintage 2015 was the first season after these vines were minimally pruned (they were previously lighted hedged); that is, the pre-project yield data were collected under a different canopy management regime than the data collected during the project. Another is the on-going effect of the imperfect irrigation system; the noticeable section in the southeast corner of the block evident in all maps in Figure 3.15 is associated with this.

3.2.3 Selection of an approach to modelling changes in fruit composition in the veraison to harvest period

Figure 3.16 illustrates the application of the first step of the Trought and Bramley (2011) approach – the modelling of changes in fruit composition over time in the veraison to harvest period – for selected measures from both the Taylors and Kingston sites and using a range of dependent variables as representations of time. In each case, the data plotted are the mean values for the attributes shown calculated from measurements made on the 30 samples collected from the locations shown in Figures

3.6 and 3.12. In all cases, these have been fitted with quadratic polynomials, except for TA for which an exponential decay function was used. As can be seen, for these single year data, close descriptions of the change in the various measures of fruit composition in the veraison to harvest period can be derived, whether time is measured in terms of days after some starting point, or on the basis of thermal time – in this case degree days with lower and upper limits of 10 and 36°C. The use of thermal time was in anticipation of it enabling common curves to be fitted over different years. Our assumption in this approach was that, for all practical purposes, vineyard management was the same each year meaning that seasonal conditions were the only likely driver of between-year differences, with thermal time accommodating the effects of these. However, as illustrated in Figure 3.17, when fruit compositional data were regressed against thermal time in such a way that the linear and quadratic (or decay for TA) terms were kept constant over the two years, but the intercept term was allowed to vary by season, it was clearly necessary to use season-specific intercept terms; the 'global fit' function in Sigmaplot was used for this. Clearly therefore, the use of thermal time as a between-season 'normaliser' did not work for these data. This suggests either that crop phenology post-veraison is not as temperature controlled as was anticipated and/or that other factors (e.g. crop water availability, the specific weather conditions at flowering and fruit set, etc.) drive between-season differences (Cooley et al., 2017). However, the merit of the Trought and Bramley (2011) approach lies

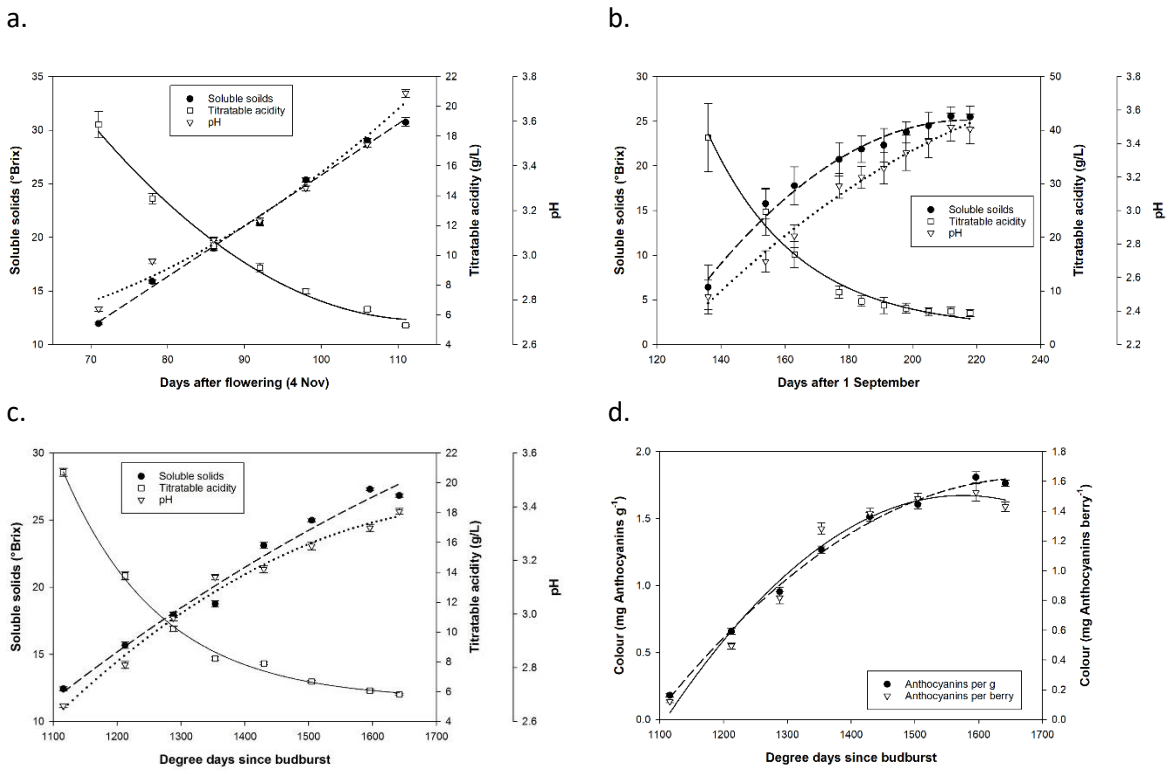
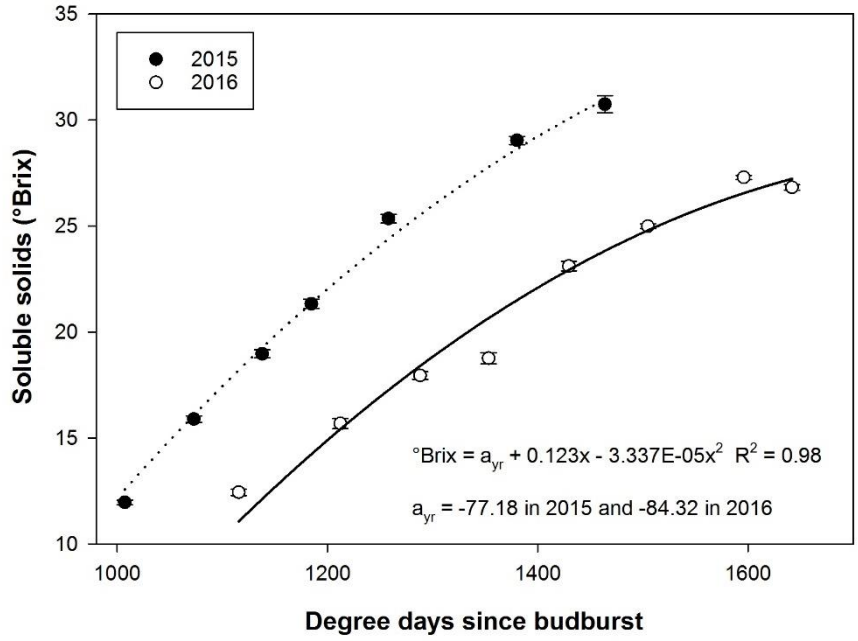


Figure 3.16 Changes in attributes of fruit composition at the Taylors and Kingston sites in 2015 and 2016 over the veraison to harvest period when time is expressed in terms of days or thermal time after a set event. The graphs show juice pH, TA and °Brix (a) as a function of days after flowering at Taylors, 2015; (b) as a function of days after 1 September 2014 at Kingston (note that phenological dates were not recorded in the 2014-15 season); and (c) as a function of degree days after budburst at Taylors, 2016. (d) shows colour (anthocyanins) at Taylors in 2016. In all cases, R^2 for the regressions was 0.96 or greater. Error bars represent the standard error of the mean.

a.



b.

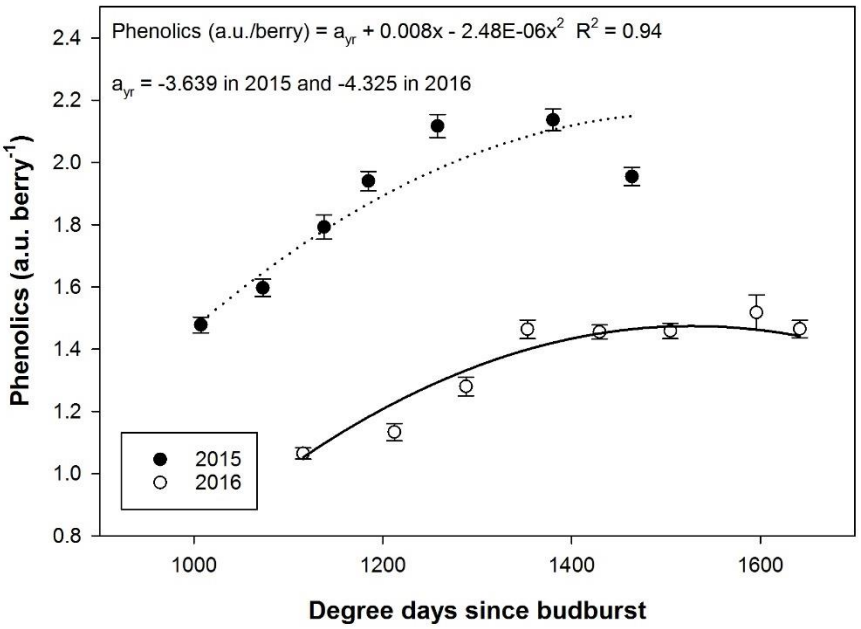


Figure 3.17 Changes in (a) soluble solids and (b) berry phenolics at the Taylors site in 2015 and 2016 when thermal time is used in an attempt to fit common curves to describe veraison to harvest phenology over two seasons. Error bars represent the standard error of the mean.

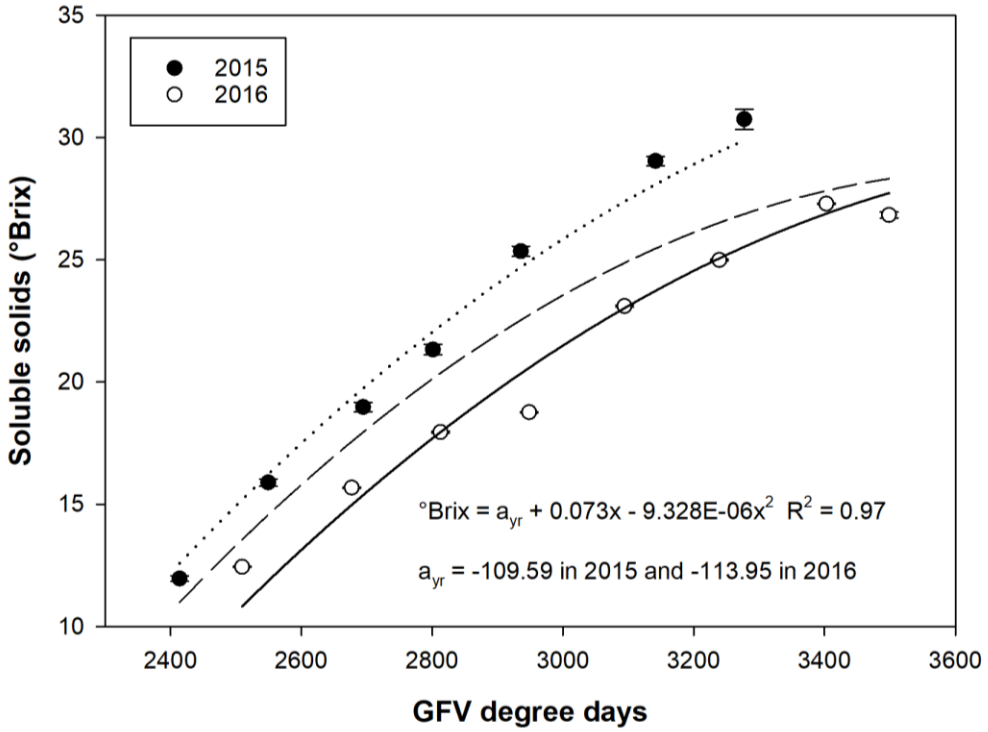
in its use of estimated/modelled juice compositional data rather than raw data so as to remove the effects of sampling and laboratory errors; that is, the effects of within vine, bunch to bunch variation, and/or difficulty in taking a representative sample from a vine and any sub-sampling or analytical errors in the laboratory.

One interpretation of the results of Cooley et al. (2017) is that changes in grape berries during the post-veraison period are a part of the grapevine senescence process and are therefore not driven by temperature in the same way that phenology earlier in the season is (Peter Clingeleffer, CSIRO – pers. comm.). If correct, then provided that the date of veraison is precisely defined, using days post-veraison as the dependent variable in predicting fruit compositional change should enable prediction across seasons. Figure 3.18a shows the same data as in Figure 3.17a, but with time expressed on the basis used in the GFV model of Parker et al. (2011). The additional dashed line, which is the 'common fit' to data from both years emphasises the fact that the limitations of a 'temperature only'-based analysis remain. However, Parker et al. (2013) have demonstrated how the GFV approach seemingly does enable robust discrimination between varieties in terms of their dates of flowering and veraison, based on analysis of data collected over a period of around 50 years from more than 120 European locations; similar data from New Zealand are consistent with the Parker et al. (2013) results (Amber Parker, Lincoln University, NZ and Mike Trought, NZ Plant and Food Research – pers. comm.).

Parker et al. (2013) identified critical degree day summations at veraison of 2601 (+/- 5.6) GFV degree days (henceforth denoted by GFV days) for Shiraz and 2849 (+/- 6.6) for Petit Verdot. The fit of a quadratic function to predict total soluble solids as a function of GFV days (e.g. Figure 3.18a) indicated that at Taylors, veraison (i.e. TSS = 8 °Brix) occurred at 2281 GFV days in 2015 and 2305 GFV days in 2016, corresponding to 7 January in 2015 and 6 January in 2016. These dates are somewhat earlier than the date corresponding to 2601 GFV days; that is, 23 January in 2015 and 18 January 2016. However, vineyard technical staff at Taylors identified veraison, defined as 50% berries colouring as occurring on 11 January 2015 and 13 January 2016. In other words, the difference between our predicted date of veraison and the vineyard staff estimate is in the order of the error (5.6 GFV days) of the Parker et al. (2013) critical value for Shiraz. Similarly, at Kingston, the modelled estimate of the date of veraison was 29 December 2014 and 1 January 2016 compared to dates predicted from the Parker et al (2013) value of 23 January 2015 and 3 January 2016. However, field inspection suggested that veraison in 2015 occurred between 15 January (~5% berries coloured) and 2 February (~95% berries coloured), whereas in 2016, veraison occurred around 20 January. It is beyond the scope of the present project to explore the reasons for these discrepancies. Two obvious explanations, aside from curve fitting errors, relate to the use of irrigation in Australia and its presumed non-use at the European locations which provided the Parker et al. (2013) dataset and also the likely higher crop load in Australia compared to Europe, especially in the case of the Kingston site (Parker et al., 2014). For southern hemisphere datasets, the appropriateness of August 29 as 'day 60' is also unclear (Amber Parker, Lincoln University, NZ – pers. comm.)

Notwithstanding the difference between the Parker et al. (2013) critical degree day summations, field observations and our modelled veraison dates, we persisted with the use of GFV degree days to define the date on which veraison occurred, based on the assumption that this is the date when berry TSS is at 8 °Brix, noting that the effect of the aforementioned discrepancies is a constant in any given year. For the TSS data at Taylors, this leads to a much closer between-season alignment of phenology (Figure 3.18b), especially earlier in the season, an observation that is consistent with those of Cooley et al. (2017). However, the divergence between the 2015 and 2016 data shown in Figure 3.18b raises concerns as to the use of the GFV model as a robust predictor of soluble solids at harvest – which it never claimed to be - especially in Australia. Other temperature-based models are likely similarly poor predictors. However, with veraison defined as occurring at 8 °Brix and, for the present purpose, with

a.



b.

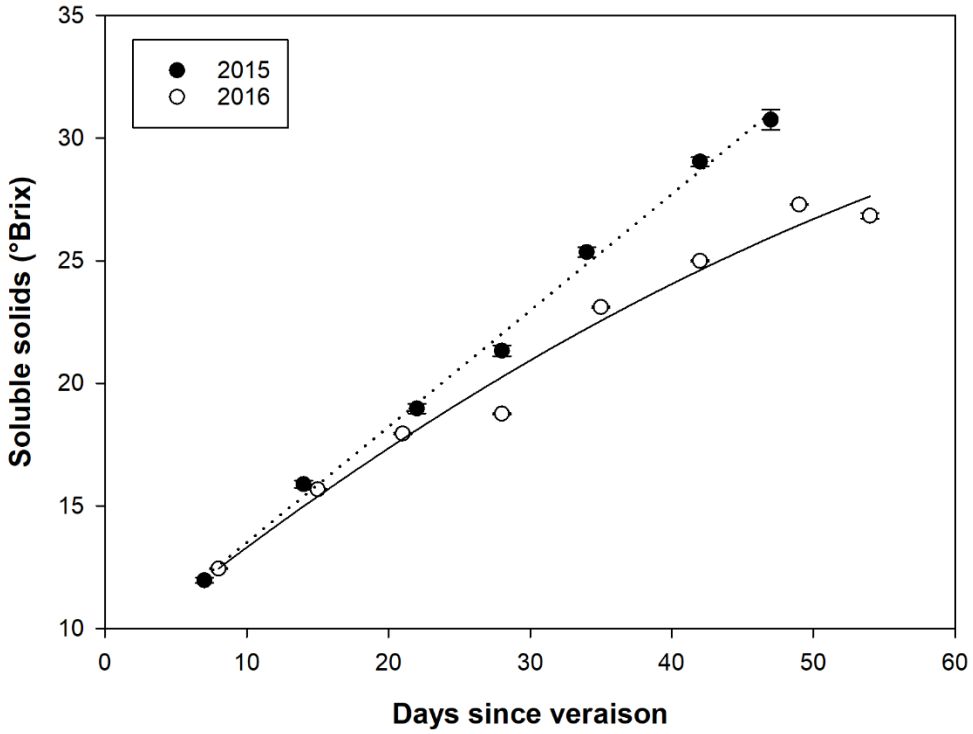


Figure 3.18 Changes in soluble solids at the Taylors site when the GFV model (Parker et al., 2011) is used to (a) calculate thermal time and from this (b) estimate the date of veraison (8 °Brix). In (a) the fitted curves for each year share common linear and quadratic terms but separate intercepts, except for the dashed line which is the fit for both years combined (all terms common). In (b), since the definition of veraison is fixed, the intercept term is shared and different linear and quadratic terms fitted for each year:
2015: °Brix = 8.79 + 0.417x + 5.32E-06 x^2 R^2 = 0.99
2016: °Brix = 8.79 + 0.474x – 0.0023 x^2 R^2 = 0.98

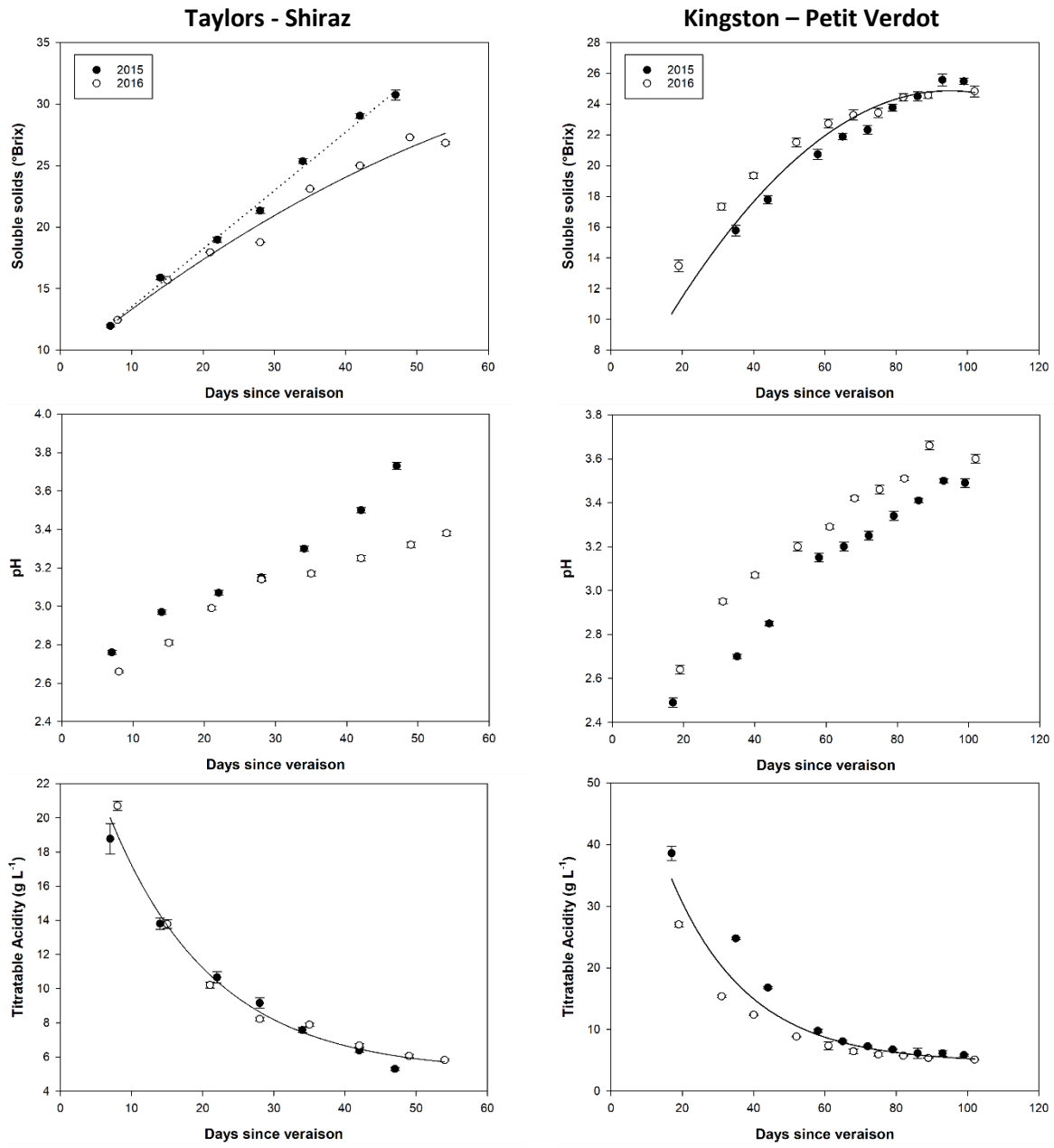


Figure 3.19 Changes in soluble solids, juice pH and titratable acidity (TA) at the Taylors and Kingston sites in 2015 and 2016. The curves fitted to the TA data at each site and to soluble solids at Kingston were common to the two years; see Figure 3.18b and discussion thereof in regard to soluble solids at Taylors. Common fits were only used where deemed justified.

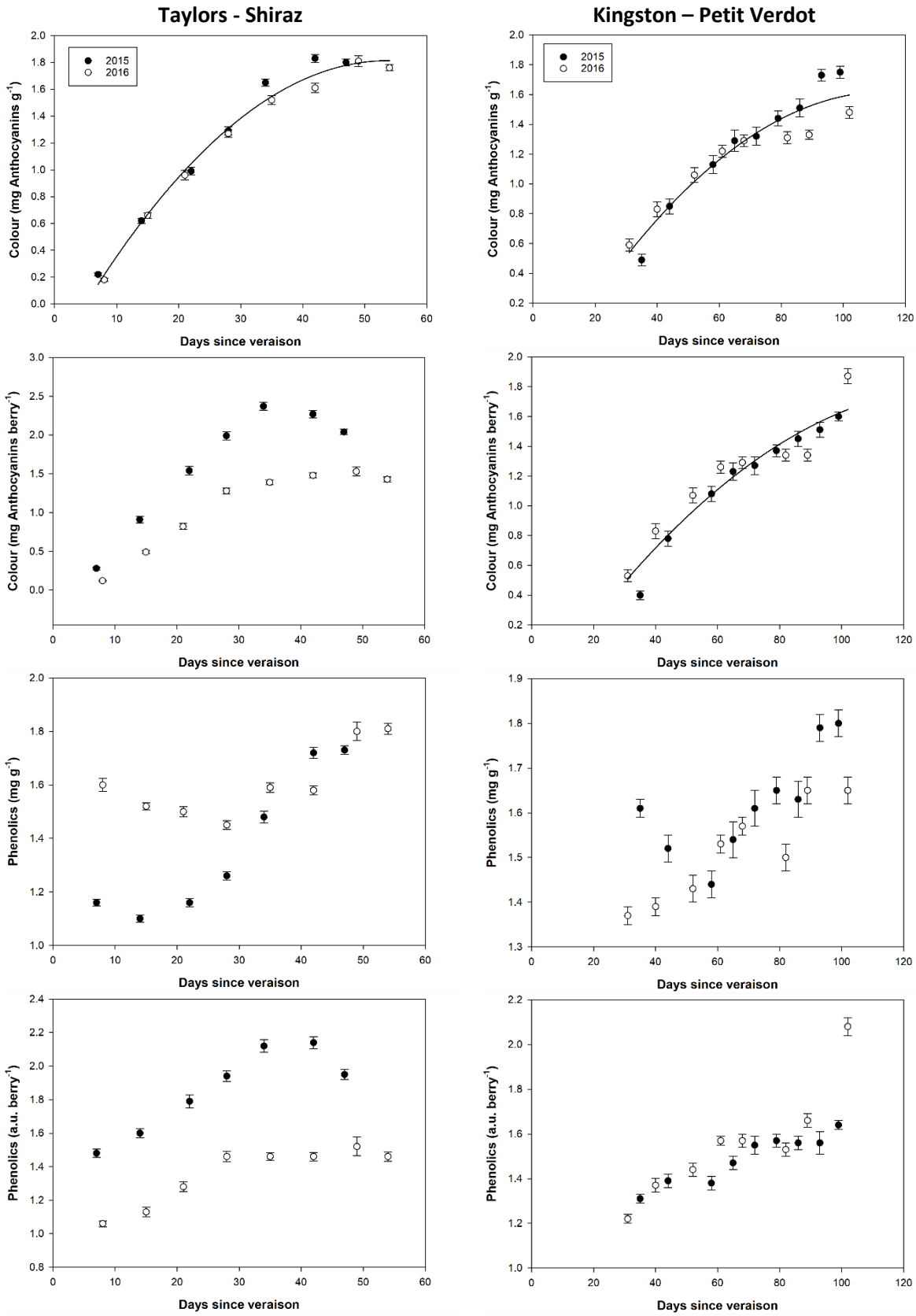


Figure 3.20 Changes in colour and phenolics at the Taylors and Kingston sites in 2015 and 2016. Where fitted, curves were common to the two years.

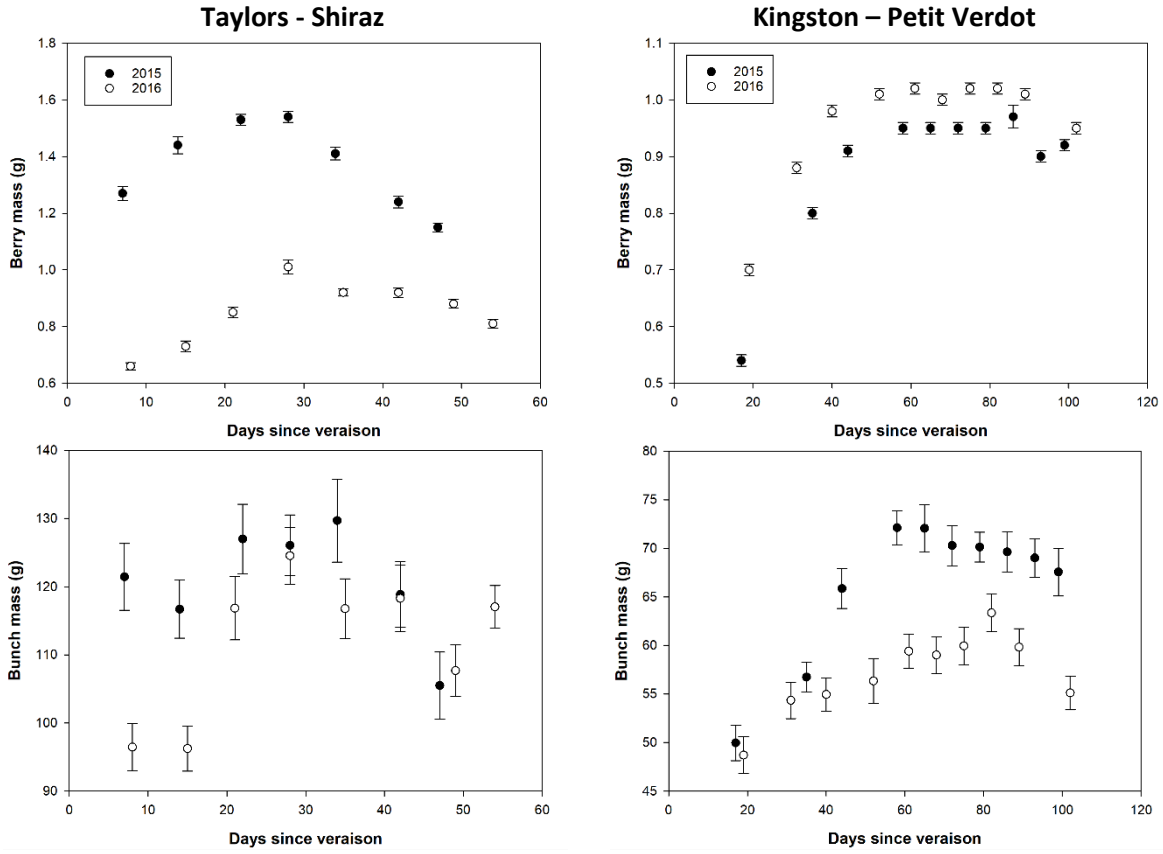


Figure 3.21 Changes in berry mass and bunch mass at the Taylors and Kingston sites in 2015 and 2016.

this date identified by the fit of our soluble solids data to GFV degree days, changes in the range of attributes measured across the two sites are provided in Figures 3.19-3.21. Whilst some attributes appear to show a remarkable consistency from year to year, many do not, even in the case of those for which a common model appears at first glance to be appropriate (Figures 3.19 and 3.20). A likely reason for this is the inter-annual variation in berry mass and bunch mass (Figure 3.21). Indeed, notwithstanding the apparent robustness of the GFV model (Parker et al., 2011, 2013) other work has concluded that the leaf area to fruit mass ratio determines the time of veraison (Parker et al., 2014); no doubt variation in this ratio also contributes to the error in other GFV-based estimates of key phenological dates.

Overall, it was concluded that attempts to fit common between-season phenological models was either not supported by the data across the range of grape attributes measured, and/or that we have insufficient site years of data to enable greater confidence in the use of common models. Accordingly, for the remainder of the present analysis, we conclude that season-specific models of berry compositional change are required and used these to estimate values of the various fruit compositional attributes of interest, as per Trought and Bramley (2011).

3.2.4 Relating fruit composition to indices of vine vigour and yield

Pairwise correlation analysis of fruit compositional attributes at harvest and indices of vine vigour and yield revealed surprisingly few significant correlations (Table 3.1), in contrast, for example, to the work of Bramley et al. (2011b) or Lamb et al. (2004). One possible reason for this at the Taylors site (Shiraz) is the impact of berry shrivel and loss of berry mass from around the middle of the veraison to harvest period; Shiraz is known to be subject to such shrivel (McCarthy, 1999) which can be clearly seen in Figure 3.21. Whilst such loss of berry mass is less evident at the Kingston site, there is nevertheless a point in the middle of the veraison to harvest period at which it ceases to increase (Figure 3.21). One implication of such a loss of yield is that the date of harvest is clearly not the time of maximum yield and, as such, 'yield' is a somewhat arbitrary measure in a temporal sense. Accordingly, and for both sites, the pairwise correlations between fruit compositional attributes and indices of vine vigour and yield were also conducted for the sampling date closest to 'peak berry mass', denoted in Table 3.1 by the subscript 'mid'. The correlations were grouped into those relating indices of vigour and yield, those between indices of fruit composition and vine vigour, those between fruit composition and yield, and between different attributes of fruit composition (Table 3.1).

As would be expected, there were close correlations between the various indices of vine vigour at Taylors, whether measured in the current season or pre-project seasons and whether derived from remote or proximal sensing (Table 3.1). This result is consistent with those reported in Sections 3.2.1, 3.2.2 and in Figure 3.1 and confirms previous work which suggests that patterns of variation in vine vigour at veraison are stable from year to year (Bramley 2010, 2019 and references therein). However, and most unusually given Figures 3.1-3.5, yield and vine vigour were not significantly correlated (P>0.05) at Taylors in 2015, and whilst the correlation between the Crop Circle measure and yield was significant in 2016, the expected positive correlation between airborne PCD and yield was not significant. At Kingston, yield and vine vigour (PCD) were surprisingly negatively correlated in both seasons; in 2015 Crop Circle PCD was highly significantly and closely positively correlated with both pre-project yield and the modelled duration of the veraison to harvest period, but PCD and yield were negatively correlated in 2016. Possible reasons for these results, which led to the Kingston data being regarded with a degree of caution, are discussed in Section 3.2.2.

Consistent with previous work, indices of vine vigour at veraison in 2015 were negatively correlated with TSS at harvest at Taylors in 2015, but not in 2016, and whilst there was no correlation between PCD and TA at harvest (not shown), the correlation between these variables in the veraison to harvest 'mid' point in 2015 was highly significant (P<0.0001), a result that lends weight to concerns over the arbitrariness of harvest in the context of 'time' and the assessment of fruit quality at harvest. In contrast, and whereas PCD and colour were not significantly correlated in 2015, in 2016 the correlation was highly significant and, as expected, indicated that higher vigour led to lower colour, whether measured mid-season or at harvest (Table 3.1). At Kingston, expected significant negative correlations between vigour and juice pH and positive correlations between vigour and TA were seen mid-season in 2015, but not at harvest; colour was also significantly correlated with vigour in 2016, although unexpectedly, the correlation was positive, in contrast to the previously observed results (e.g. Bramley et al., 2011b).

At Taylors, there were no significant correlations (P>0.05) between yield and any element of fruit composition across the two study years, except in 2016 when colour was negatively correlated with yield, albeit not as strongly as for vine vigour (above), and with a more significant, albeit fairly weak

Table 3.1 Selected pairwise correlations amongst and between indices of vine vigour, yield and fruit composition.

Attributes		Taylors		Kingston	
		2015	2016	2015	2016
Vigour and Yield					
Average $PCD_{2008-14}$	Crop Circle	0.8240****	0.6068***		
PCD this year	Crop Circle	0.9623****	0.6555****		
Average $PCD_{2008-14}$	PCD this year	0.8190****	0.6008***		
Yield this year	Crop Circle	-0.2382^{NS}	0.5143**	-0.3996*	-0.6396***
Yield this year	EM38^{A}	-0.4587*	-0.0649^{NS}	0.5704**	-0.3294^{NS}
PCD this year	Yield this year	-0.2668^{NS}	0.3212^{NS}		
PCD this year	EM38	-0.2352^{NS}	-0.4171*		
Crop Circle	Average $Yield_{2009-14}$			0.8711****	-0.6202***
Yield this year	Average $Yield_{2009-14}$			-0.5157**	0.3012^{NS}
Yield this year	Days V to H^{B}			0.7341****	-0.0571^{NS}
Vigour and Fruit composition					
Crop Circle	TSS at harvest	-0.5622**	-0.1086^{NS}		
PCD this year	TSS at harvest	-0.5025**	-0.1959^{NS}		
Average $PCD_{2008-14}$	TSS at harvest	-0.3463^{NS}	0.1458^{NS}		
Crop Circle	Juice pH at harvest	-0.3259^{NS}	0.0554^{NS}		
PCD this year	Juice pH at harvest	-0.3024^{NS}	0.1085^{NS}		
Average $PCD_{2008-14}$	Juice pH at harvest	-0.1708^{NS}	0.0315^{NS}		
Crop Circle	Juice pH_{mid}	-0.4688**	-0.0145^{NS}	-0.5407**	0.1293^{NS}
PCD this year	Juice pH_{mid}	-0.4569*	-0.2078^{NS}		
Average $PCD_{2008-14}$	Juice pH_{mid}	-0.4029*	-0.2401^{NS}		
Crop Circle	TA at harvest			0.1173^{NS}	-0.0364^{NS}
Crop Circle	TA_{mid}	0.6910****	-0.0892^{NS}	0.8028****	-0.1145^{NS}
PCD this year	TA_{mid}	0.6453****	-0.0806^{NS}		
Average $PCD_{2008-14}$	TA_{mid}	0.5560**	-0.0121^{NS}		
Crop Circle	Colour g^{-1} at harvest	-0.1931^{NS}	-0.6010****	0.3774*	0.3570^{NS}
Crop Circle	Colour g^{-1}_{mid}	-0.3747^{NS}	-0.5781***	0.3918*	0.7979****
PCD this year	Colour g^{-1} at harvest	-0.2833^{NS}	-0.4422*		
PCD this year	Colour g^{-1}_{mid}	-0.3860*	-0.3141^{NS}		
Average $PCD_{2008-14}$	Colour g^{-1}_{mid}	-0.2499^{NS}	-0.3302^{NS}		
Yield and Fruit composition					
Yield	TSS at harvest	-0.3588^{NS}	-0.1468^{NS}	-0.5451**	0.0359^{NS}
Yield	TSS_{mid}	-0.1858^{NS}	-0.0907^{NS}	-0.8487****	-0.8850****
Yield	Juice pH at harvest	-0.3458^{NS}	0.1376^{NS}	-0.5316**	-0.4536*
Yield	TA at harvest	-0.0544^{NS}	0.0140^{NS}	0.5399**	0.3090^{NS}
Yield	Colour g^{-1} at harvest	0.2143^{NS}	-0.4893**	-0.6201***	-0.4911**
Yield	Colour g^{-1}_{mid}	0.0689^{NS}	-0.4089*	-0.9119****	-0.8610****

Table 3.1 Contd…

Attributes		Taylors		Kingston	
		2015	2016	2015	2016
Fruit composition					
Brix at harvest	Juice pH at harvest	0.7435****	0.1901^{NS}	0.7237****	0.4464*
Brix at harvest	TA at harvest	0.0243^{NS}	-0.1138^{NS}	-0.6166***	-0.0901^{NS}
Brix at harvest	Colour g^{-1} at harvest	0.0648^{NS}	0.1916^{NS}	0.5479**	0.2653^{NS}
TA at harvest	Juice pH at harvest	-0.0143^{NS}	-0.2229^{NS}	-0.6008***	-0.3252^{NS}
TA at harvest	Days V to H	-0.0598^{NS}	0.3972*	0.4254*	-0.2191^{NS}
TA_{mid}	Days V to H	0.3847*	0.4339*	-0.0521^{NS}	-0.0808^{NS}
$Brix_{mid}$	Days V to H	-0.5890****	-0.5185**	-0.8249****	0.0637^{NS}
$Brix_{mid}$	TA_{mid}	-0.7014****	-0.0694^{NS}	-0.1809^{NS}	-0.4377*
Juice pH_{mid}	TA_{mid}	-0.7361****	-0.3368^{NS}	-0.7415****	-0.7794****
$Brix_{mid}$	Colour $g^{-1}{}_{mid}$	0.4140*	0.6298***	0.9241****	0.7883****

[A]EM38 denotes bulk electrical soil conductivity (EC_a) – see section 3.1.2.
[B]Days V to H is the modelled number of days between veraison (TSS=8 °Brix) and harvest (TSS=25.2 °Brix at Taylors and 24 °Brix at Kingston).
$_{mid}$ denotes measures made during the veraison to harvest period prior to any berry decline – see text for further explanation.
The significance of the correlations is denoted by ^{NS}, Not Significant (P>0.05); *, P<0.05; **, P<0.01; ***, P<0.001; and ****, P<0.0001.

correlation at harvest compared to that for the veraison to harvest 'mid' point. In contrast, at Kingston, in 2015 there were strong and expected negative correlations between yield and TSS, juice pH and colour, and a positive correlation with TA; again, the correlations tended to be stronger and more significant at the veraison to harvest 'mid' point than at harvest.

TSS, juice pH and TA are arguably all more appropriately measures of fruit maturity than of quality *per se* and would generally be expected to be correlated; positively in the case of TSS and pH and negatively in the case of TA. Fruit with higher TSS (i.e. riper, more mature) would also be expected to have more colour. Thus, some of the results in Table 3.1 are surprising. For example, TSS and juice pH were not correlated at Taylors in 2016 and bizarrely, neither were juice pH and TA, yet TA was positively correlated with the estimated duration of the veraison to harvest period suggesting that a longer ripening period led to more acidity in the fruit – which is somewhat counter-intuitive. The 2015 results were more expected with TA being strongly negatively correlated with both TSS and pH in the middle of the veraison to harvest period. There was also a strong negative correlation between TSS and the duration of the veraison to harvest period. This makes sense: higher TSS fruit is riper sooner than fruit of lower TSS. This same result was observed at Kingston in 2015 when the other correlations were consistent with previous work (e.g. Bramley et al., 2011b), but in 2016, there few significant correlations other than the positive linkage between TSS and colour.

Recently, Edwards et al. (2017) found that strategies such as fruit thinning (i.e. deliberately reducing yield) were unlikely to deliver a benefit in terms of fruit quality; they suggested that focussing on improving the bunch environment was likely to be more beneficial. As a part of that work, they

normalised their data on a per g sugar basis in order to better understand the source:sink interactions between vigour and yield and their implications for berry composition. Accordingly, we tested a similar strategy and examined the relationships between indices of vine vigour and yield and the gross production of sugar (i.e. g sugar berry^{-1} as opposed to TSS), and also the amount of colour and phenolics produced as a function of the amount of sugar produced (colour or phenolics produced berry^{-1} divided by sugar berry^{-1}); the results are shown in Table 3.2 for both measurements made at harvest and in the mid-point of the harvest to veraison period.

Whereas correlations between TSS and either vine vigour or yield tend to be negative, the correlations between sugar produced and these indices at Taylors tended to be positive, presumably reflecting the impact of higher yields at a site producing well below its potential yield, although many were not significant. Conversely, at Kingston where achieving yield potential (i.e. maximising yield) is effectively a production objective, the correlation between sugar produced and indices of vigour and yield tended to be negative or not significant indicating that the minimally pruned Petit Verdot vines were struggling to ripen the high yields of this late maturing variety. However, the main message from Table 3.2 is that, with respect to the data collected in this study, accounting for berry sugar content did not assist in understanding yield:compositional interactions at Taylors with most correlations not significant, whilst at Kingston, the results across the two years were equivocal and also not significant in many instances.

Overall, the results reported led to the conclusion that implementation of the approach of Trought and Bramley (2011) in using Crop Circle PCD as a predictor of fruit composition was not justified. Trought and Bramley (2011) used this approach as a means of modelling changes in fruit composition in the few weeks prior to harvest to explore spatial and temporal variation in the development of a 'juice quality index'. In many respects, their results were similar to those reported here in that the strength of their predictions of TSS, juice pH and TA using Crop Circle PCD were temporally variable and quite weak in some cases. Theirs was a 'proof of concept' piece of work aimed at exploring the utility of a juice index as a guide to strategies such as selective harvesting and gaining understanding of the evolution of fruit composition and its spatial variability. Here, our objective was to address the question of whether yield or vine vigour (which we sought to use as a surrogate for yield) and fruit quality were correlated. Given that these correlations were weak, based on the available data, we did not consider attempts to predict fruit composition from Crop Circle PCD were justified.

3.2.5 Discussion – the yield:quality nexus

Trought (2005) has questioned the existence of an inverse relationship between yield and fruit quality noting that it is largely anecdotal, and citing Sinton et al. (1978), Gray et al. (1994) and Chapman et al. (2004) in suggesting that whilst excessive yield may result in inferior wine, the reverse is not true, with low yields offering no guarantee of quality. In the case of the Chapman et al. (2004) study, low yields seemingly contributed to lower quality. Matthews (2016) has similarly cast considerable doubt over the basis for the worldwide wine dogma which suggests that higher yields mean lower quality and that it is therefore not possible to achieve high quality fruit at high yield. From the first principles of plant physiology, in a place where there is a sufficient combination of sunlight, warmth and water, it is difficult to conceive a reason why a grapevine should not be able to have high yield at high quality – providing it is supplied with the other things (good nutrition, absence of disease or other constraints) that it needs to do so. Edwards et al. (2017) make a similar inference. One might therefore not expect

Table 3.2 Correlation between berry sugar (g berry^{-1}), sugar-adjusted colour (Colour$_{sug}$; mg anthocyanins g^{-1} sugar) and phenolics (Phenolics$_{sug}$; a.u. g^{-1} sugar) and indices of vine vigour and yield.

Attributes		Taylors		Kingston	
		2015	2016	2015	2016
Crop Circle	$Sugar_{mid}$	0.5085**	0.6110***	-0.2012^{NS}	0.3384^{NS}
Crop Circle	Sugar	0.1211^{NS}	0.3715*	0.1186^{NS}	-0.2597^{NS}
Average $PCD_{2008-14}$	$Sugar_{mid}$	0.4626*	0.3356^{NS}		
Average $PCD_{2008-14}$	Sugar	0.3101^{NS}	0.2453^{NS}		
PCD this year	$Sugar_{mid}$	0.5156**	0.3643*		
PCD this year	Sugar	0.2195^{NS}	0.0420^{NS}		
Yield	$Sugar_{mid}$	0.0199^{NS}	0.3155^{NS}	-0.2370^{NS}	-0.4032*
Yield	Sugar	0.4166*	0.3300^{NS}	-0.1410^{NS}	0.1982^{NS}
Average $Yield_{2009-14}$	$Sugar_{mid}$			-0.1396^{NS}	-0.0750^{NS}
Average $Yield_{2009-14}$	Sugar			0.0669^{NS}	0.3448^{NS}
Crop Circle	$Colour_{sug, mid}$	0.0235^{NS}	-0.3223	0.3679*	0.7012****
Crop Circle	$Colour_{sug}$	0.2138^{NS}	-0.3330^{NS}	0.4203*	-0.1974^{NS}
Average $PCD_{2008-14}$	$Colour_{sug, mid}$	0.1206^{NS}	-0.1288		
Average $PCD_{2008-14}$	$Colour_{sug}$	0.0918^{NS}	-0.3367^{NS}		
PCD this year	$Colour_{sug, mid}$	0.0183^{NS}	-0.2398		
PCD this year	$Colour_{sug}$	0.1314^{NS}	-0.1265^{NS}		
Yield	$Colour_{sug, mid}$	0.0199^{NS}	-0.1419	-0.8610****	-0.6187***
Yield	$Colour_{sug}$	0.4166*	-0.2629^{NS}	-0.5916***	0.0747^{NS}
Average $Yield_{2009-14}$	$Colour_{sug, mid}$			0.3831*	-0.3696*
Average $Yield_{2009-14}$	$Colour_{sug}$			0.5006**	-0.1274^{NS}
Days V to H	$Colour_{sug, mid}$			-0.6223****	-0.2234^{NS}
Days V to H	$Colour_{sug}$			-0.3715^{NS}	0.0159^{NS}
Crop Circle	$Phenolics_{sug, mid}$	-0.2577^{NS}	-0.4669**	0.1310^{NS}	0.0163^{NS}
Crop Circle	$Phenolics_{sug}$	0.3102^{NS}	-0.3049^{NS}	0.0197^{NS}	-0.3075^{NS}
Average $PCD_{2008-14}$	$Phenolics_{sug, mid}$	-0.0842^{NS}	-0.3456^{NS}		
Average $PCD_{2008-14}$	$Phenolics_{sug}$	0.2516^{NS}	-0.2870^{NS}		
PCD this year	$Phenolics_{sug, mid}$	-0.2413^{NS}	-0.4285*		
PCD this year	$Phenolics_{sug}$	0.2515^{NS}	-0.1149^{NS}		
Yield	$Phenolics_{sug, mid}$	0.0044^{NS}	-0.4248*	-0.7154****	0.2602^{NS}
Yield	$Phenolics_{sug}$	0.3456^{NS}	-0.1501^{NS}	-0.5037**	0.2162^{NS}
Average $Yield_{2009-14}$	$Phenolics_{sug, mid}$			0.2522^{NS}	0.0433^{NS}
Average $Yield_{2009-14}$	$Phenolics_{sug}$			0.1545^{NS}	-0.1960^{NS}
$Phenolics_{sug, mid}$	$Colour_{sug, mid}$	0.8411****	0.6659****	0.8704****	0.2677^{NS}
$Phenolics_{sug}$	$Colour_{sug}$	0.8776****	0.8306****	0.7944****	0.7730****

The significance of the correlations is denoted by ^{NS}, Not Significant (P>0.05); *, P<0.05; **, P<0.01; ***, P<0.001; and ****, P<0.0001. Other descriptors are as per Table 3.1.

Note that in contrast to other measures of fruit composition which used modelled data (see section 3.2.2, here the sugar-adjusted measures of colour and phenolics were calculated from actual analytical data along with measures of berry mass.

yield and quality to be inextricably linked. The present results lend little weight to the suggestion, at the within-vineyard scale, that they are; that is, they do not provide much evidence at the within-vineyard scale for the existence of a yield:quality nexus reflective of industry dogma. It must be said however, that four site years of data from just two contrasting sites growing two contrasting varieties is barely sufficient to end the argument, especially given the unusual nature of some of the data collected in the present study compared to previous work (Bramley 2010, 2019 and references therein). In one example of that previous work, Bramley and Hamilton (2004) demonstrated that patterns of within-vineyard variation in yield were stable in time such that the lowest and highest yielding zones were always the lowest and highest, whereas their rank order in terms of quality could change. They inferred that this fluctuation of the rank order of yield-based zones in terms of fruit quality was due to seasonal variation in the absolute value of the mean yield. Thus, in a constrained season, a 'high' yielding zone could conceivably be lower yielding than the long term average for the block. It is perhaps not hard to conceive that in such a season, the 'low' yielding zone might not produce particularly high quality fruit.

Trought et al. (2008) and Trought and Bramley (2011) have shown how, in a cane pruned Marlborough Sauvignon Blanc vineyard, fruit quality assessed on the basis of TSS, juice pH and TA did appear to be closely related to vine vigour, a result that is consistent with those of Bramley et al. (2011b,c) in much higher yielding spur pruned vineyards in the Murray Valley. In both cases, vine vigour was clearly controlled by a combination of soil and topographic variation. However, this NZ work also showed that there was no relationship between yield and vine vigour (Bramley et al., 2011d) or, by inference, yield and quality. Analysis of data from additional seasons in the same NZ vineyard (Bramley and Trought, unpublished) suggests that these relationships (or the lack thereof) are maintained across seasons. The lack of a yield:vigour relationship, and consequent lack of a yield:quality relationship was ascribed to the careful selection of similarly sized canes during the hand pruning process. Clearly therefore, at least some aspects of canopy management are important here. In the present study, both sites were spur pruned, albeit to contrasting canopy sizes and architectures, yet the evidence for existence of a yield:quality nexus at either site was, at best, weak. In that regard, the present results are consistent with those of Edwards et al. (2017).

Much of the previous Australasian work on vineyard variability was done in vineyards where there was either a clear '*terroir* effect' or was conducted in such a way that one could be readily discerned. Thus, for example, variation in soil depth (Bramley and Janik, 2005) and topography was clearly driving the variation in yield (Bramley and Hamilton, 2004) and quality (Bramley, 2005) observed in a Coonawarra vineyard; likewise in the Murray Valley and Marlborough (NZ) vineyards studied by Bramley et al. (2011b,d) and Trought and Bramley (2011 –see comments above); topography was again key in vineyards in Padthaway (Bramley and Hamilton, 2007), Eden Valley (Bramley, 2017) and the Grampians (Scarlett et al., 2014; Bramley et al., 2017), whilst the effect of soil salinity, in turn driven by topography, was critical to the performance of a Clare Valley vineyard (Bramley et al., 2002). In all of these studies, clear yield:quality interactions were evident when examined in the context of differences between 'zones', identified using high resolution spatial data, that were reflective of the expression of some element of *terroir*. In the present study, the area of high EC_a at the Taylors site (Figures 3.3-3.5) is suggestive of a *terroir* effect (Figure 3.13, Table 3.1), yet it was not the objective of the present work to gain a detailed understanding of this, and in fact, only two of our target vines (Figure 3.6) were located in this area. Similarly, the interaction between topography and early season temperature at the Kingston site (see Figure 3.15 and discussion thereof) is a clear *terroir* effect, and whilst our sampling strategy (Figure 3.12) did canvass this, it did so with arguably too few samples.

Obviously, the weak yield:quality interaction seen in the present study is somewhat in contrast to these previous studies. Figure 3.4 suggests that the area of higher soil EC_a at the Taylors site does have a yield impact; whether it also has a fruit compositional impact is unclear. Meanwhile, one-way analysis of variance coupled with the Tukey-Kramer significance test on target vine data at harvest suggests that, whereas the low-lying part of the Kingston block did yield significantly differently (P<0.05) to the remainder of the block in both 2015 and 2016, the only significant difference (P<0.05) in terms of fruit composition was with respect to juice pH in 2016. In other words, an impact of variation in the land underlying the vineyard on yield, does not always infer a *terroir* impact on fruit composition or quality.

One problem in resolving the yield:quality debate is that, as noted above, many of the commonly used indices of 'quality' are much more appropriately regarded as indices of maturity; total soluble solids, juice pH and TA are certainly in this category, whilst the extent to which anthocyanins and phenolics are robust indicators of fruit quality remains equivocal. Francis et al. (1999) and Gishen et al. (2002) have noted the relationship between juice colour and wine quality and therefore the potential utility of colour as a quality index. On the other hand, anecdotal evidence suggests that many wineries do not routinely use colour assessment to make harvesting decisions or to direct product streaming. The wine sector therefore remains faced with the need for measures of fruit composition that are objective, robust and truly reflective of 'quality'. Arguably, they should also be reasonably independent of measures of maturity given that, as indicated above, for many vineyards, the date of harvest is clearly somewhat arbitrary in the context of yield accumulation (or loss), vine phenology and changes in fruit composition during (and after) the ripening period. One possible solution to this problem, as Trought (2005) has noted, is to assess everything at a constant TSS, but of course, this is not possible in a pragmatic vineyard management sense given that TSS is spatially variable - to which many studies including this one attest. Another possibility is to identify compounds that indicate suitability for particular product streams, as has been done, for example, in the case of some cool climate Shiraz through analysis of rotundone to determine it's 'pepperiness' (Scarlett et al., 2014; Bramley et al., 2017). Interestingly, those studies found that spatial variation in rotundone was unrelated to variation in vine vigour, with soil and topographic variation apparently the main drivers of variation in rotundone concentration. However, since rotundone is known to develop later in the season (unpublished data from Wine Australia project AWR 1701) and is favoured by cool conditions (Zhang et al., 2015a,b), an apparently peppery site might be rendered un-peppery by either warm seasonal conditions or an early harvest. It is also a fact that as rotundone occurs at very low concentrations, its analysis is both complex and expensive, characteristics that do not lend themselves towards rapid analysis and decision making during the stressed vintage season. It appears therefore, that the question of the yield:quality nexus will remain vexed until we can be certain that 'quality' is something that we can measure robustly. Since sensory perceptions of quality vary amongst consumers, even if an analyte or suite of analytes can be identified that are readily analysable, supporting sensory research will be required to guide interpretation of their analysed concentrations. Given also the short-range spatial variation in vine vigour and yield, for progress to be made in properly understanding any nexus between yield and quality, as was argued during the development of this work, it is important that indices of quality can be analysed at the same spatial intensity as is provided by remote or proximal canopy sensing and/or yield monitoring and mapping. Section 5 seeks a solution to this requirement.

This page intentionally blank

4 Calibrating passive remote sensing against active proximal canopy sensing

As described in Section 3, a major intent of this project was to seek to use the Crop Circle™ proximal canopy sensor as a predictor of fruit composition. The work was done on three premises: that variation in vine vigour and yield follows similar patterns – which appears to be the case in most Australian vineyards where this has been investigated (Bramley, 2010, 2019 and references therein); that robust relationships between PCD and fruit composition might be more readily defined from multiple seasons using an active proximal sensor compared to passive remote sensing; and that given a greater adoption of remote sensing compared to yield mapping, the implications of the work might be more readily adopted if it was cast in the context of canopy sensing rather than yield monitoring. We also had the initial view that since imagery is typically only acquired at veraison, but our fruit sampling was planned to be done over the veraison to harvest period (Section 3), we needed a basis for relating canopy condition at sampling to canopy condition at veraison, so that the imagery acquired at veraison could be used as a predictor of fruit composition whenever sampled. In other words, we wished to calibrate the *passive* imagery acquired commercially at veraison, using imagery from an *active* sensor used at the time of sampling. This was thought to be potentially useful given the observation of Trought and Bramley (2011) that the ability of imagery acquired on a single occasion to predict fruit composition throughout the veraison to harvest period was markedly temporally variable. Finally, and irrespective of considerations of fruit quality, since passive remote sensing is much more commonly used than active proximal sensing, it was considered important to explore the potential for calibrating passively sensed imagery with an active sensor.

4.1 Methods and materials

4.1.1 Remotely sensed imagery

In addition to the pre-project imagery described in section 3.2.1, remotely sensed imagery was purchased for both the Taylors (2015, 2016) and Kingston sites (2015 only). These images are presented in Section 3.2.2 (Figures 3.13-3.15). Lamb et al. (2004) established veraison as the optimal time for acquisition of remotely sensed imagery targeted at understanding vineyard variability, leading to the recommendation (Proffitt et al., 2006) that it be acquired within a two week period centred on veraison. The logistics of operating a commercial aircraft over different wine regions in which different varieties are grown, along with the need to acquire imagery in cloud-free conditions, means that service providers can only use a 'best guess' approach to selecting the date on which to fly. In this case, airborne digital multi-spectral video imagery (Specterra Services, Leederville, WA) was acquired at Taylors on 22 January 2015 and 15 January 2016. For Kingston, 2015 imagery was acquired on 16 January; we were unable to obtain imagery in 2016 for the Kingston site as the provider declined to fly the Riverland due to a lack of orders for imagery for other vineyards. All imagery was provided as 'PCD' – the ratio of infrared:red reflectance (see section 3.1.3).

4.1.2 Proximal canopy sensing

Crop Circle sensing was undertaken at Taylors on 16 January 2015 and 14 January 2016 and at Kingston on 15 January 2015 and 18 January 2016. On all of these dates, the sensor was mounted for sensing the canopy from above (Figure 4.1a, b). The filters used for generation of PCD were red (650 nm) and near infrared (NIR; 760 nm). Trought and Bramley (2011) used Crop Circle imagery acquired from the side in a vertically shoot positioned, cane pruned Marlborough (NZ) Sauvignon Blanc vineyard. This imagery was shown to provide essentially the same information about patterns of variation in vine vigour as airborne (i.e. from above) remotely sensed imagery (Bramley et al., 2011d). Here, it was of interest to know whether the same was true when this sensor was used in more sprawled Australian conditions. Accordingly, we also scanned the Taylors vineyard in 2015 from the side (Figure 4.1c). Alternate rows were scanned and in the case of the side-mounted scanning, the equipment was adjusted at the end of each row to ensure that the same side of the row was scanned irrespective of the direction of travel. The Kingston site was considered too sprawled for scanning from the side to be feasible given previous experience with a different canopy sensor trialled in a Murray Valley vineyard (Bramley et al., 2007) in which variation in the distance between the sensor and target, along with actual interference of the target (long sprawling canes) with the sensor conspired against its utility. In the present work, the sensor was mounted in such a way that the distance between the sensor and canopy (~40 cm) was as constant as possible, and appropriate to the sensor field of view.

As explained in section 3.1.3, vine sampling was undertaken at approximately weekly intervals during the veraison to harvest period. On each sampling occasion, the sampled transects (Figures 3.6 and 3.12) were re-scanned with the Crop Circle sensor using the 'above canopy' configuration (Figure 4.1a,b) at a speed of approximately 8 km/h and no greater than 11 km/h. Since the Crop Circle logs data at 1 Hz, this generated PCD data at intervals of approximately 2.2 m.

4.1.3 Image interpolation and spatial and statistical analysis

Interpolation of Crop Circle PCD data followed a similar procedure to that employed for yield mapping or EM38 mapping (Section 3.1.5); that is, local block kriging using VESPER (Minasny et al., 2005), with exponential variograms, a data cloud of 100 points and blocks of 10 m. Images were interpolated onto a 2 m raster grid as per standard practice in our PV research.

Commercially acquired airborne imagery was provided at 40 cm resolution. To enable overlay with other data (e.g. yield maps, high resolution soil survey – see Figure 3.5), the imagery needed to be re-projected to the same 2 m grid as used for other data layers. This was done using the focal statistics function available in the ArcGIS software suite (v10.4.1; ESRI, Redlands, CA, USA). To examine relationships between Crop Circle and airborne imagery, different approaches were explored. In the first, the trace of the Crop Circle proximal sensor (n = 4609 points) was used as a template for extracting values from the Airborne image (smoothed to 2 m) and the airborne data regressed against the Crop Circle point data. In the second, the airborne data (smoothed to 2 m) were regressed against the interpolated Crop Circle data at 50 randomly selected points; that is, values were extracted from 50 randomly selected pixels in the 2 m raster. In the third, and in order to remove any effects of smoothing, values were extracted from the 40 cm airborne image at locations corresponding to the

a.



b.



c.



Figure 4.1 Configuration of the Crop Circle™ sensor when mounted to sense the canopy either from above (a) at Kingston and (b) at Taylors, or (c) from the side at Taylors.

trace of where Crop Circle data were collected. These were then kriged (see above). Finally, values of kriged Crop Circle and airborne Imagery were extracted from locations corresponding to the Crop Circle trace and regressed against each other. In all cases, PCD data were used.

To calibrate the airborne imagery against the Crop Circle data collected from the sampling transects, the locations of the target vines sampled on the particular sampling occasion were used as the basis for the calibrations. Mean PCD values were extracted from a 3 x 3 array of 2 m pixels in the remotely sensed image, centred on these locations. These were then regressed against the mean Crop Circle values collected from within 5 m of the target vine. This approach was used to accommodate positional errors in both the remote and proximally sensed data and while it means that the PCD are not specific to the individual target vines, as can be clearly seen in all the imagery acquired during this project, adjacent vines tend to express very similar PCD values.

Regressions between remote and proximally sensed data were undertaken in JMP (v.11.0.0, SAS Institute, Cary, NC, USA) as before with other elements of spatial and statistical analysis and map display as described in Section 3.1.5.

4.2 Results and discussion

Patterns of variation in the Crop Circle data when sensed from above the canopy were very similar to those seen in the pre-project remotely sensed imagery acquired at veraison during the seven seasons prior to the project (Figure 4.2). However, using the Crop Circle from the side led to somewhat noisier data and while the image obtained from the side contained many similar features to that obtained from above, either remotely or proximally, a number of artefacts were apparent, especially along the northern edge of the block; the reasons for these remain unclear. Even when the data from the two northernmost rows are excluded from the image interpolation, the Crop Circle image from the side remained somewhat different to that from above (Figure 4.2). It is inferred that this is due to the impact of the loosely sprawled canopy on the distance between the sensor and the canopy which, as a consequence, is more variable from the side (Figure 4.1c) than when the sensor is mounted above the canopy (Figure 4.1a,b). Thus, whereas Bramley et al. (2011d) showed Crop Circle imagery from the side to be essentially the same as remotely sensed imagery in a tightly confined VSP canopy in Marlborough, NZ, even in fairly small canopies such as at Taylors, a modest degree of sprawl clearly mitigates against the quality of images obtained. For this reason, we have henceforth only used Crop Circle canopy sensing in vineyards with the sensor mounted above the canopy – which intuitively should lead to a more similar view of the vine to that reflected in airborne remotely sensed imagery.

As noted in section 3.2.2 (see also Figure 3.13), patterns of variation in the remote and proximally sensed PCD imagery obtained at veraison in 2015 were very similar. However, the relationship between the airborne and Crop Circle point data was noisy (Figure 4.3, bottom left graph; R^2_{adj} = 0.44) when the trace of the Crop Circle proximal sensor (n = 4609 points) was used as a template for extracting values from the airborne image (smoothed to 2 m). When values were extracted from both the smoothed airborne image and the interpolated Crop Circle image at 50 randomly chosen locations, the relationship between the remote and proximal data was much tighter (Figure 4.3, bottom centre graph; R^2_{adj} = 0.72). This result reflects the benefit of interpolation in removing noise from the raw Crop Circle dataset. Thus, when a 'new' remotely sensed image (Figure 4.3, right hand map, middle

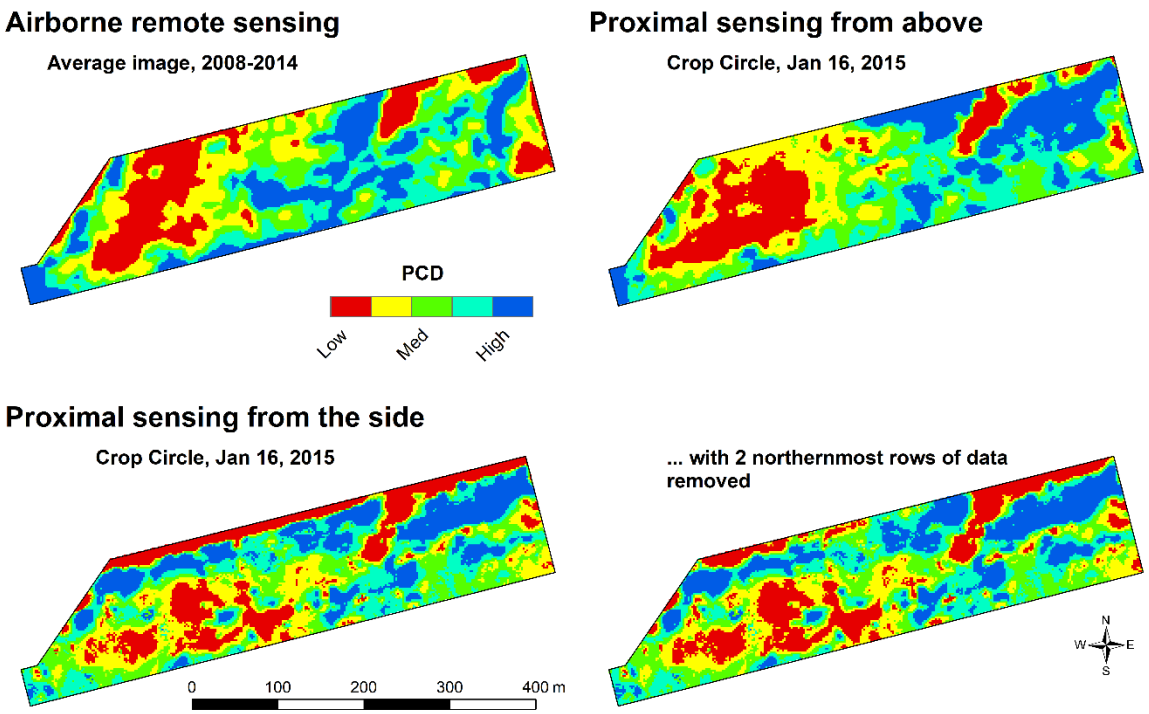


Figure 4.2 Comparison between Crop Circle imagery collected either from above or to the side of the canopy, with pre-project remotely sensed imagery at Taylors. In all maps, the PCD data have been classified on the basis of 20th percentiles.

row) was generated by kriging PCD values extracted from the raw 40 cm image at locations corresponding to the Crop Circle trace (Figure 4.3, centre map, top row), the relationship was tighter still (Figure 4.3, bottom right graph; R^2_{adj} = 0.76). Note that the use of adjusted R^2 values accommodates the effects of different numbers of samples used in these regressions. The conclusions to be drawn from Figure 4.3 however, are that the remote and proximally sensed imagery are indeed similar – as they ought to be – and that, the kind of approaches used here provide an appropriate way of calibrating passive airborne imagery against proximally sensed imagery obtained using an active sensor.

Linear regressions, analogous to that seen in the bottom centre graph in Figure 4.3, but based on the 30 target vines sampled on each sampling occasion when transects of Crop Circle data were also collected, enabled re-calibration of the remotely sensed imagery obtained at veraison, to canopy vigour (i.e. PCD) as measured using the Crop Circle through the veraison to harvest period (Figure 4.4). Note the use of common legends in Figure 4.4 based on the 20th percentile classification of either the 40 cm remotely sensed imagery (top left) or the Crop Circle image obtained at veraison. Because each image post veraison is essentially a linear transformation of that obtained at veraison, the result is a series of maps that reflect the de-vigouration of the canopy due to drying over the veraison to harvest period; re-classification of any of these maps in Figure 4.4 on the basis of 20th percentiles simply results in a map that looks like the top centre map, reflecting that each map is indeed simply a linear transformation of the veraison image. Although generally interesting, we did not consider this valuable in relation to the use of Crop Circle as a predictor of fruit compositional change during the

veraison to harvest period, and in light of the results reported in Section 3, we did not pursue this avenue of calibration work further.

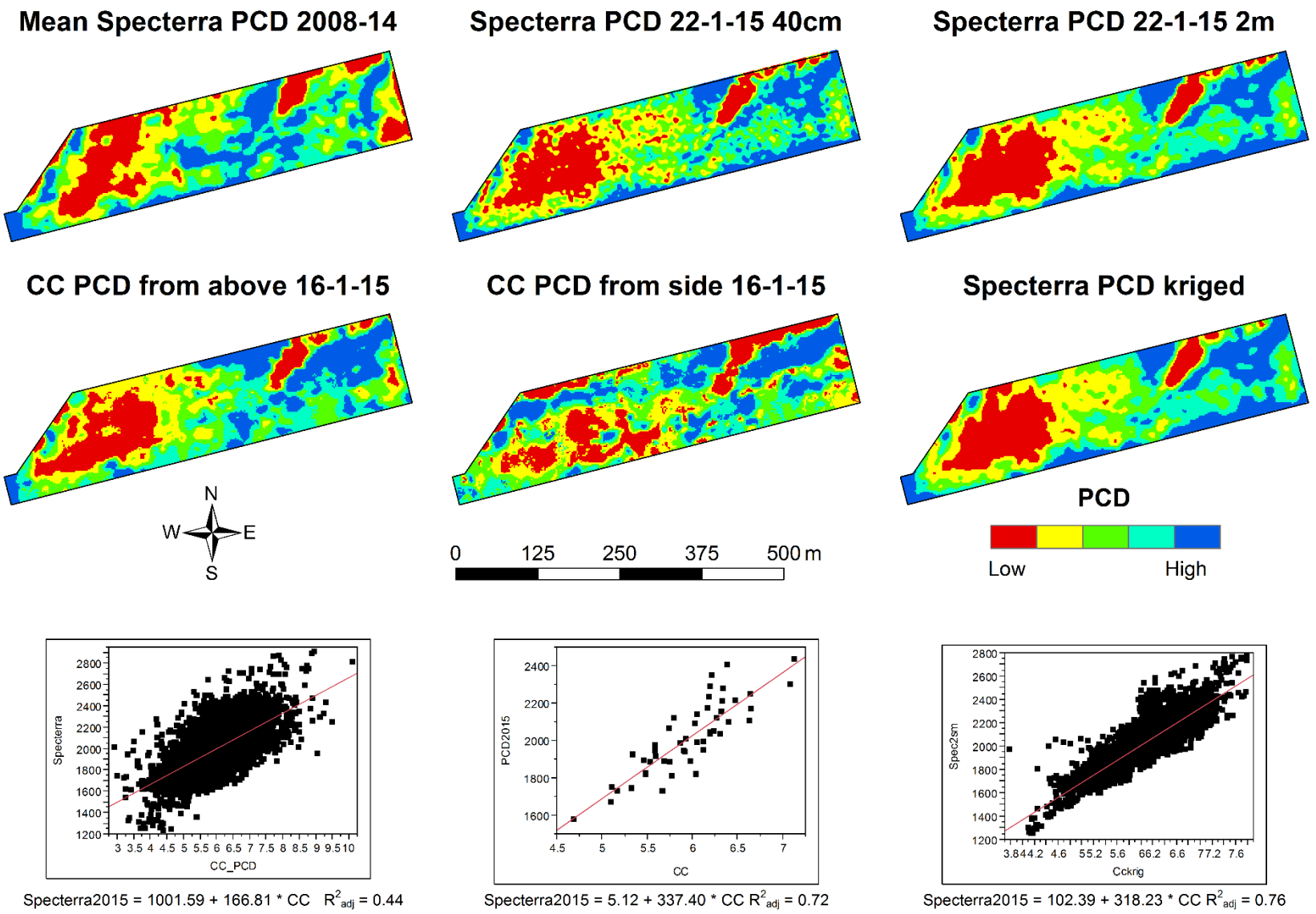


Figure 4.3 Relating proximally and remotely sensed imagery at Taylors. See text for further explanation.

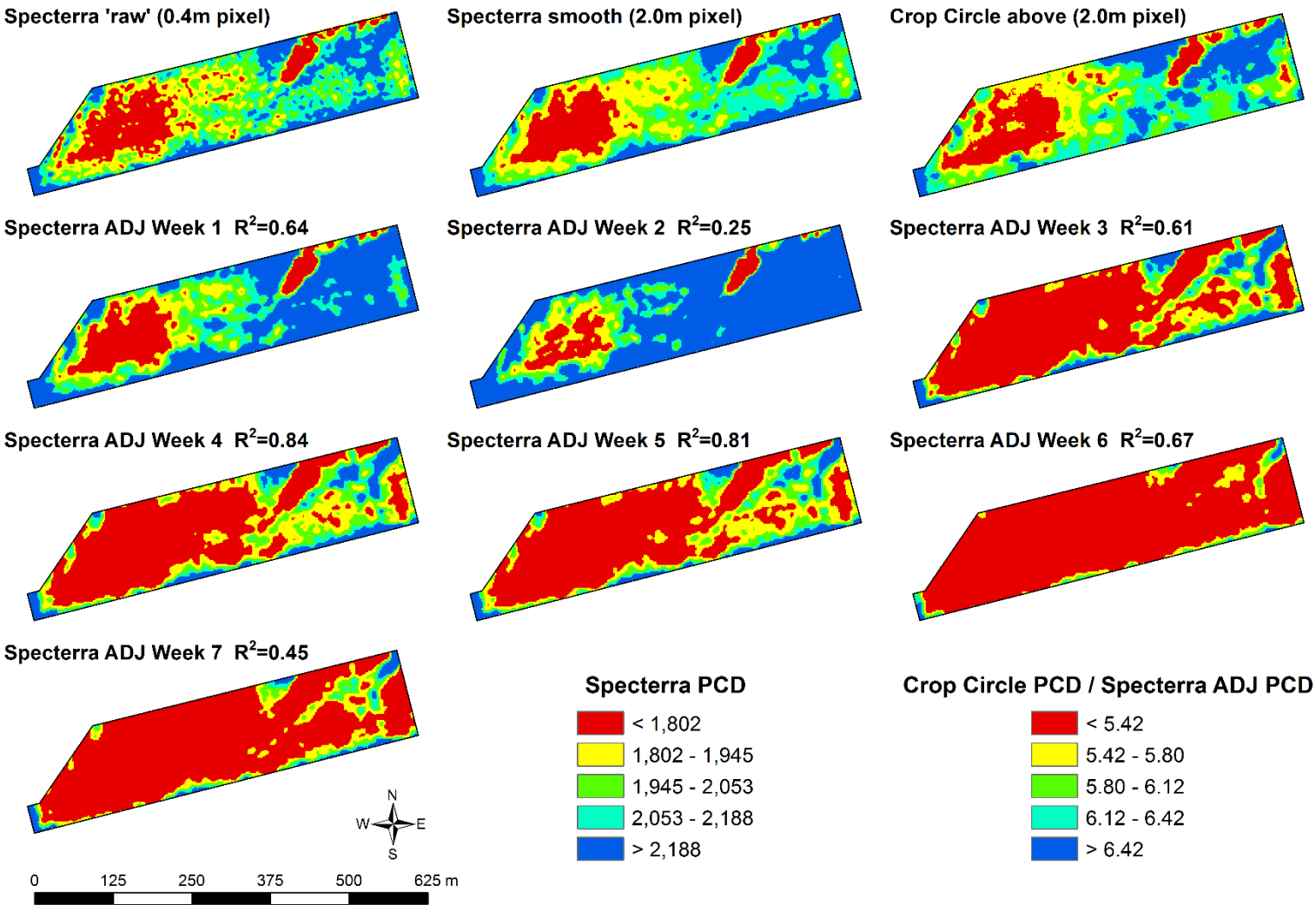


Figure 4.4 Adjusting remotely sensed imagery acquired at veraison, to measurements made using an active sensor in the veraison to harvest period at Taylors. See text for further explanation.

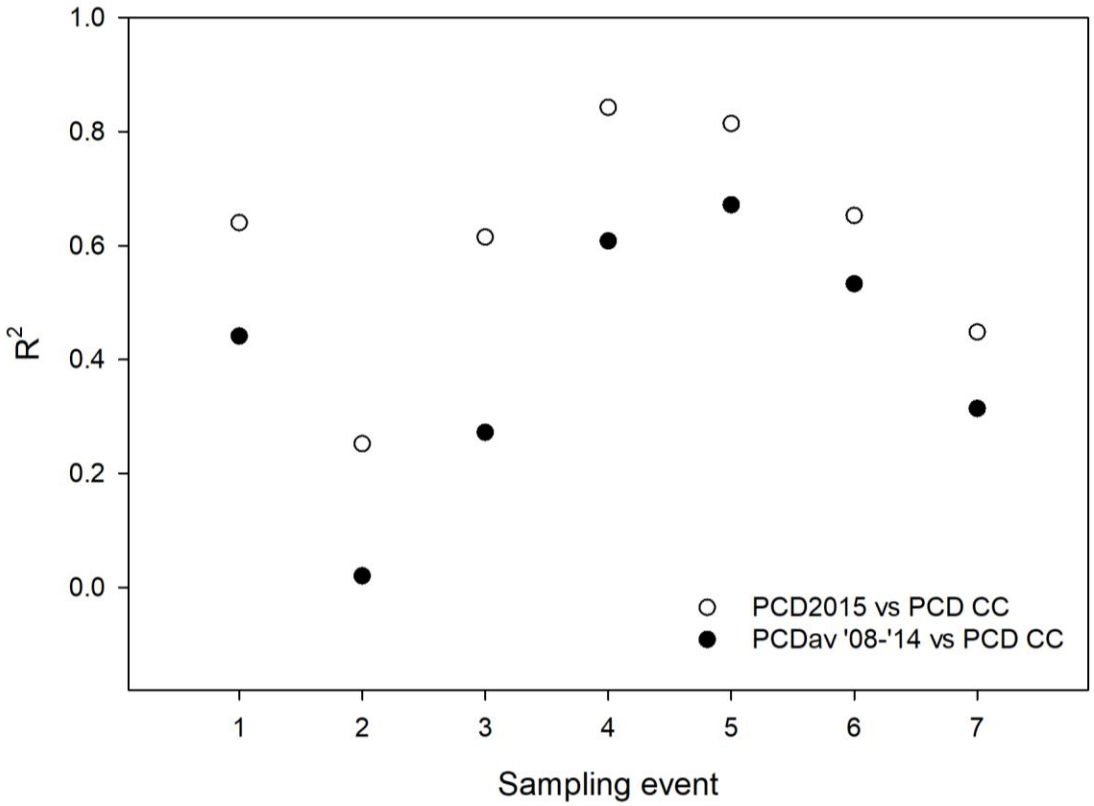


Figure 4.5 Variation in the strength of the relationship (linear regression) between proximally sensed PCD (PCD CC) during the veraison to harvest period at Taylors in 2015 and remotely sensed imagery obtained either at veraison in 2015 (PCD2015) or over a seven year period pre-project (PCDav '08-'14).

It is, however, interesting to note the marked impact of drying between weeks 2 and 3 in what was a dry 2015 season. Also of interest is the change in the strength of the regression relationship between Crop Circle and remotely sensed PCD (Figure 4.5). As with the time series of changes in berry and bunch mass in the veraison to harvest period (Figure 3.21) there is clearly a point in the ripening season when the inter-relationships between various vine physiological measures break down. Again, this suggests that possible confusion over the existence of a yield:quality nexus is due to a reliance on data collected at harvest which, the present study suggests, may be far from optimal.

Finally, and notwithstanding that we did not consider Figure 4.4 to be useful in the context of the overall project objectives, an obvious reason to use an active sensor to calibrate data collected using passive remote sensing, is to enable comparison between seasons. Regression relationships were derived between the Crop Circle (CC) and remotely sensed (RS) PCD data collected at veraison:

2015: $PCD_{RS} = -1.445 + 333.926\ PCD_{CC}$ $R^2_{adj} = 0.92$

2016: $PCD_{RS} = 610.832 + 127.711\ PCD_{CC}$ $R^2_{adj} = 0.41$

These equations were then used to generate 'calibrated' PCD images (PCD_{cal}) based on the airborne data (Figure 4.6). The extent to which such an adjustment is useful probably requires data from more

than two seasons. Here, it is evident that, presumably due to the dry conditions, vine vigour at veraison, as measured using PCD, was substantially reduced in 2016 compared to 2015. This is consistent with the observations of vineyard management.

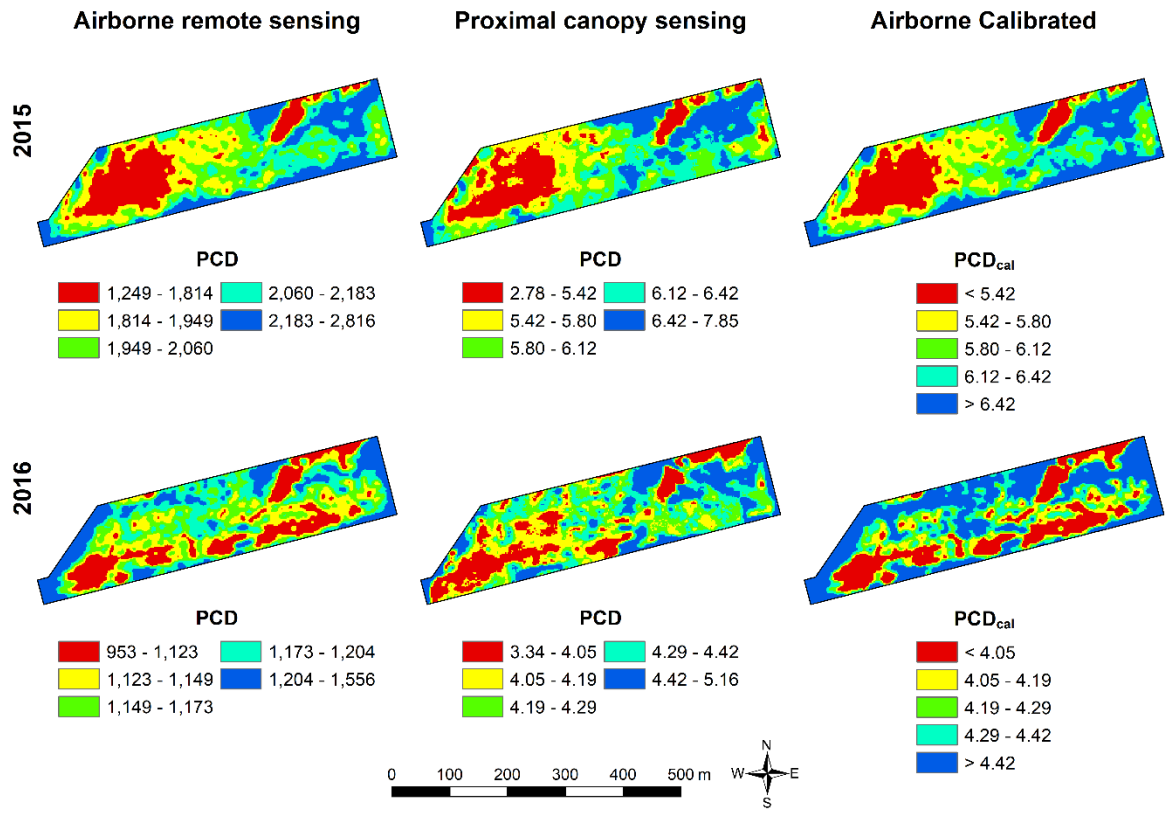


Figure 4.6 Calibration of airborne remotely sensed imagery using an active proximal sensor (Crop Circle). Here, the airborne and proximal images (left and centre column of maps) are the same as those shown in Figure 3.14 and have been classified on the basis of 20th percentiles. The derivation of the calibrated images (right hand column) is explained in the text; these use the same classification as for the proximally sensed maps. Note that if the 2016 map were classified using the 2015 values, almost the entire map would be red, highlighting the effect of the dry 2015 and 2016 seasons on vine vigour in 2016.

This page intentionally blank

5. Towards an on-the-go fruit quality sensing capability

An essential premise of this project was that, in order to better understand the yield:quality nexus, it needed to be explored at fine scale using the tools of precision viticulture (PV) to provide information at high spatial density and resolution rather than rely on data collected on a whole block, vineyard or regional basis. A yield monitor logs data at 1 Hz and the data are then thinned to a 3 second equivalent (Bramley and Williams, 2001) for yield map interpolation; as noted in section 4, commercially available airborne remote sensing typically has a resolution of 40-50 cm. So to enable examination of the yield:quality nexus at the scale that we intended, fruit quality or compositional data were required to be collected at a similar spatial intensity.

5.1 Initial work using the Multiplex™ sensor

Bramley et al. (2011a) were able to install a minimally modified version of the hand-held Multiplex™ sensor (Force-A, Paris, France) on a harvester at Taylors Wines and successfully used this to log anthocyanins on-the-go during harvest. This work led to the commercialisation of an on-the-go variant of the Multiplex and our intention was to use this sensor in the present project via ongoing collaboration with Force-A.

Multiplex is a fluorescence-based sensor in which light is shone onto the target and the resultant 'excitation' of the target is measured in terms of the amount of reflected fluorescent light at a range of wavelengths; further details are provided by Bramley et al. (2011a), Cerovic et al., (2008) and Ben Ghozlen et al. (2008a,b). Two key indices may be generated which have been shown to correlate well with anthocyanins, both derived from measures of far-red fluorescence (FRF) following excitation with red, green or blue (R,G,B) light – the $Anth_{RG}$ index and FERARI. $Anth_{RG}$, calculated as $\log(FRF_R/FRF_G)$, provides one measure of anthocyanin content in mature berries, with high values of $Anth_{RG}$ indicating low anthocyanin concentrations and low values of $Anth_{RG}$ indicating high concentrations (Cerovic et al. 2008, Ben Ghozlen et al. 2010a,b). Because $Anth_{RG}$ is calculated as a ratio, it is thought to be immune from the effects of varying distances between the sample and the sensor, which, for any given measurement, are the same for both FRF_G and FRF_R. $Anth_{RG}$ is therefore considered appropriate for operation of Multiplex in the field, for which the sensor is held close to a target bunch when a reading is taken. Of course, sample–sensor distances may vary between samples, while the size and tightness of bunches also varies such that differing proportions of the sensor field of view may be occupied by berries, rachis, leaves or even canes. Leaves need to be avoided otherwise the measurement of berry anthocyanins is corrupted by unscreened chlorophyll fluorescence of leaves. The FERARI index (Ben Ghozlen et al. 2010a), is calculated as $\log(5000/FRF_R)$. Because this index derives from FRF_R alone, it is subject to variation in the sample–sensor distance, bunch tightness, etc. (Ben Ghozlen et al. 2010b).

During the first year of this project, an on-the-go version of the Multiplex was installed at both the Taylors and Kingston sites (Figure 5.1). However, its use was not sufficiently successful for us to be able to have confidence in the results obtained, especially in terms of the consistency of the results obtained for $Anth_{RG}$ and FERARI. At Taylors in 2015 the map of $Anth_{RG}$ (Figure 5.2a) showed similar spatial patterns to variation in yield and vine vigour (Figure 3.13) and in particular reflected the area of high soil EC_a (Figure 3.3). However, there was no similarity between the maps for $Anth_{RG}$ and FERARI

a.



b.



c.



Figure 5.1 The on-the-go Multiplex sensor (a) installed on a Gregoire harvester at Taylors Wines, and in operation at (b) Taylors Wines and (c) Kingston Estate.

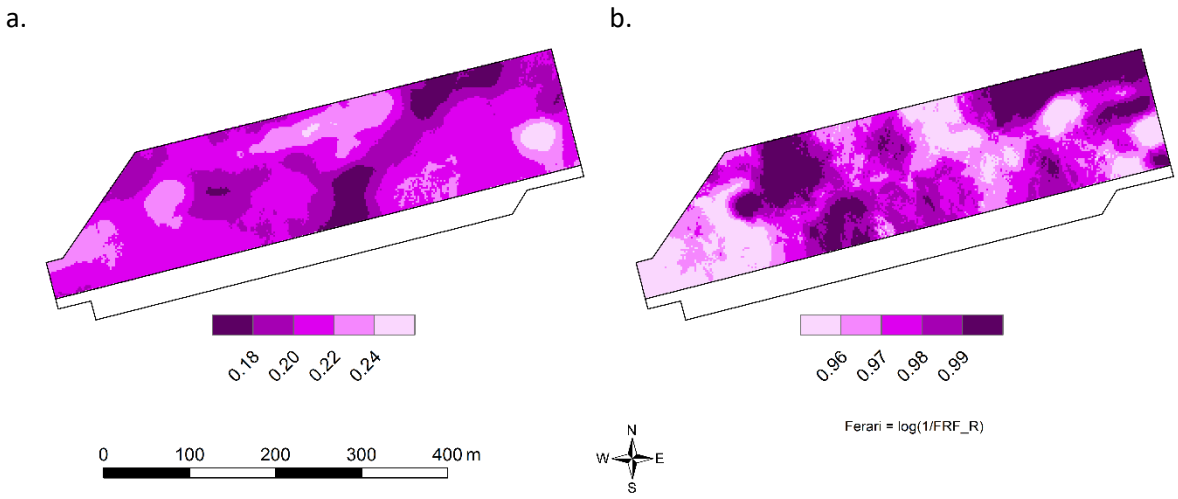


Figure 5.2 Variation in the (a) $Anth_{RG}$ and (b) FERARI indices of grape anthocyanins at Taylors as measured using an on-the-go Multiplex sensor (Figure 5.1a,b), vintage 2015.

(Figure 5.2b) which is what would be expected if the sensor was working well and assuming no effect on FERARI of variation in the sample-sensor distance. Likewise, there was no similarity between the yield map and the FERARI map, which is what would be expected assuming that the depth of fruit on the discharge belt can be treated as a surrogate for yield. In contrast, at Kingston in 2015, there was no apparent similarity between the $Anth_{RG}$ map (Figure 5.3a) and any other Kingston data layer (see section 3) whilst the FERARI map (Figure 5.3b) bore a strong resemblance to the yield map; in other words, in this instance, FERARI was essentially a surrogate for yield, given the interfering effect of the depth of fruit on the harvester discharge belt and its impact on the sensor-sample distance. It was also a fact that in generating the maps shown in Figures 5.2 and 5.3, we were concerned at the high proportion (generally > 70%) of sensor data collected that was discarded in the data cleaning and filtering process recommended by Force-A. In the end, it was agreed that the sensor we used may have been subject to interference from ambient UV as was the case with our initial foray into the use of Multiplex in hand-held mode (Bramley et al., 2011a).

Regrettably, it was not possible for Force-A to reconfigure the on-the-go sensor in readiness for vintage 2016 and as a result, and simply as a means of acquiring some project-useful data, we reverted to the hand-held version of the sensor. At Taylors, for vintage 2016, we used a sampling strategy based on a grid comprising every 12th vine in every fifth row, modified to enable generation of a robust variogram by the random omission of some grid nodes and re-inserting these at vines located adjacent to existing grid nodes (Bramley 2005). The resulting map of $Anth_{RG}$ and its conversion to a measure of anthocyanins per unit berry surface area (Anth_a (Cerovic et al., 2014); Figure 5.4) again showed a pattern of variation in berry anthocyanins similar to the patterns of variation in this vineyard seen in maps of other attributes (Figures 3.3 and 3.13) with the patterns of variation in these indices being stable in the period leading to vintage. However, the FERARI map (Figure 5.5) bore no resemblance to these, even when great care was used to ensure a constant sensor-sample distance.

At Kingston in 2016, the size of the vineyard meant that only a subsection of the vineyard could be surveyed with the hand-held Multiplex. Nonetheless, neither the Anth_a nor $Anth_{RG}$ maps in the approximately 4.25 ha area surveyed showed any spatial variation, whilst the FERARI map bore no resemblance to other data layers (Figure 5.6). In this instance, we concluded that interference from

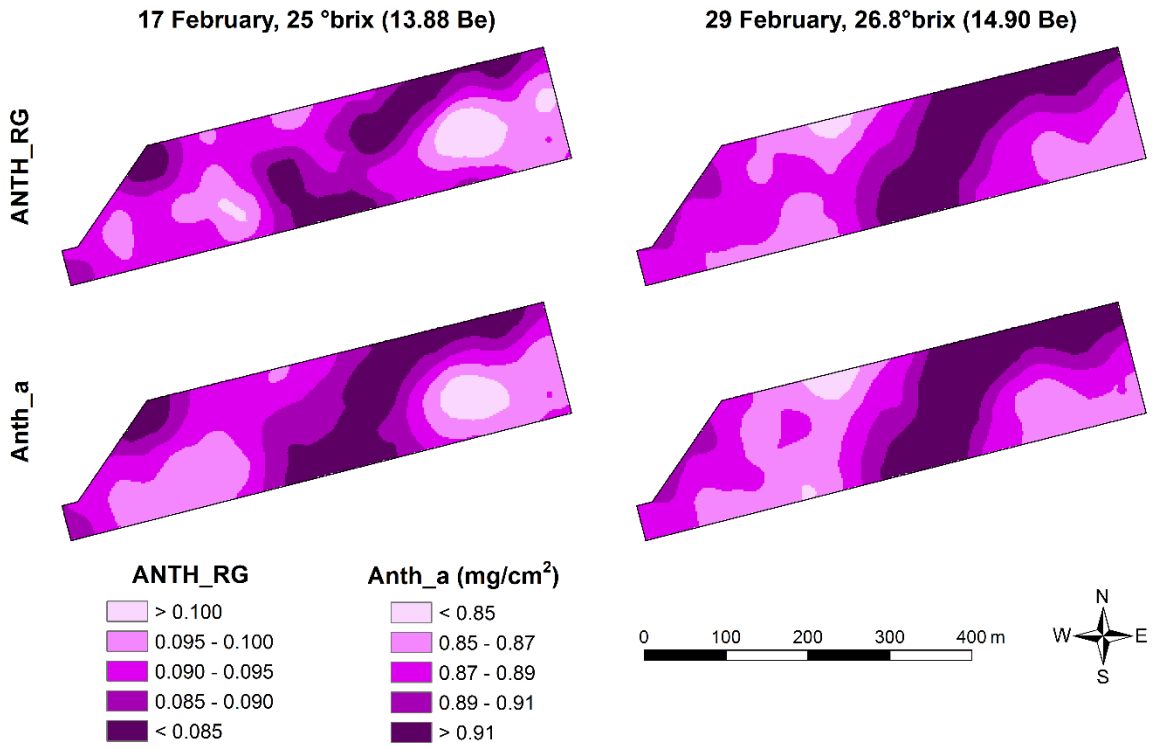


Figure 5.4 Variation in the $Anth_{RG}$ and Anth_a indices assessed using measurements made on 266 vines using a hand-held Multiplex in 2016. Note that this block was harvested on 1 March and these maps therefore represent anthocyanin status one (right hand column) and 13 (left hand column) days prior to harvest.

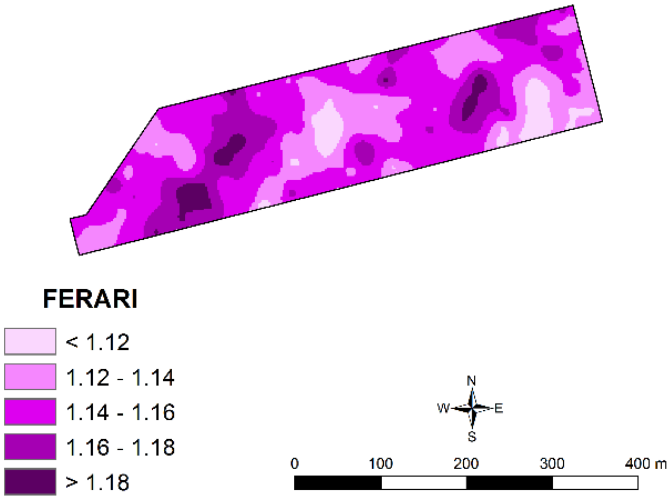


Figure 5.5 Variation in the FERARI index assessed using measurements made on 266 vines using a hand-held Multiplex, one day prior to harvest in 2016.

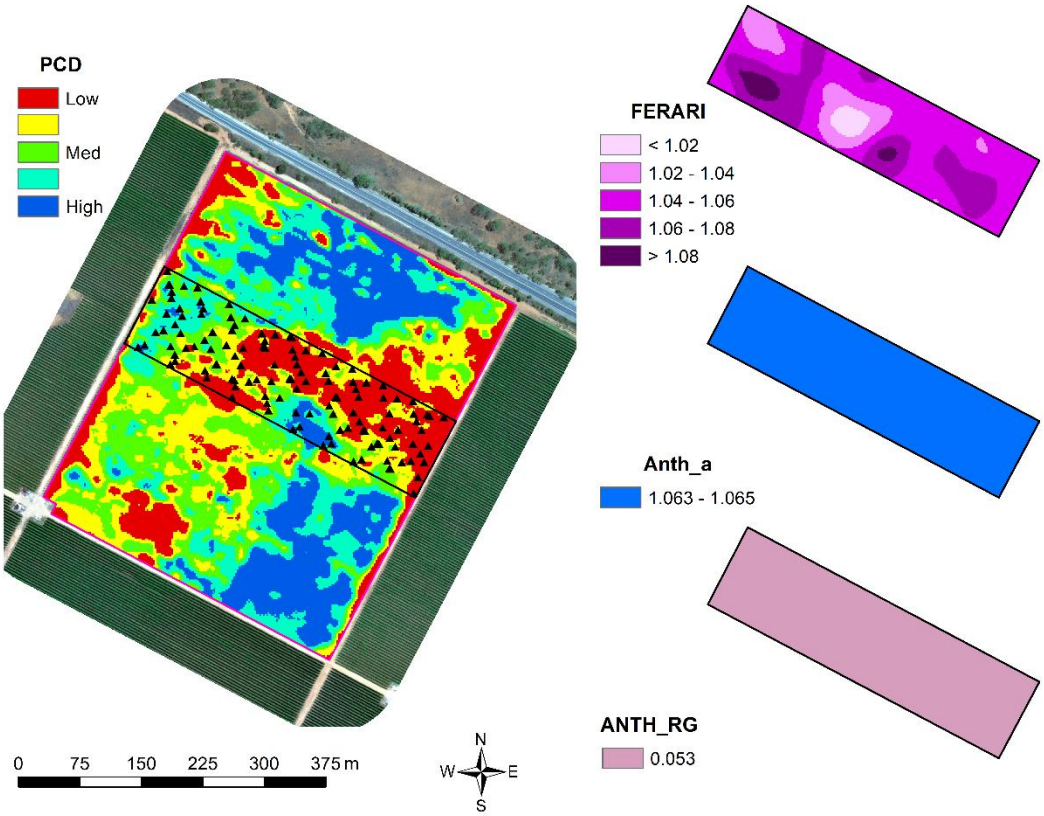


Figure 5.6 Variation in the apparent content of anthocyanins in a 4.25 ha area within the Kingston site measured using a hand-held Multiplex sensor, vintage 2016. Also shown is the 2016 Crop Circle image and the locations of the 132 vines that were sampled for this analysis.

leaves (see above) was a major constraint given that at Kingston, the minimally pruned, high yielding production system, results in vigorous canopies with large numbers of small bunches that are not arranged in a readily discernible fruiting zone. Many bunches were not large enough to properly fill the sensor field of view.

Overall, and with some reluctance given the effort expended, and recognising that our analysis was limited to assessment of anthocyanins, we decided to abandon use of the Multiplex for fruit quality assessment. Instead, and given progress made in the laboratory analysis of grapes and wine using NIR sensing (Cozzolino et al., 2006; Dambergs et al., 2014), we decided to pursue the opportunity for an NIR-based on-the-go fruit quality sensing option.

5.1 Methods and materials

5.1.1 Site details

The decision to move away from the Multiplex coincided with severe frost and hail damage to approximately one third of the Kingston site in October and November 2016 respectively. At around the same time, it emerged that the Taylors site had been severely impacted by herbicide damage. Accordingly, for this work, two new vineyard blocks were used. The first was a different block at

Taylors – close to the previous one, but unaffected by spray damage. This block was also planted to Shiraz on own roots in 2005 with row and vine spacings of 3.3 and 1.8 m. The block is divided into two sub-blocks, with the first (3.65 ha) planted to clone BVRC on own roots; the second (4.01 ha) is planted to clone 1654 on 110 Richter rootstock. The management of the two sub-blocks is otherwise the same, with 'finger and thumb' pruning to 60 buds per vine, a permanent cordon and a ballerina canopy in which half of the shoots are allowed to sprawl and the other half are vertically positioned by permanent foliage wires. This site overlays deeper alluvial soils compared to the Taylors site used in the previous work (sections 3 and 4), a result of which being that the canopy tends to be larger and so requires approximately 0.9 ML ha^{-1} irrigation water annually.

The second site was also a block of Shiraz, in this case at The Lane Vineyard in the Adelaide Hills; this block (3.21 ha excluding headlands) is also being used in project AWR 1602 for Wine Australia-funded research into rotundone. Row and vine spacings are 2.7 and 2.0 m respectively. This block is also divided into two sub-blocks planted to different clones, both on own roots; 2626 (1.65 ha) and 1127 (1.56 ha). In contrast to the Taylors site, this vineyard at The Lane is cane pruned with a vertically shoot-positioned canopy. The block receives supplementary irrigation as required with a maximum annual application of approximately 0.5 ML ha^{-1}. Crop thinning to a target yield of around 6-7.5 t ha^{-1} is used in most years and the block is mechanically harvested, albeit by a harvester not fitted with a yield monitor.

5.1.2 Pre-project data

A similar array of information was available for the Taylors site as for the block used for the other elements of the work (see sections 3 and 4) – remotely sensed imagery, previous yield maps, etc. For reasons of expediency and in light of the results reported in Figures 3.3, 3.5 and 3.13, we focussed on the remotely sensed imagery for characterising the variability of the vineyard including that acquired at veraison in 2017 (Figure 5.7). In contrast, The Lane had no prior engagement in PV or the acquisition of related data and so our sampling strategy was solely reliant on imagery purchased at veraison 2017 (Figure 5.8).

5.1.3 Vine sampling and NIR sensing

At The Lane, we used the target vine sampling strategy being used for AWR 1602. Thus, 140 target vines were identified for NIR sensing (see below; Figure 5.8). These were the same vines sampled for rotundone analysis in AWR 1602. In addition, 24 vines located on two transects as indicated in the legend to Figure 5.8 were used for bunch sampling for the purposes of calibration of the NIR sensor (see below). These 24 vines were located one vine to the north of those used for the rotundone work to avoid removal of fruit required for rotundone analysis. Sampling of these vines (five bunches per vine) along with NIR sensing of the sampled bunches and the other target vines (see below) took place 1-3 days prior to harvest in both 2017 and 2018.

At Taylors, clustering of the pre-project imagery (Figure 5.7) enabled identification of two transects, one in each sub-block and 30 sampling locations that covered the range of vineyard variation (Figure 5.9).

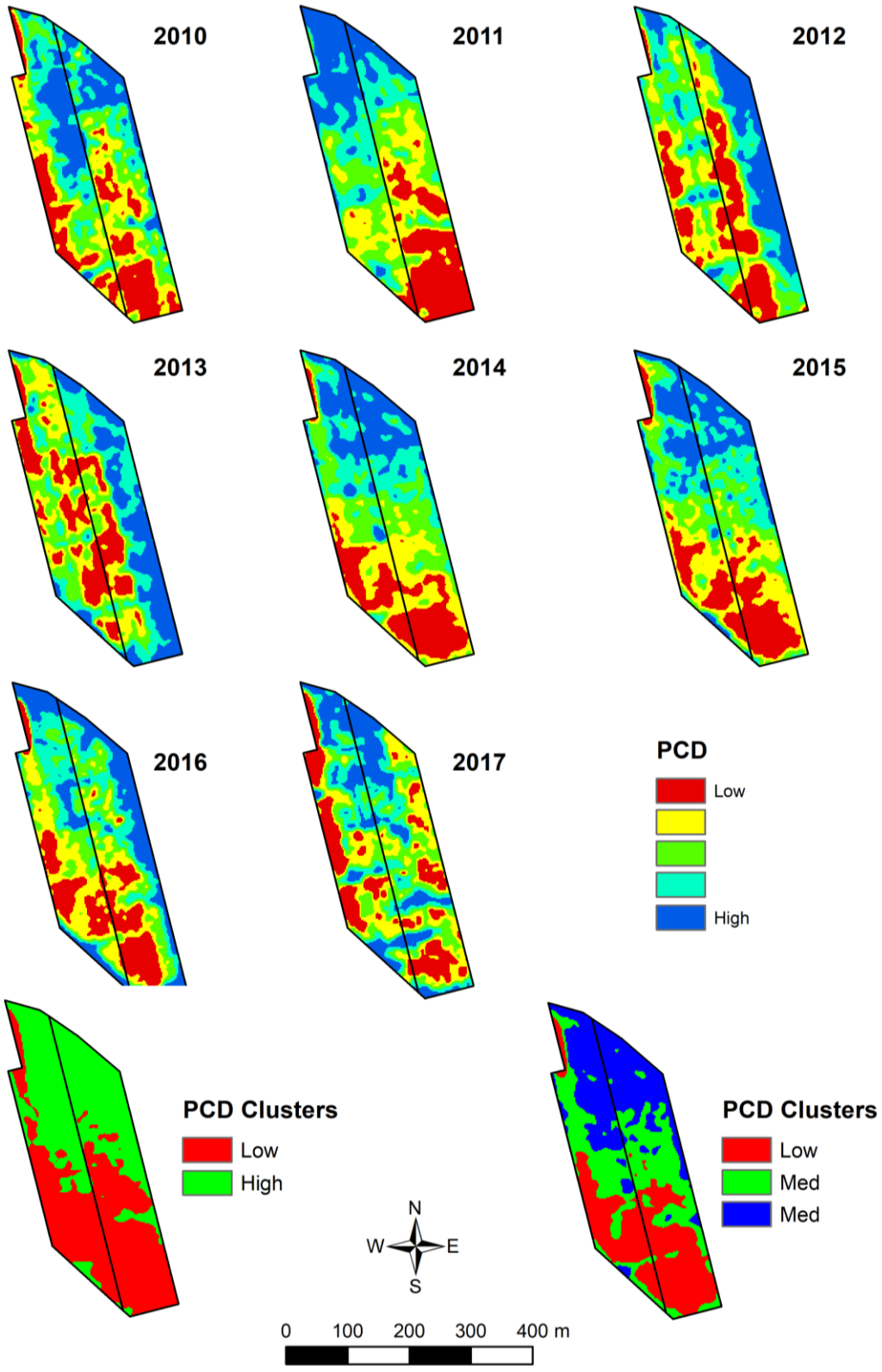


Figure 5.7 Remotely sensed PCD imagery of the Taylors site used for development of an NIR grape sensing capability, acquired at veraison in the 2010-2017 vintage seasons. Also shown are the results of clustering the images using *k*-means; two and three cluster solutions are shown. Note that the imagery from 2012 and 2013 was excluded from this cluster analysis due to the residual effects of a trial conducted in 2012 on the eastern boundary.

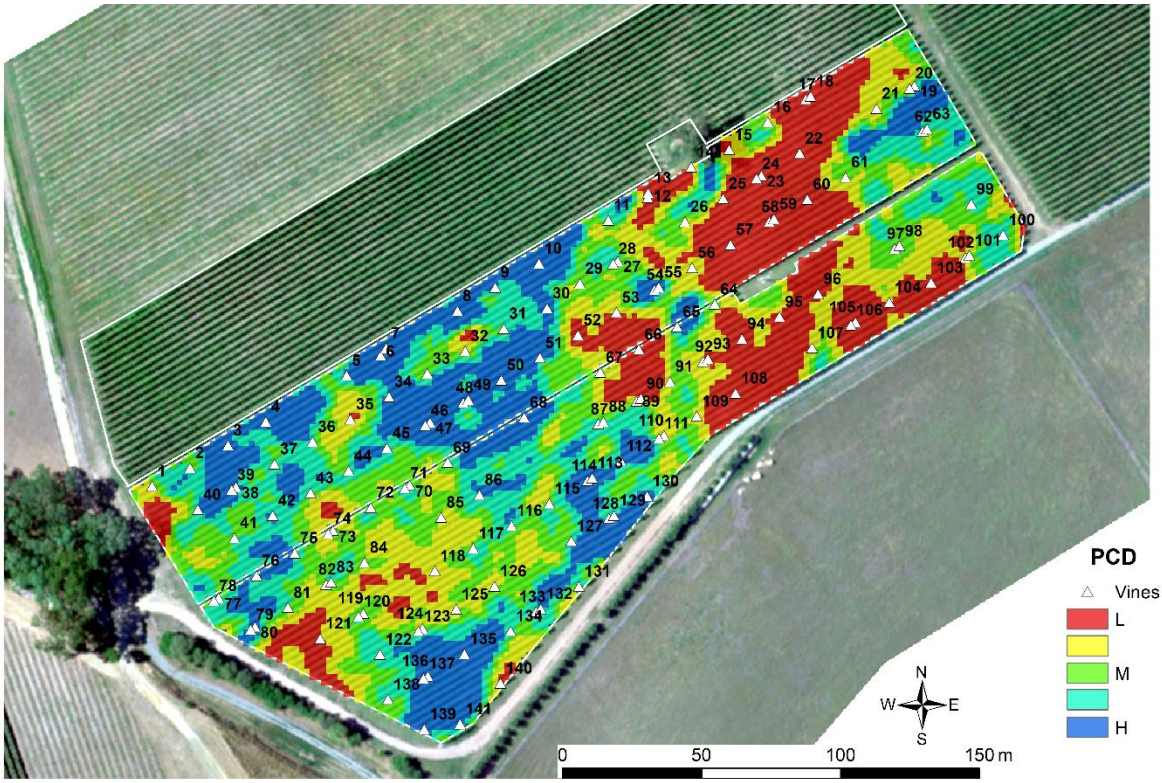


Figure 5.8 Remotely sensed PCD imagery of The Lane site acquired at veraison in 2017. Also shown are the locations are the target vines used for NIR sensing. Sample sites used for sensor calibration lay in two transects running between vines 41 and 63 and vines 79 and 99; a sub-sample of 24 of these target vines were used for calibration.

In addition to the 30 sampling locations used for sensor calibration, a further 185 vines were scanned with the NIR, giving a total of 215 vines used for NIR sensing. For vintage 2017, we used an SVC HR-768si field portable spectroradiometer (Spectravista Corporation, Poughkeepsie, NY, USA; https://www.spectravista.com) which scans between 350-1900 nm in nominal bandwidths of 1.5 nm from 350-1000 nm and 3.8 nm from 1000-1900nm over 768 channels; in effect, this means that the full spectral range (350-1900nm) is scanned in two halves – 350-1000 nm and 1000-1900 nm. This instrument (ca. $65,000) was obtained through CSIRO CAPEX funds. We used this SVC instrument – which is non-contact - fitted with a fibre optic probe (Figure 5.10a) to enable scanning of bunches on the vine with the instrument stationed on our field vehicle (Figure 5.10b), with spectra logged to a portable laptop computer (Figure 5.10c) through which locations were also logged via dGPS (Figure 5.10b). Initial commissioning and testing of this equipment quickly indicated that an external light source was also required to reduce the effects of variable ambient light and to ensure that NIR reflectance was of sufficient measurable strength (Figure 5.10a). At each target vine, three randomly-chosen bunches were scanned; in general, one of these was close to the trunk and the other two were either side of the trunk, but within 1 m of it. For the vines used for calibration, five bunches were sampled for laboratory analysis and all of these were also scanned in the field using the NIR sensor.

In 2018, in addition to scanning all target vines with the SVC instrument, they were also scanned with an STS-NIR miniature spectrometer (Ocean Optics, Largo, FL, USA; https://oceanoptics.com/; Figure

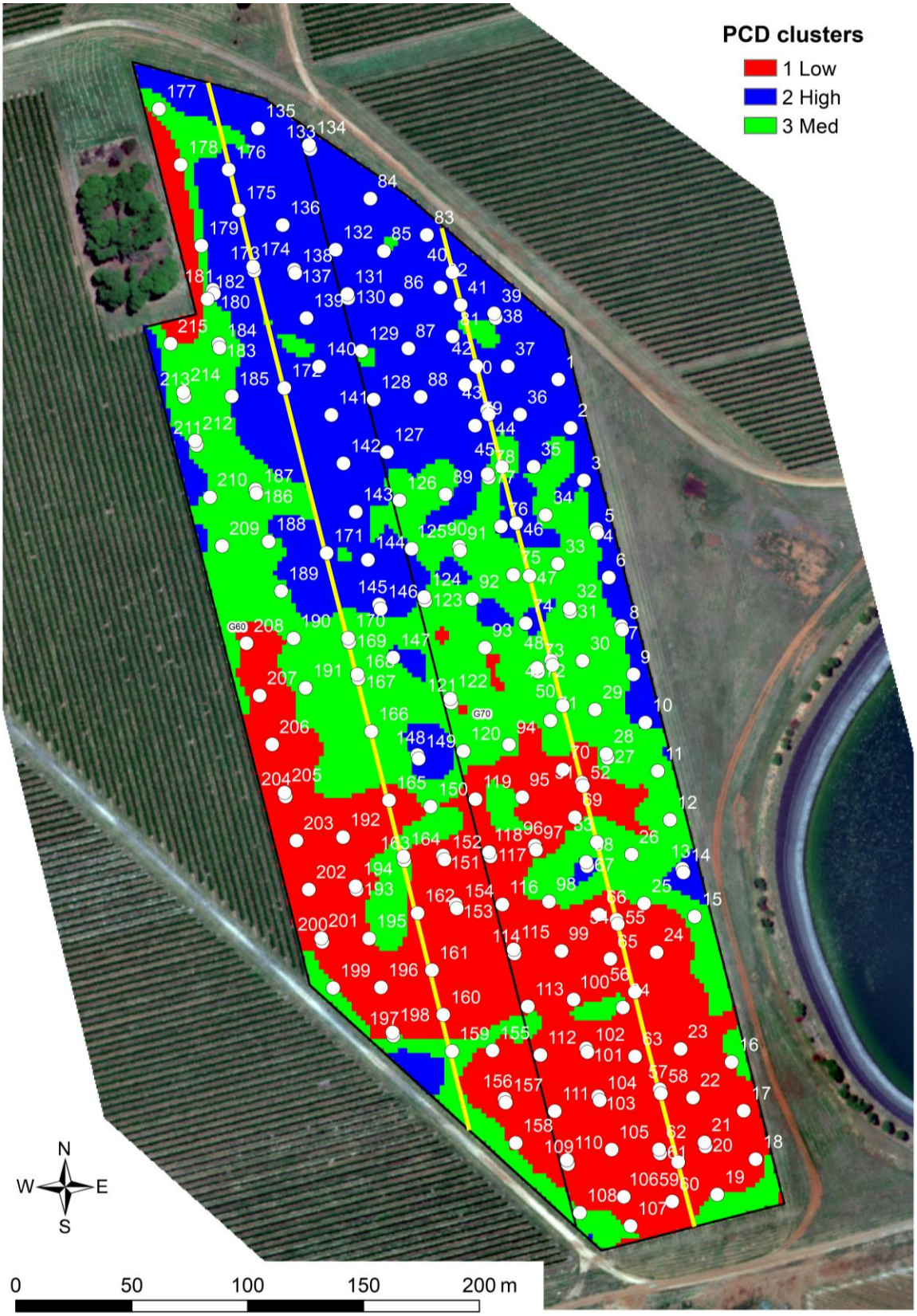


Figure 5.9 Sampling strategy used for hand-held NIR work at the Taylors site. Note that the vines used for calibration were located on the two transects denoted by the yellow lines. The sub-block to the west is clone BVRC on own roots; that to the east is 1654 on 110 Richter.

a.



b.



c.



d.



e.

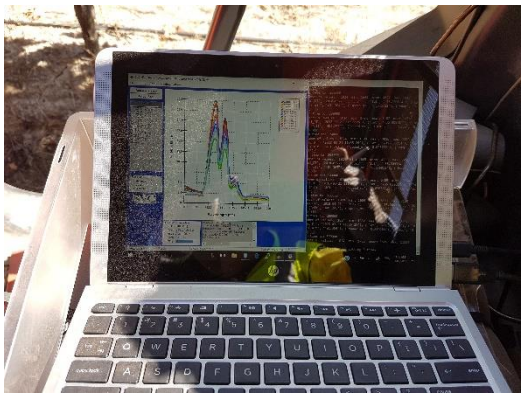


Figure 5.10 NIR scanning of fruit in 2017 and 2018. In 2017, just the SVC instrument was used (a) with logging onto a laptop (b) which was also used to record location; note the dGPS positioned above the canopy of the target vine (c). In 2018, we also used the STS sensor (d); both the SVC (left hand window) and STS data (right hand window) were logged simultaneously (e), with the same three bunches on each target vine scanned with each instrument.

5.10d). This is the same as the instrument used for on-the-go logging on the harvester (see section 5.1.4) and was used to try to link the results obtained from the on-the-go and hand-held sensing. This instrument (ca. $4,000 and purchased for the project) senses in the 650-1100 nm range and is controlled by a Raspberry Pi computer which in turn is configured and controlled using a conventional windows laptop; as with the SVC instrument, an external light source was used (Figure 5.10d). We were able to set up simultaneous logging of both the SVC and STS spectra with a shared dGPS data stream (Figure 5.10e). For the scanning of target vines, we again scanned three randomly selected bunches (as above), but the bunches scanned on each target vine were not necessarily the same bunches for each instrument, except in the case of those used for sensor calibration to wet chemistry, which were scanned using both instruments; of course, we could not guarantee that the sensor field of view was necessarily filled by an identical section of each scanned bunch. The decision not to scan the same bunches with each instrument was based on the time required for the field work (at each site, collection of these data took several hours; a full day at the larger Taylors site) and also the fact that our primary motive here was to understand the spatial structure in the data collected over the whole block, as opposed to bunch to bunch or within-vine variation. Previous work (e.g. Bramley, 2005; Scarlett et al., 2014) suggests that this approach was justified.

5.1.4 On-the-go scanning

Results obtained in 2017 with the hand-held SVC instrument were sufficiently encouraging to justify attempting implementation of an on-the-go NIR scanning solution mounted on a harvester. The SVC spectrometer is not robust enough to cope with the harsh environment of the harvester, and given its value, we were reluctant to use it under harvesting conditions. Instead, a more robust and cheaper NIR solution was sourced; hence the decision to purchase two of the STS instruments (see above). Initial testing in the laboratory indicated that, within the more restricted wavelength range of the STS sensor, similar spectral signals were provided by this instrument as by the SVC. Accordingly, the decision was made to design a system that could be installed on the Taylors harvester.

A frame was constructed to go over the harvester discharge shoot and was mounted immediately above the yield monitor (Figure 5.11a). To this, a light was fitted, along with the fibre optic from the STS spectrometer (Figure 5.11a,b). A battery pack power supply was fitted, in addition to connection to the power source from the tractor, to make sure the system continued to operate when the tractor was not running. This was done so that tractor operators did not need to worry about turning the system on and off, particularly due to the complexity of turning the Raspberry Pi on and off and establishing the Bluetooth connection between this and the tablet PC used for logging. Both the spectrometer and the Raspberry Pi computer used to control it were enclosed in a climate controlled container (Figure 5.11c) so that both could operate in stable conditions, particularly with respect to temperature. A bespoke Python script was developed to run on the tablet PC, controlling the STS spectrometer via a WiFi connection to the Raspberry Pi, and taking readings at a rapid rate. To deal with uncertainty as to the optimal sensor settings due to ambient lighting conditions, the script captured readings with several integration times (see below). This script logged the spectral data, together with accurate GPS coordinates for later processing. This prototype system was then used during harvest of the Taylors field site (Figure 5.11d) and we also attempted to collect packets of data from other blocks on an opportunistic basis during harvest. Unfortunately, due to the vagaries of the timing of harvest events during the 2018 vintage, and the fact that Taylors uses two harvesters, often in tandem, only very limited additional mappable data were collected. Given our focus in this work of

proving the concept of on-the-go NIR sensing, our main effort was to deliberately focus on the target site (Figure 5.9).

The STS sensor captures spectra with various integration times - the time taken for the STS spectrometer to take a measurement. We captured data with several different integration times and subsequently selected the dataset with the most suitable integration time in terms of retaining the maximum spectral peak without saturating the sensor readings, and also sensitivity in respect of the amount of input illumination. The integration times for the harvester STS and the hand-held STS were different to enable collection of optimal spectra data; 50,000 µs for the harvester and 150,000 µs for the hand-held STS. For the western sub-block (Figure 5.9), the harvester fitted with the STS sensor harvested the entire sub-block (9 March), whereas the eastern sub-block (Figure 5.9) was harvested by two machines (14 March) and so only had alternative rows scanned.

a. b.





c. d.





Figure 5.11 Harvester-mounted NIR system developed for on-the-go sensing of fruit composition at Taylors Wines, vintage 2018. The sensing system was mounted above the yield monitor (a) and comprised a fibre-optic sensor and light source (b), with the actual spectrometer and controlling Raspberry Pi computer housed in a refrigerated box (c). The system was successfully deployed (d) for harvest of both the sub-blocks used for this study (Figure 9) enabling calibration against target vine and comparison with hand-held fruit scanning on the vine.

5.1.5 Laboratory analysis

Methods of sample processing and laboratory analysis were as described in Section 3.1.4. However, in addition to the chemical analysis of fruit and the use of the NIR sensors in the field, the laboratory fruit samples were also scanned with the hand-held NIR instruments in the laboratory.

5.1.6 Spectral analysis

Data collected from the target vines using either the SVC or STS instruments is measured as reflectance. As indicated, spectra were collected on three bunches on each target vine. Collected sample spectra were brought into The Unscrambler X (v. 10.3, CAMO Software AS, Oslo, Norway; https://www.camo.com) for multivariate analysis. Spectral data were checked for abnormal/different spectra and these were taken out of the dataset. Retained spectra were then averaged on a per vine basis to give one spectrum per vine. In the case of the harvester data, the dataset was also clipped to the block boundaries to remove data collected in headlands or when the harvester was idle. For the SVC dataset, spectral values for < 600 nm were removed from the dataset – because the 350-600 nm range presented as noise, and also to enable comparison with the STS data; for such comparison, the data were also clipped to 1200 nm.

During scanning, a white reference and a 'dark' reading were taken at the beginning and end of each event, and also periodically (no less than hourly). A white Spectralon reference (Labsphere, New Hampshire, USA) was used for the white reference sample while the fibre optic was covered with a dark cap for the dark readings. In the case of the harvester mounted system, the white and dark readings were obtained prior to set-up on the harvester and assumed to be constant throughout. The white and dark readings were used to transform the primary / raw reflectance data from the spectrometers to a reflectance percentage:

Reflect % = (sample reflectance - dark reading) / (white reference – dark reading)

Reflect% readings were then transformed into absorbance readings using:

$ABS = Log_{10} (100/reflectance)$.

This transformation allows easier linear correlation with wet chemistry data (Les Janik - pers. comm.). The data were then put through a Baseline Correction Transformation in Unscrambler which transforms a sloped baseline into a horizontal baseline. The 'baselined' spectral data were then run through a Principal Component Analysis (PCA) and location specific scores generated for the first 2-3 principal components for subsequent mapping.

Preliminary multivariate analyses, along with the results reported in section 3, led to the decision to focus on calibration against laboratory measures of berry colour (anthocyanins) and phenolics. Initially this was done over the entire spectral range using partial least squares in Unscrambler, but difficulties encountered with between-instrument and between-season comparisons (see results below), led to a focus on the 960-990 nm range. The Predict function in Unscrambler then allowed us to predict fruit compositional aspects across the whole vineyard using the PLS model (obtained from hand sampling

spectra and fruit chemistry) in conjunction with the spectra obtained from the on-the-go sensor on the harvester.

5.1.7 Spatial analysis

For the data collected on-the-go, map interpolation followed the same procedure as described in section 3.1.5. For target vine data, global point kriging in VESPER (Minasny et al., 2005) was used for map interpolation onto the same 2 m grid as used for on-the-go data, using either exponential or spherical variograms and with a maximum distance of 200 m. As a part of arriving at an appropriate methodology, the use of common variograms across different datasets (cf. Bramley et al., 2017) was also explored, as was the mapping of individual compared to average spectra (see 5.1.6 above).

5.2 Results and discussion

Initial analysis of absorbance collected using the SVC instrument at selected wavelengths in 2017 suggested spatial variability in spectral signals at both The Lane and Taylors sites and offered motivation for further developing the NIR-based analysis (Figures 5.12 and 5.13). Variation in spectral data was seemingly unrelated to vine vigour (PCD) at The Lane (Figure 5.12) although at Taylors, there was a suggestion of some alignment between spatial variation in spectral data and variation in yield (Figure 5.14).

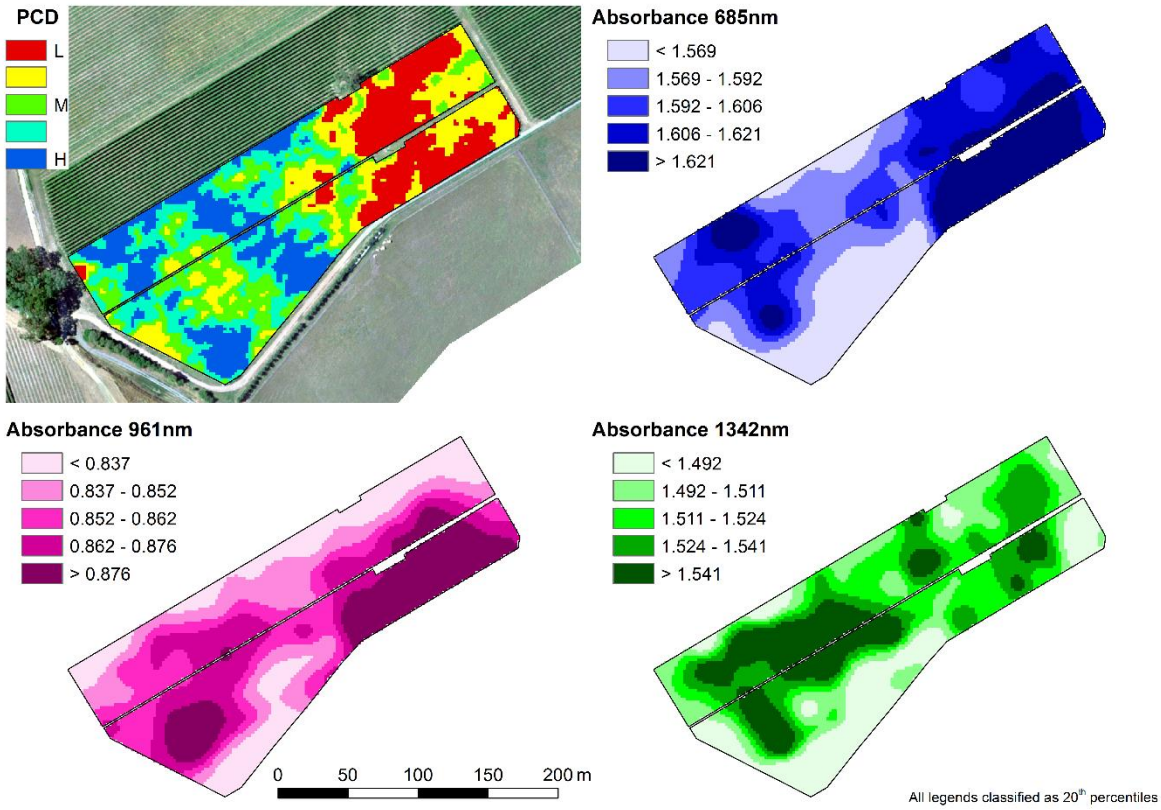


Figure 5.12 Variation in the spectral signal and vine vigour (PCD) obtained from grapes the day before harvest at The Lane, vintage 2017.

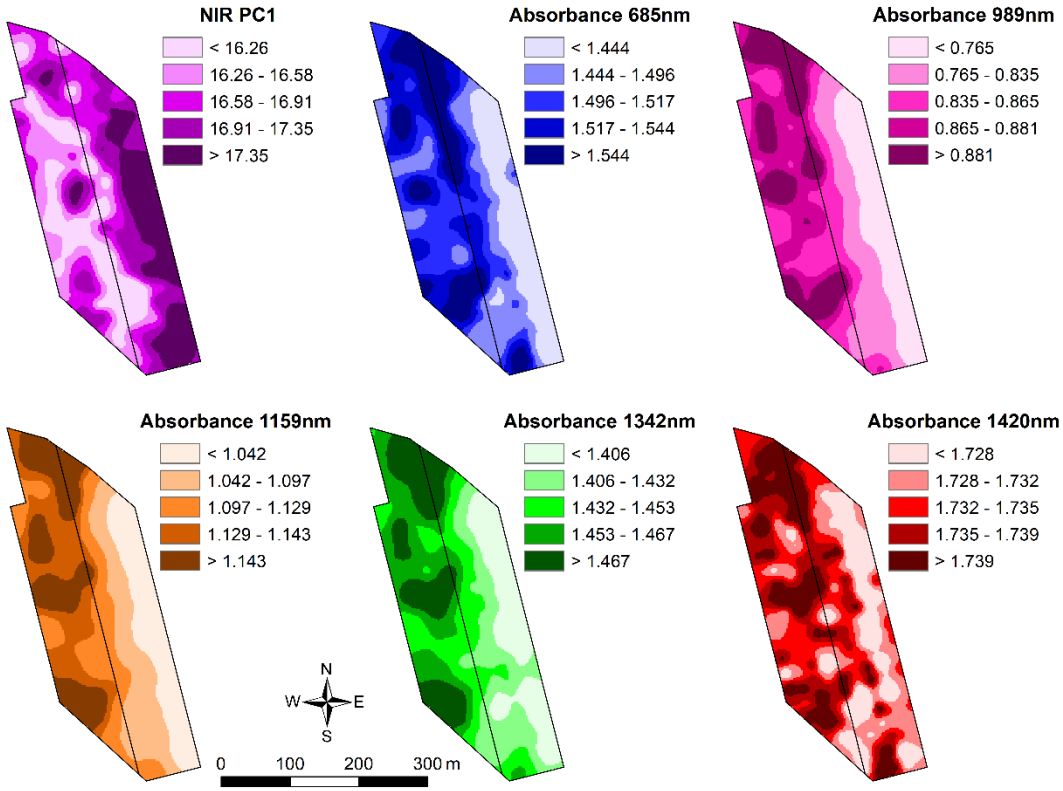


Figure 5.13 Variation in the spectral signal obtained from grapes the day before harvest at Taylors, vintage 2017.

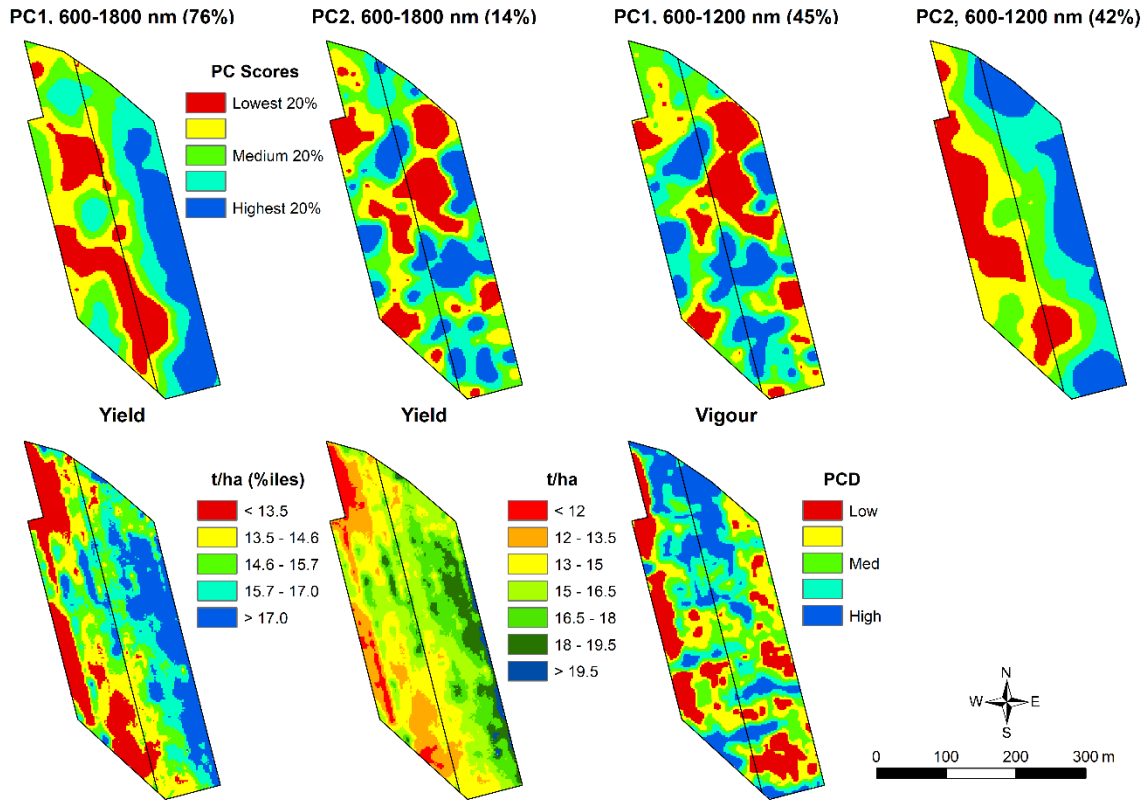


Figure 5.14 Comparison of variation in the spectral signal obtained from grapes the day before harvest at Taylors, and variation in yield and vine vigour, vintage 2017.

Of interest in Figure 5.14 are the results of the principal components analysis. When this was applied to the entire spectral range (with wavelengths < 600 nm excluded – see above), the first principal component (PC1) which indicated some alignment with yield, accounted for 76% of the variation in the spectra collected from 215 vines; PC2 accounted for just 14%. However, when the spectral range was curtailed at 1200 nm, both PC1 and PC2 accounted for a similar proportion of the spectral variation, but with the spatial structure of PC1 matching that of PC2 when the entire spectral range was included. This observation led to concerns over the merit or appropriateness of comparing maps derived from principal components calculated from differing bases, and also raised questions as to the effects of the map interpolation process on the analysis. In turn, consideration of these issues led to questioning of the appropriateness of averaging spectra prior to the multivariate and spatial analysis. The question of spectral averaging and of using individual or common variograms for mapping is canvassed in Figure 5.15.

In general, and irrespective of the spectral range canvassed, the principal component mapped, or the proportion of spectral variance which it accounted for, maps derived from average spectra (i.e. the average of the spectra obtained from the three bunches scanned) showed similar patterns of spatial variation to maps derived from just a single bunch (denoted as either ‘a’, ‘b’ or ‘c samples’ in Figure 5.15). Where there were obvious differences (e.g. PC2, 600-1800 nm, individual variogram), the much smoother map in comparison to others in the same column is indicative of the effects of the fitted

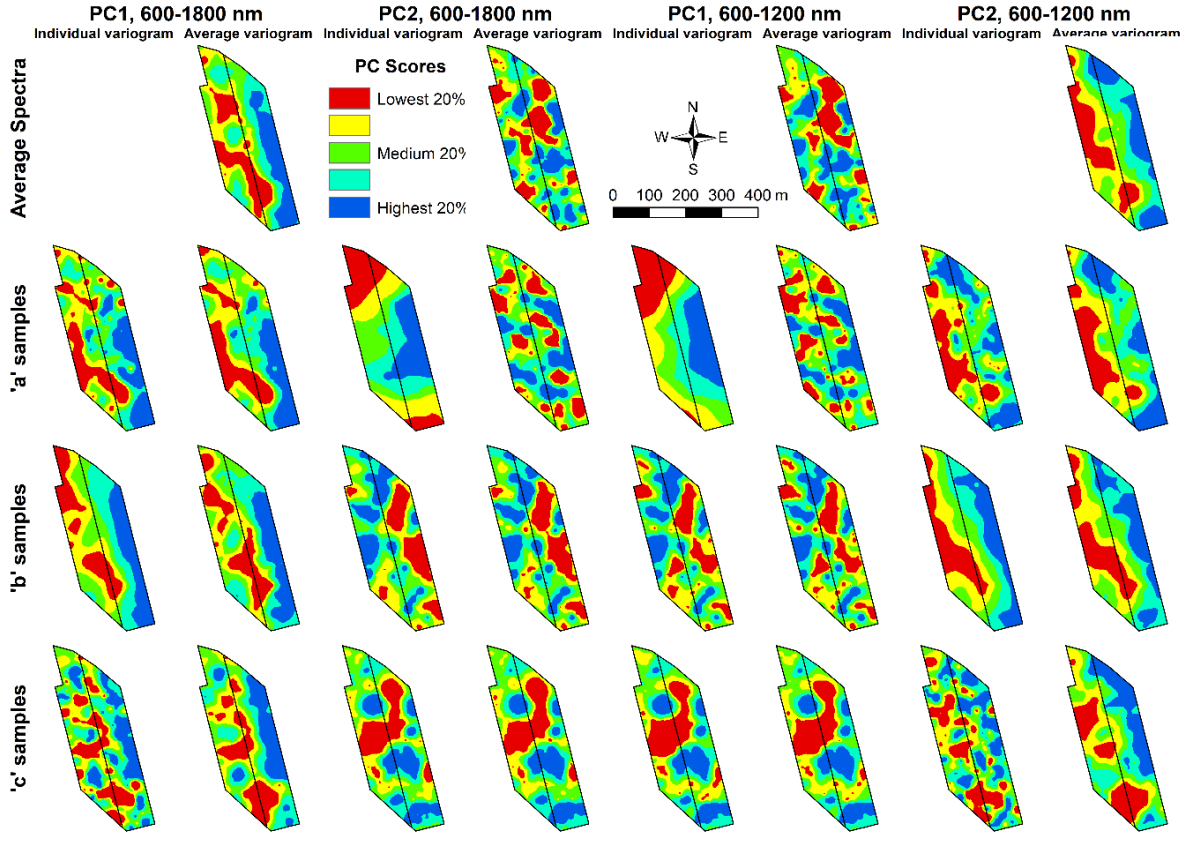


Figure 5.15 Examination of the appropriateness of spectral averaging and of the effect of variogram fitting on spectral map comparisons using data collected at Taylors with the SVC sensor, vintage 2017.

variogram giving a poor description of the spatial structure and/or of a high 'nugget' variance (Webster and Oliver, 2007). Note here that the allocation of any of the triplicate bunch data to either 'a', 'b' or 'c samples' is arbitrary and as such, Figure 5.15 presents just one of a very large number of possible iterations of this kind of analysis. In terms of the effects of variogram fitting on map generation, Figure 5.15 provides a comparison of the effects of map interpolation using either individual variograms (i.e. variograms that are specific to the 'a', 'b' or 'c sample' datasets being mapped), or the variogram obtained when the average spectra derived from averaging those from the triplicate bunches was the dataset used for variogram generation and map interpolation. As can be seen, variogram choice has very little effect on the resultant maps. The exceptions are those cases where the use of an individual variogram leads to an apparently abnormally smooth map (e.g. PC2, 600-1800 nm, individual variogram), a problem which is seemingly corrected by re-interpolation using the variogram derived from the average spectra. Overall therefore, it was concluded from Figure 5.15 that the averaging of the triplicate spectra was an appropriate step in our data processing. A repeat of this analysis using the data collected using the SVC at Taylors in 2018 (Figure 5.16) lends weight to this conclusion. Comparison of maps of spectral data collected across the two years using both the SVC and STS hand-held instruments and also the STS system used on-the-go was somewhat discouraging (Figure 5.17). Whilst spatial structure is evident in the mapped spectral principal components, there was little obvious similarity in the patterns of variation amongst the maps. Recognising that for any individual instrument or season, maps of PCs 1 and 2 would be expected to be different, given that different factors (absorbances at different wavebands in this instance) likely contribute to the different PCs, the lack of similarity in spatial patterns amongst any pairs of maps was initially a surprise. An exception was the comparison between the SVC PC1 over the full spectral range in 2017 (top left map in Figure 5.17), PC2 from the same instrument in 2017 (bottom row, second from left) and the maps for both PC1 and PC2 obtained from the on-the-go STS sensor deployed on the harvester (right hand maps in Figure 5.17). However, these harvester-derived maps highlight a difficulty in that the five-day gap between harvest of the eastern and western sub-blocks seemingly has a major impact on the analysis when the data from the two harvest events are combined prior to generation of the principal components. Whether this five-day gap is due to changes in fruit composition (see section 3) or is reflective of changed lighting conditions, or both, is not known.

This result led to realisation of a significant difficulty with the analysis of these data using a principal components analysis-based approach. Our initial intent in this work was to prove the concept of using NIR analysis as a means of assessing spatial variability in fruit composition. In this respect it was 'fruit composition' or 'quality' in its most general sense that we were interested in, rather than any specific compositional attribute. This is why we focussed initially in generating maps derived from principal component scores rather than calibration against specific analytes, especially given the conclusion (section 3), that the analytes typically measured are not necessarily robust indicators of 'quality'. However, the results shown in Figure 5.17 highlight a problem with this approach in that one can have no confidence that the grape attributes reflected by PC1 and PC2 are constant across sensors or seasons; clearly this is not the case when different wavelength ranges are used, but it is also highly likely not the case even when the same wavelengths are considered across seasons. Thus, for example, there is little similarity between the SVC-derived maps for 2017 and 2018 (Figure 5.17). Likewise, there is little similarity between the SVC and STS data in 2018 when considered over the same wavelength range. Finally, whereas the maps of PC1 and PC2 derived from SVC data in 2017 show different patterns, those in the maps of PC1 and PC2 derived from the same sensor in 2018, are quite similar. In other words, it is not possible to separate out a sensor effect from a seasonal effect and therefore

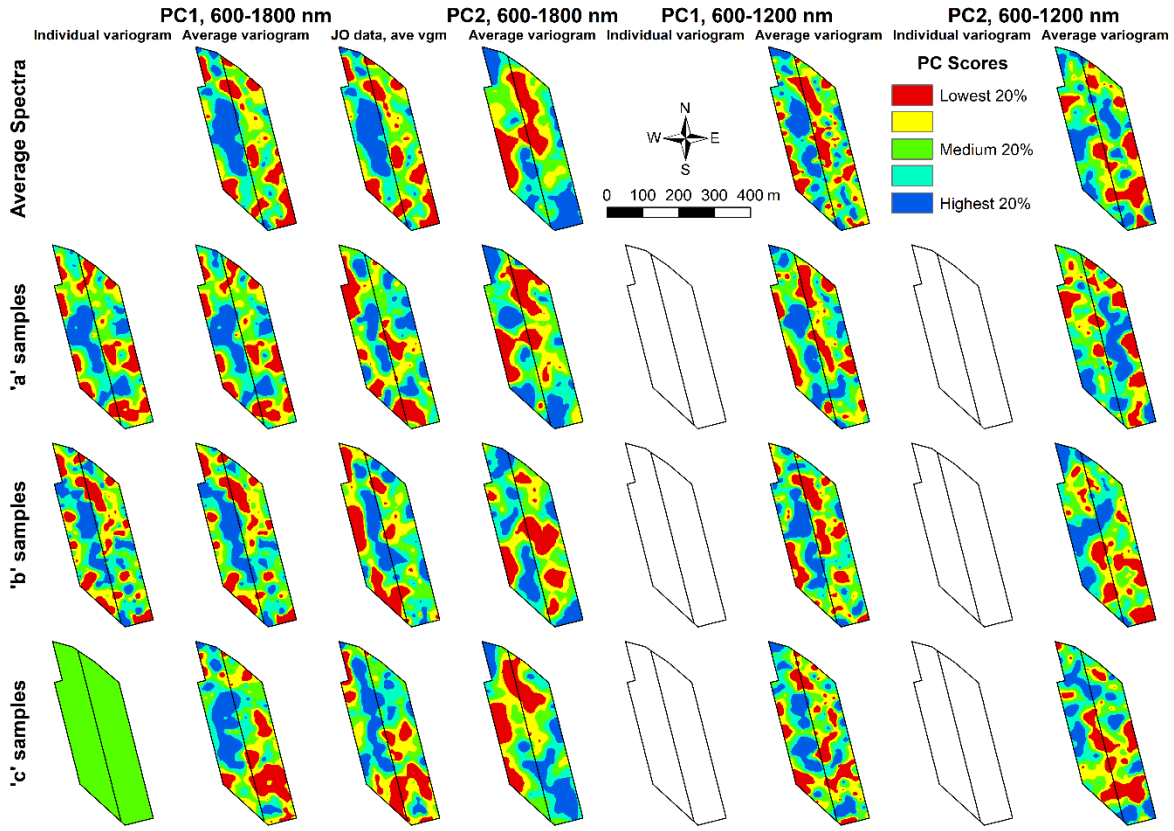


Figure 5.16 Examination of the appropriateness of spectral averaging and of the effect of variogram fitting on spectral map comparisons using data collected at Taylors with the SVC sensor, vintage 2018.

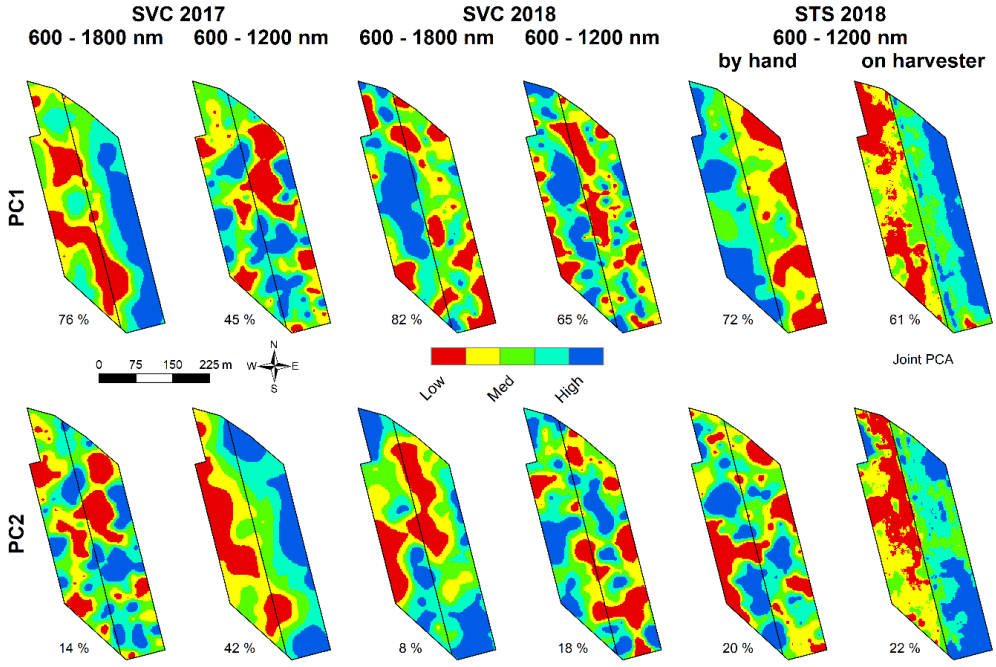


Figure 5.17 Comparison between sensors and seasons in the principal components analysis of grape NIR data at the Taylors site.

not possible using the approach followed here, to assess temporal stability in the patterns of variation in fruit composition. All that can be concluded from Figure 5.17, and therefore also from Figures 5.12-5.16, is that whatever is driving the variation in NIR absorbance, which we assume to be fruit composition, is spatially variable. As demonstrated in section 3, fruit composition is also temporally variable and the time of harvest is seemingly somewhat arbitrary from a plant physiology point of view. So, it can be inferred that variation in the signal obtained from the NIR sensor, in the absence of calibration against specific analytes, is reflective only of the fact that the composition of different bunches is different, and takes no account of which analytes are driving those differences. That said, for the on-the-go data in Figure 5.17, the fact that two sub-blocks harvested five days apart are clearly discriminated by NIR suggests that it is a potentially sensitive tool in assessing variation in fruit composition, assuming that this difference is not solely a consequence of different ambient lighting during the two harvest events.

These issues are further highlighted in Figure 5.18 in which the on-the-go data have been processed either on a per sub-block / harvest event basis (top row of maps), or together. Thus, in the top row of maps, the processing of the spectral data and generation of principal components has been done for the two sub-blocks individually. In the bottom row of maps, the dataset has been combined. Whilst this latter approach enables continuity in the spatial variation across the sub-block boundary to be seen, and also retains some elements of the spatial variation apparent when the sub-blocks are analysed separately, much of the variation seen in the individual sub-block analysis is not retained when the analysis is undertaken for the entire management unit. In other words, the composition of the PCs is not constant – and likely neither is the fruit composition given the five day period between

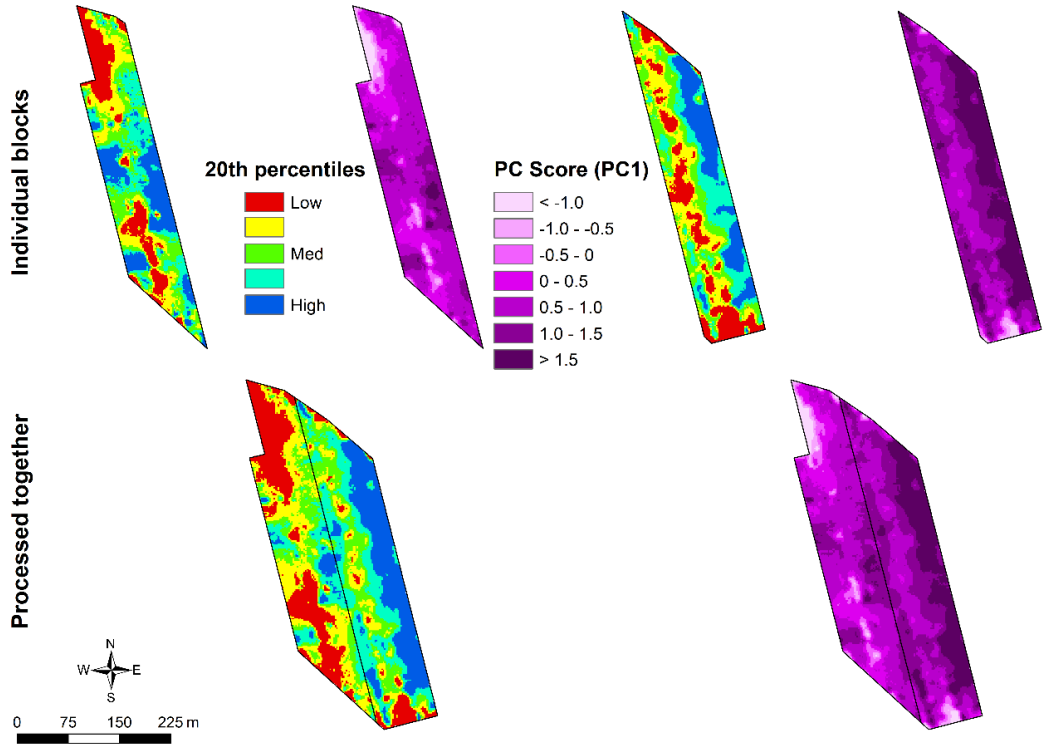


Figure 5.18 Differences in variation in apparent fruit composition, as assessed using NIR on-the-go during harvest, when data collected from the two sub-blocks at Taylors are analysed either individually, or as a single entity. Note that the two sub-blocks were harvested five days apart from each other.

harvest events. Note that the effect of the five day difference in harvest date does not impact the data collected with hand held sensors since these data were all collected on the same day. Note also that the difference in harvest date notwithstanding, this block (i.e. the two sub-blocks collectively) is managed uniformly as a single management unit. As indicated above, and in spite of the bright light positioned alongside the sensor, differences in ambient lighting between the two harvest events may also have had an impact; of course, the use of the bright light was intended to remove /reduce these.

In light of concerns as to how maps based on principal component scores should be interpreted, calibrations of the spectral data against berry anthocyanins and phenolics were explored. Mindful that our objective here was to prove the concept of on-the-go NIR sensing, and in an attempt to keep this analysis relatively simple, and also minimise the effects of between-sensor differences, we chose to focus on the 960-990 nm wavelength range for the calibrations. This wavelength range corresponds to a marked peak absorbance area of the spectrum which is also relatively free of noise (Figure 5.19). The calibrations were generated using the PLS procedure in Unscrambler. Regressions of the predicted values for anthocyanins and phenolics against the laboratory standard analysis resulted in the maps shown in Figures 5.20-5.23 which, in turn, were based on the equations detailed in Table 5.1. As can be seen, the predictions are, at best, fairly weak. Note that here we have focussed on concentration per berry rather than per g as the predictions were stronger on the per berry basis.

Presumably due to the weak predictions of anthocyanins and phenolics berry^{-1}, coupled with the smoothing that is inherent to map interpolation using kriging, the maps of anthocyanins and phenolics berry^{-1} derived from NIR prediction were somewhat discouraging. Whether classified on the basis of equal intervals (Figures 5.20 and 5.22) or quantiles (20th percentiles; Figures 5.21 and 5.23), the degree of apparent spatial variation in anthocyanins and phenolics berry^{-1} was small. Furthermore, there was no consistency between the maps either across years or, in the case of 2018, across sensors. Given that the same wavelength range (960-990 nm) was used for all analyses, this latter result is certainly counter-intuitive. Accordingly, in Figures 5.24-5.27, absorbance at the single wavelength of 980 nm is

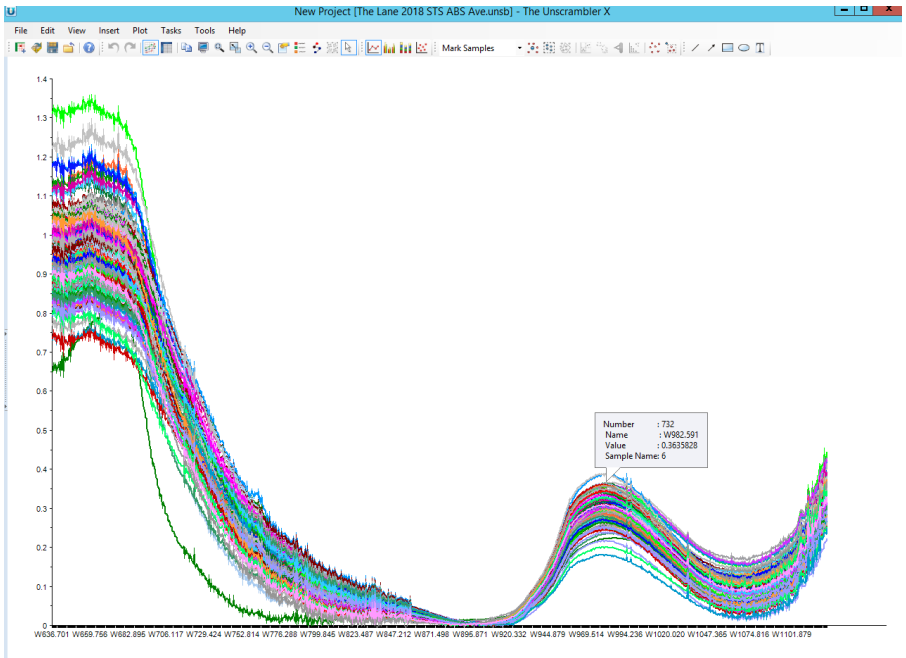


Figure 5.19 Screen dump from Unscrambler X (The Lane, STS sensor) highlighting the peak NIR absorbance at 960-990 nm. The data shown are The Lane, vintage 2018.

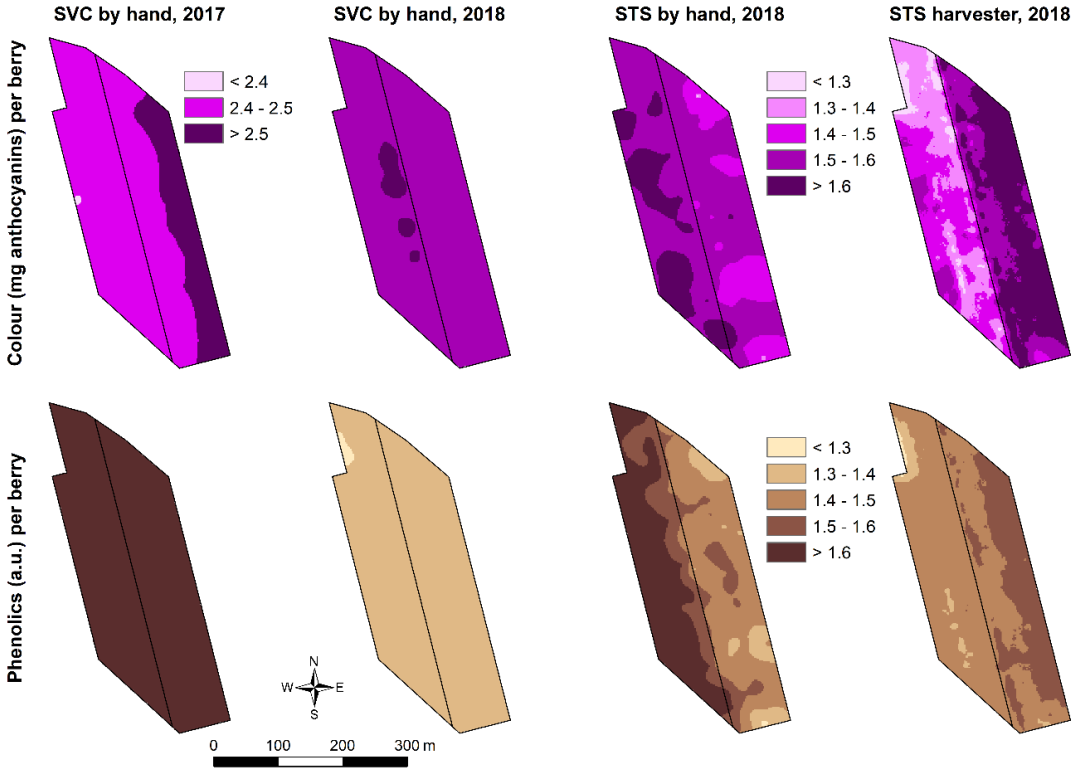


Figure 5.20 Apparent variation in berry anthocyanins and phenolics at the Taylors site when assessed using NIR sensing in the 960-990 nm spectral range – equal interval classification.

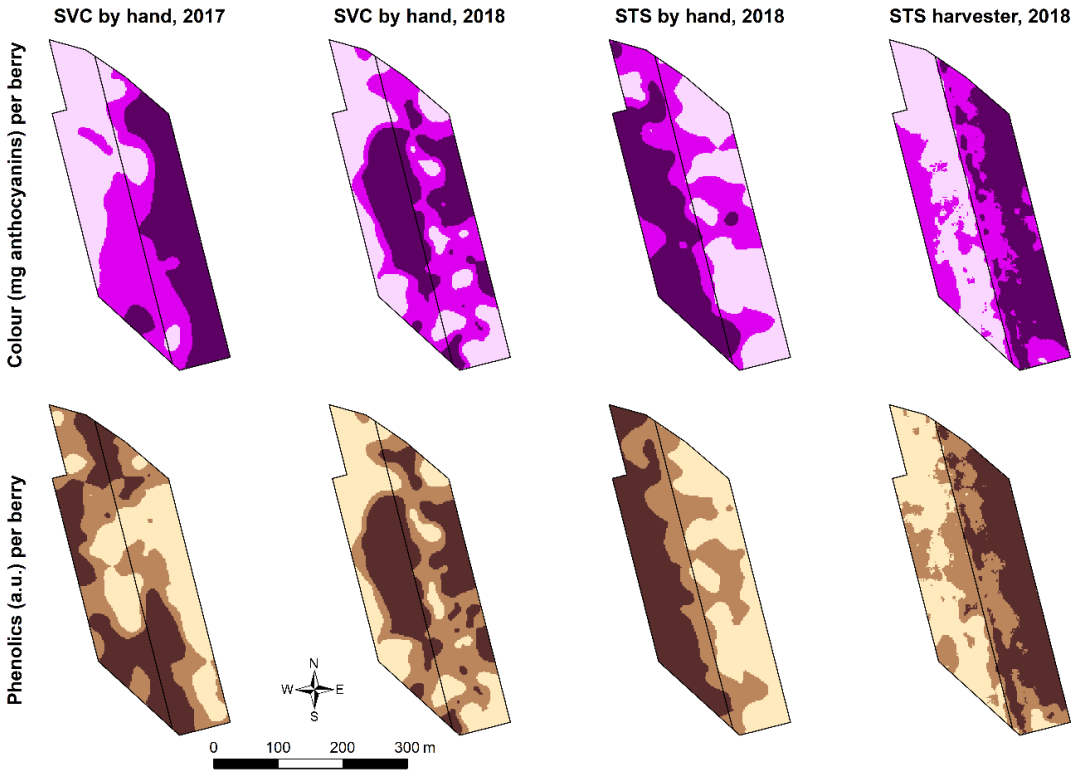


Figure 5.21 Apparent variation in berry anthocyanins and phenolics at the Taylors site when assessed using NIR sensing in the 960-990 nm spectral range – 20th percentile (quantile) classification.

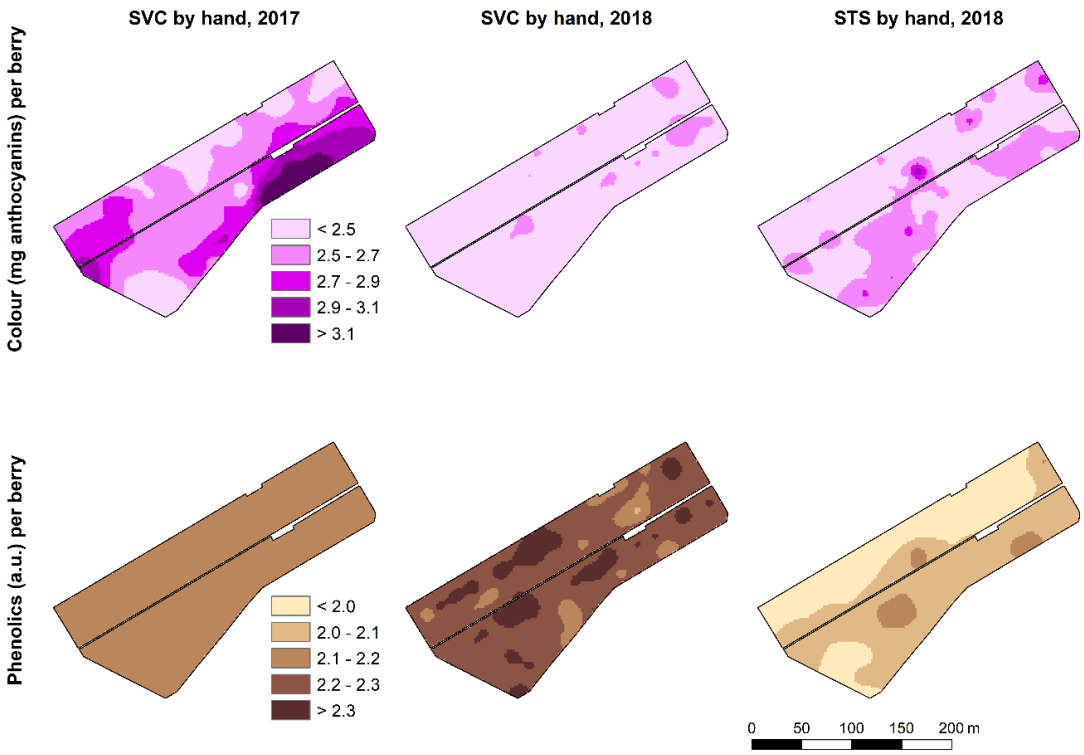


Figure 5.22 Apparent variation in berry anthocyanins and phenolics at The Lane site when assessed using NIR sensing in the 960-990 nm spectral range – equal interval classification.

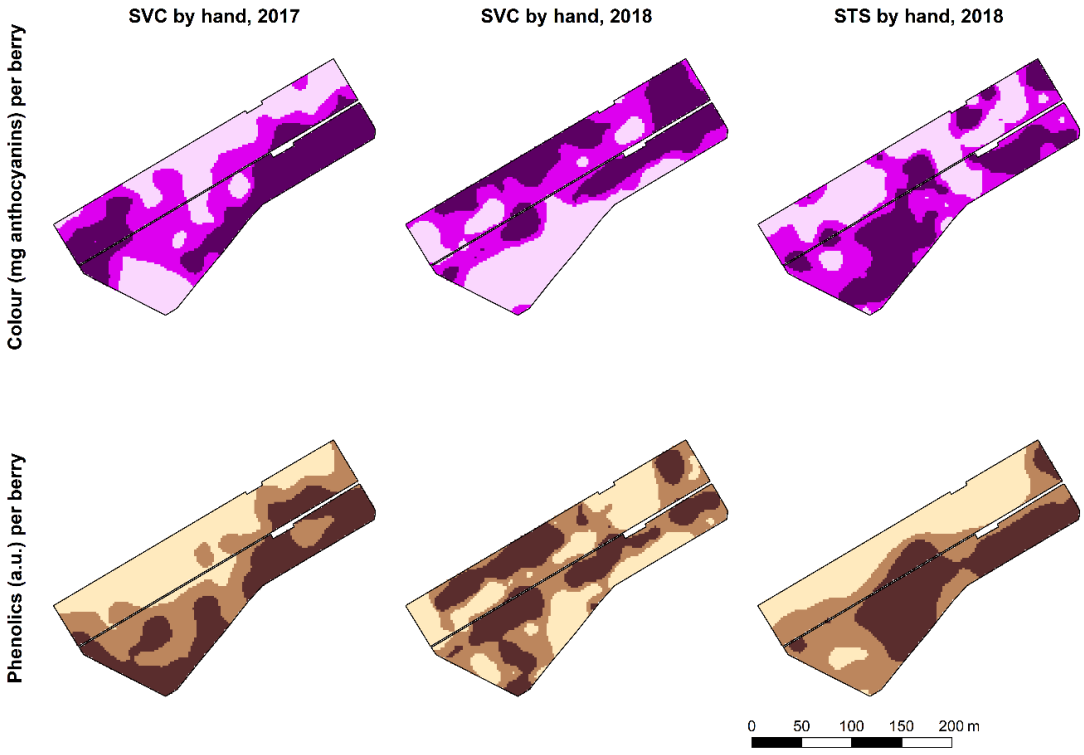


Figure 5.23 Apparent variation in berry anthocyanins and phenolics at The Lane site when assessed using NIR sensing in the 960-990 nm spectral range – 20th percentile (quantile) classification.

Table 5.1 Regression equations describing the relationship between concentrations of either anthocyanins (mg berry^{-1}) or phenolics (absorbance units (OD280 nm) berry^{-1}) measured using the methods of Iland et al. (2004) with the concentrations predicted from analysis of NIR spectra in the 960-990 nm range ($Pred_{NIR}$).

Year	Site	Sensor	Anthocyanins	R^2	Phenolics	R^2
2017	Taylors	SVC	$Pred_{NIR}$ = 0.19 lab + 1.63	0.19	$Pred_{NIR}$ = 0.38 lab + 1.16	0.26
	The Lane		$Pred_{NIR}$ = 0.44 lab + 1.52	0.29	$Pred_{NIR}$ = 0.20 lab + 1.71	0.20
2018	Taylors	SVC	$Pred_{NIR}$ = 0.25 lab + 1.52	0.25	$Pred_{NIR}$ = 0.21 lab + 1.47	0.13
		STS_{hand}	$Pred_{NIR}$ = 0.40 lab + 0.36	0.36	$Pred_{NIR}$ = 0.45 lab + 0.86	0.40
		$STS_{harvester}$	$Pred_{NIR}$ = 0.36 lab + 0.99	0.29	$Pred_{NIR}$ = 0.45 lab + 0.86	0.40
	The Lane	SVC	$Pred_{NIR}$ = 0.33 lab + 1.62	0.19	$Pred_{NIR}$ = 0.43 lab + 1.15	0.28
		STS_{hand}	$Pred_{NIR}$ = 0.58 lab + 1.02	0.47	$Pred_{NIR}$ = 0.48 lab + 1.02	0.25

Here, partial least squared regression of NIR spectra against laboratory analysis has been used to generate predictions ($Pred_{NIR}$) of anthocyanins and phenolics. The above equations are the regression relationships between these predicted values and the actual wet chemistry measurements.

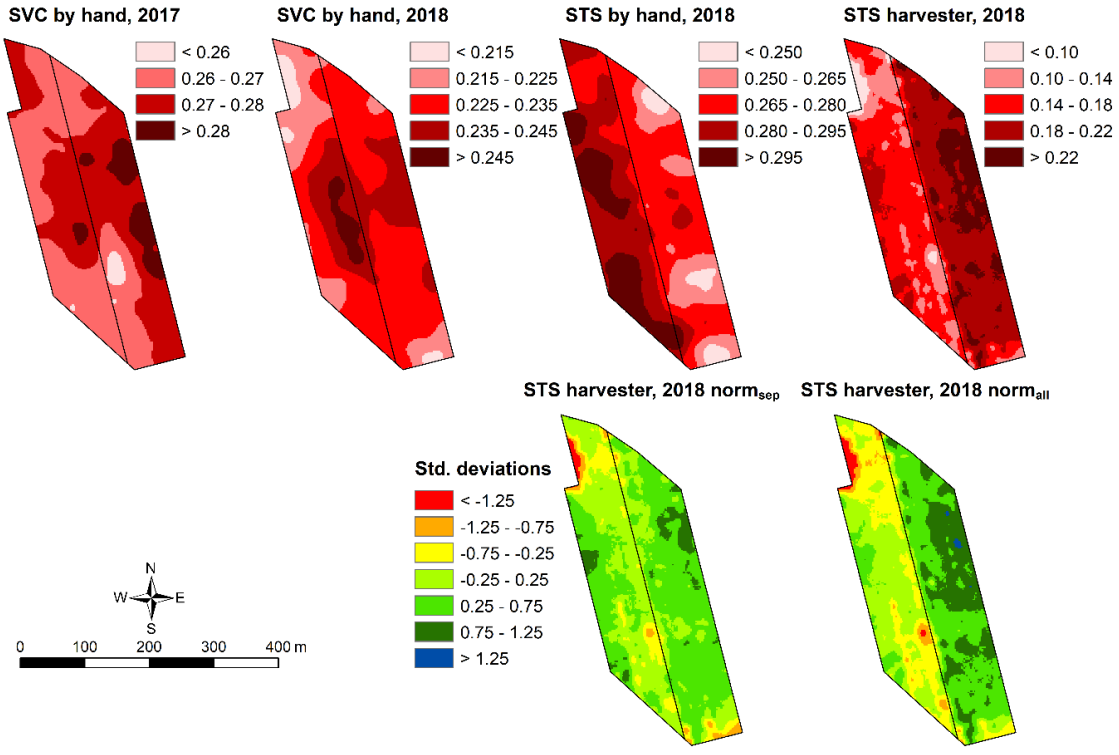


Figure 5.24 Variation in absorbance at 980 nm at the Taylors site – equal interval classification.

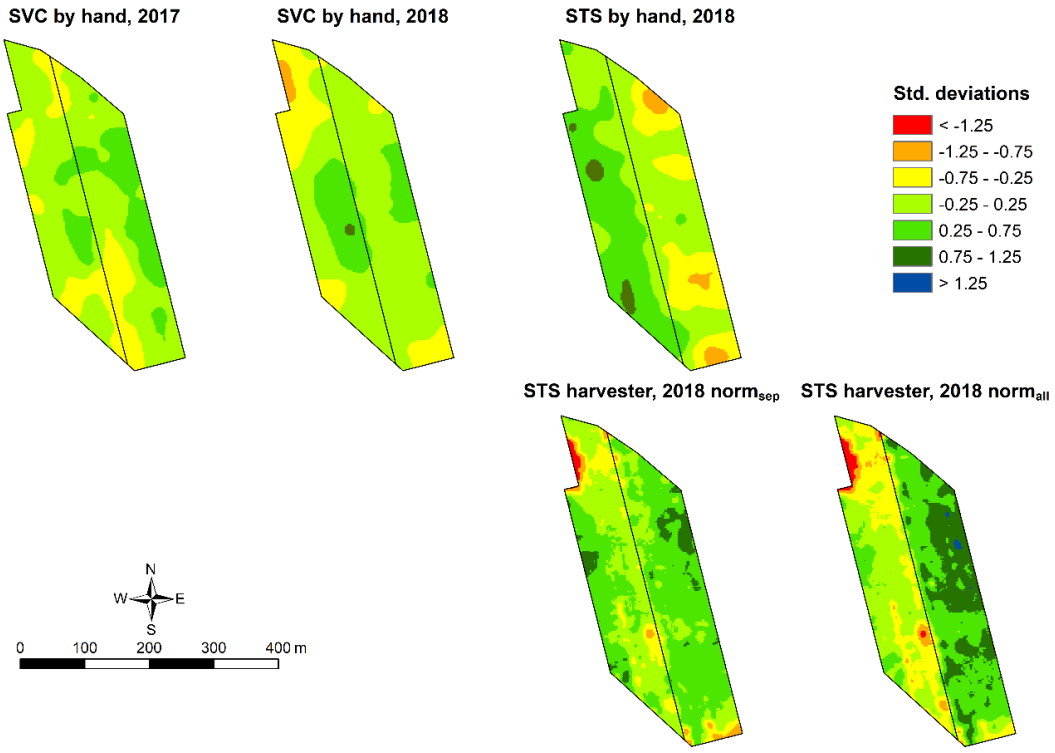


Figure 5.25 Variation in absorbance at 980 nm at the Taylors site – normalised data.

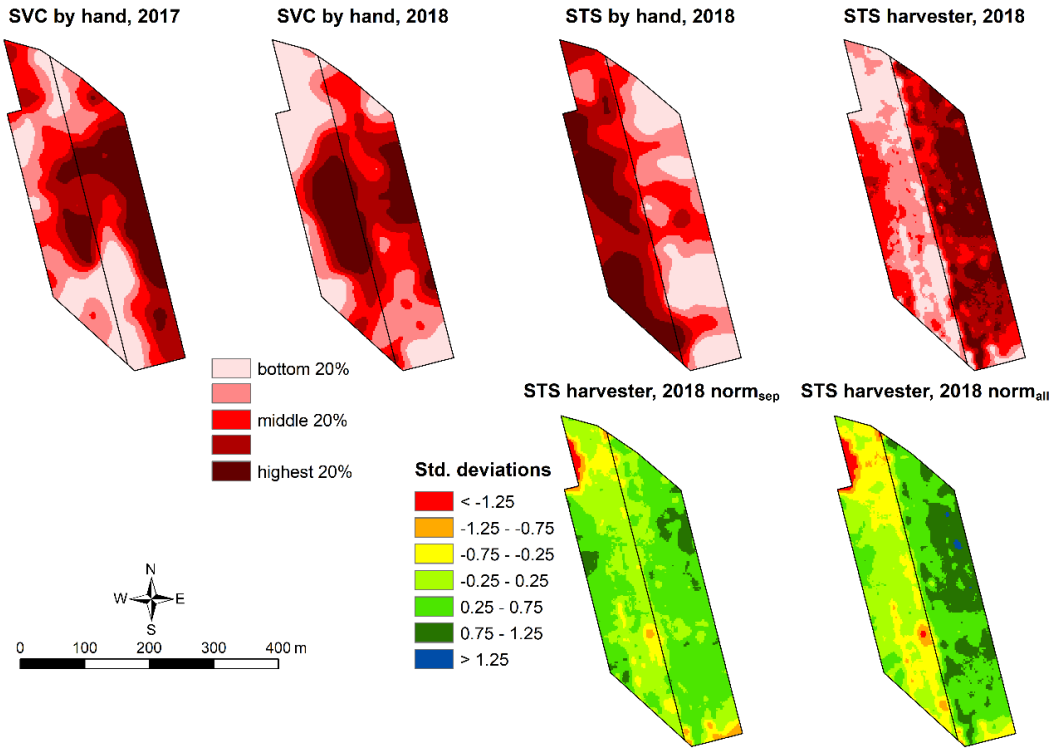


Figure 5.26 Variation in absorbance at 980 nm at the Taylors site – 20th percentile (quantile) classification.

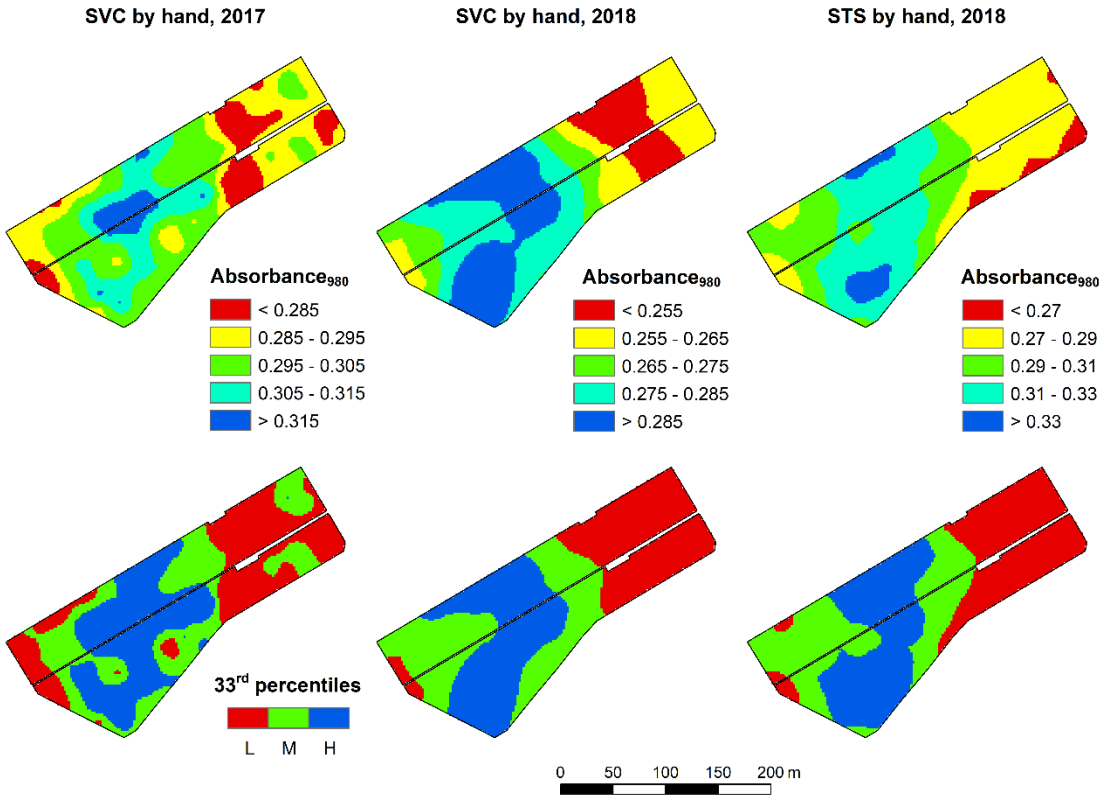


Figure 5.27 Variation in absorbance at 980 nm at The Lane.

mapped. At Taylors, there is again little similarity in patterns of variation across sensors or years whether the classification is expressed in terms of equal interval (Figure 5.24), normalised data (μ=0, σ=1; Figure 5.25), or quantiles (Figure 5.26.). In contrast, the results from The Lane (Figure 5.27) are much more encouraging and suggest, as would be expected, that the SVC and STS sensors provide the same information at similar wavelengths; they also tend to suggest some similarity across years. One possible reason for these equivocal results is the proximity of 980 nm to a part of the spectrum known to be associated with NIR absorbance by water. However, even if these maps are simply reflecting berry water content, they might intuitively be expected to show greater similarity between sensors in terms of the patterns of variation. Of course, without such between-sensor similarity, assessment of the stability of patterns between seasons is made impossible.

5.3 Conclusions

The objective of this part of the project, given past success with laboratory analysis of grapes and wine (Cozzolino et al., 2006; Dambergs et al., 2014), was to prove the concept of NIR sensing of grapes, both *in vivo*, and on-the-go during harvest. Inasmuch that our results indicate an ability to capture spatial variability in fruit composition using NIR sensing, the work has been successful and suggests that pursuit of a more robust NIR sensing solution has much merit. However, for this to be a useful tool commercially, we need clarity as to which *objective* measures of fruit quality we are trying to predict using NIR, and how the results might be interpreted given the apparent temporal arbitrariness

of harvest and the impact of this on measures of fruit composition (section 3). Bindon et al. (2017) reported success in using laboratory NIR analysis in a cross-regional study to predict fruit grade and noted the need to analyse compounds which, hitherto, had not been considered as quality indicators; whether their list is either exhaustive or optimal is unclear. It also needs to be said that in spite of its history (approximately 20 years in the case of grapes and wine), the analysis of spectral data is difficult and without doubt, we were on a very steep learning curve in processing the spectral data collected in this work. Indeed, a positive outcome from this work was the convening of a workshop within CSIRO to share experiences and form a community of practice amongst users of spectral data across a wide range of targets (minerals, soils, crop and pasture plants, fruits and seafood); a similar forum amongst wine sector participants would likely be similarly valuable, as would agreement as to what the key compounds are for quality assessment. Having selected the key attributes of grape composition to be measured, we also need to be clear on the key wavelengths to be targeted.

Based on current pricing, it is considered neither feasible nor cost-effective to place an expensive instrument such as the SVC on a grape harvester. An instrument akin to the STS certainly would be feasible however, but whether the wavelength range of the instrument used here is either sufficient or optimal is unclear. However, given the time required for hand-scanning of sufficient samples for map production, along with the smoothing that arises from kriging with low support (i.e. small samples numbers), an on-the-go solution providing data at high spatial resolution will be required if the temporal stability of patterns of within-vineyard variation is to be robustly assessed, and if the yield:quality nexus is to be better understood at the within-vineyard scale.

6. Conclusions and recommendations

6.1 The yield:quality nexus

The central theme of this project was to try to better understand the so-called yield:quality nexus, to provide industry with better understanding of the link between yield and quality. Through a field-based research program, we sought to evaluate the evidence in support of the widely held belief that, not only are yield and quality inextricably linked, they are inversely correlated such that high quality fruit, and therefore high quality wines, may only derive from fruit produced at low yield. In many respects, this was a project about *terroir*. Vineyards are known to be variable, with this variability driven by the land underlying the vineyard (e.g. Bramley, 2010, 2019 and references therein). Thus, if yield and quality are inextricably linked, then an impact of variation in the land underlying the vineyard on its yield will, *de facto*, also have an impact on the quality of its fruit – and vice versa. Previous work at the within-vineyard scale (e.g. Bramley et al., 2011b, 2017) has provided compelling evidence of *terroir* being expressed at that scale. Indeed, there is good reason to suppose that our limited understanding of *terroir* is a consequence of its research having been compromised by the scale at which it has been investigated (Bramley, 2017). With this in mind, our approach was to use the tools of precision viticulture and the within-vineyard scale as the basis for investigating the yield:quality nexus.

As detailed in section 3, whereas the within-vineyard study of Bramley et al. (2011b) was suggestive of yield and quality being linked at the within-vineyard scale, through investigation of contrasting sites in the Clare Valley and Riverland, the present results provide, at best, weak evidence of a link between yield and quality. They are therefore broadly consistent with the cautionary notes of Trought (2005) and Matthews (2016) in questioning the notion of higher yields inferring lower quality. However, our results come with two important caveats. First, due to circumstances beyond our control, we were only able to collect data for two seasons. Possibly more importantly, our results tend to support the view that poor understanding of the yield:quality nexus derives from the metrics used to assess it. It is well established that juice pH, titratable acidity and total soluble solids are essentially indices of fruit maturity, even if they also have some impact on the perceived quality of fruit, especially in white grape varieties (e.g. Trought and Bramley, 2011). In red grapes, there is some basis for regarding colour (anthocyanins) and phenolics as indicators of quality (Francis et al., 1999; Gishen et al., 2002), although use of these as quality indicators has not been widely adopted by winemakers. The identification of robust, objective measures of fruit (and wine) quality has been an important element of the Wine Australia research agenda for some time, and the present results suggest that until such measures can be elaborated and adopted by industry, improved understanding of the yield:quality nexus, if indeed there is one, may remain elusive. Bindon et al. (2017) noted the desirability of including a wider range of analytes than the more restricted range commonly used. Ideally, such measures will also reflect sensory attributes such as fruit characters and astringency. On the other hand, recent work (Scarlett et al., 2014; Bramley et al., 2017) aimed at understanding variability in the concentration of rotundone, a very particular indicator of the quality of some cool climate Shiraz, does not provide evidence in support of yield and quality (in respect of this measure of it) being linked. Note that whilst yield was not measured in this work on rotundone, vine vigour which correlates with yield was. There was scant evidence of vine vigour impacting on berry rotundone concentration (Bramley et al., 2017).

Finally, somewhat paradoxically, and closely related to the previous point on the need for objective measures of quality, our results are strongly suggestive of harvest being an inappropriate time for 'quality' to be measured if the objective is to understand any relationship between quality and yield. Quite rightly, winemakers will assess the quality of fruit, both sensorially and/or using chemical analysis, in making harvesting decisions. But if either yield and/or the elements of fruit composition which drive quality are in decline at harvest, then its timing is essentially arbitrary in a physiological / phenological sense, a fact which arguably compromises our ability to better understand the yield:quality nexus. One solution to this problem which has been advocated by numerous researchers, is to make all measurements at a constant concentration of total soluble solids (i.e. a constant level of maturity). However, because TSS is known to be spatially variable (e.g. Bramley 2005), it is unclear how this might be achieved. A modelling-based solution (cf. section 3.2.3) is one option, although how this might be accepted by industry as a basis for decision making in real time is not known.

6.2 Calibration of remote and proximal sensing

Investigation of this issue was a small but potentially important element of the work. As demonstrated in section 4, calibration of passive remotely sensed imagery (e.g. from an aircraft) using imagery acquired from an active proximal sensor is clearly possible. In the present work, we did this in anticipation of being able to make use of the calibration for predicting fruit composition based on understanding of its relationship with vine vigour (as a surrogate for yield). As indicated, because the yield:quality nexus did not appear well established, we were unable to progress the use of converting passively acquired measures of vigour into robust quantitative measures using active sensing and so use these measures for further prediction of fruit composition. Nonetheless, such calibrations remain a potentially useful tool if the issues identified in 6.1 (above) can be addressed.

One element of the work which may be important is the recommendation that in (even lightly) sprawling canopies, proximal canopy sensing is best done with the sensor mounted above the canopy, rather than to the side.

6.3 On-the-go-sensing of fruit composition

Notwithstanding concerns as to whether harvest is necessarily the most appropriate time for measuring fruit composition when the objective is to understand it relationship with yield (6.1 above), it would clearly be valuable to have the ability to measure fruit compositional attributes with the same spatial intensity and resolution as is now possible for vine vigour and yield. Indeed, just as the major utility of yield mapping, and demonstrating temporal stability in patterns of yield variation, is its value in assessing what is likely to happen next year (as opposed to what happened this year), a similar ability to generate maps of fruit quality from year to year and so understand temporal stability in patterns of fruit quality variation would be very useful. Indeed, the knowledge that particular areas within vineyards consistently produce fruit suitable for different product streams to other parts of the same uniformly managed vineyards would be invaluable in underpinning strategies such as selective harvesting, which have previously been shown to be highly profitable. Given our somewhat equivocal experience with fluorescence sensing (section 5) and its present focus on a single analyte

(anthocyanins), the prospect of using hyperspectral NIR sensing to sense a range of compositional attributes (e.g. Bindon et al., 2017) was highly attractive.

This project did not seek to produce a commercialisable NIR-based on-the-go fruit sensing technology, but it did seek to prove the concept of using an NIR sensor on a harvester as an on-the-go tool for fruit analysis, and therefore to demonstrate the potential merit of developing one. We believe that we achieved this, albeit recognising that much additional work will be needed to deliver such a system. Of course, such a sensor needs to provide information that is interpretable – perhaps in terms of fruit grade (Bindon et al., 2017) or suitability for a particular wine style. Its utility is therefore heavily dependent on resolution of the issues identified in 6.1 (above) regarding objective measures of quality and the timing of their measurement – or at least, the time dependent interpretation of the measurements made. However, such a tool could also be invaluable in resolving these issues given the potential to cheaply provide many thousands of measurements within a single vineyard. It is to be hoped that Wine Australia will feel encouraged to support a continuation of this work.

6.4 Recommendations

It follows from 6.1, that an enhanced effort is needed to identify robust measures of fruit quality if the industry is to move away from its present assumption of higher yield being correlated with lower quality. As a part of this, understanding of how such measures should be interpreted in relation to the time of measurement is needed, especially if understanding of the yield:quality nexus remains a goal. As has been suggested previously, using science to underpin both the desirability of our wines and the skill used in making them, would be very much to the advantage of the Australian wine sector (Bramley, 2017). The work of Bindon et al. (2017) provides a good start, and if combined with some sort of juice quality scoring system (e.g. Trought and Bramley, 2011; N Dokoozlian, E&J Gallo Winery – pers. comm.) that is predictable by NIR, or some other appropriate sensing technology, considerable progress might be made.

As implied in 6.3, an on-the-go NIR sensor mounted on a harvester could be a rich source of information to underpin both viticultural understanding and commercial decision making. We believe that this work should be continued and hope that Wine Australia agrees. However, the work reported in section 5 highlighted three closely related issues which warrant follow-up. First, some fine tuning of the sensing systems, in order to develop greater confidence in the in-field and on-the-go calibration of NIR sensors and accommodating the varied/challenging sensing illumination conditions would be useful. Second, analysis of spectral data is difficult, especially to those who have not previously encountered it. Yet it has been used in various forms in the wine sector for at least 20 years (Dambergs et al., 2014). Just as we found benefit within CSIRO in canvassing advice as to how to proceed through the formation of a spectral analysis community of practice, so too would benefit surely arise if a coordinated attempt was made amongst Wine Australia's stakeholders and research providers, to join forces in sharing this important capability. Sharing analytical protocols and/or developing the basic steps to be followed in analysing grape (and wine) spectral data would be valuable. These could also be passed to industry.

Closely related to this last point, in the present project we collected a lot of data! We would welcome the opportunity for it to be re-analysed by an appropriate experienced and grape-astute spectroscopist. In a similar vein, if development of an on-the-go NIR sensing capability is to be

continued, the addition of such a spectroscopist to the present project team would be both valuable and is arguably essential.

7. Acknowledgements

This project was funded jointly by CSIRO and Wine Australia. However, the work would not have been possible without the participation and support of Taylors Wines, Kingston Estate Wines and The Lane Vineyard and their staff. In particular, the assistance of Ben Mitchell, Colin Hinze (now Bird in Hand) and the workshop and harvester staff at Taylors Wines, of Peter Morath, Nicole Pitman and harvester staff at Kingston Estate Wines, and of Michael Schreurs at The Lane Vineyard is gratefully acknowledged. Likewise, the support of the erstwhile project advisory team of Ashley Ratcliff (Ricca Terra Farms), Dr Richard Hamilton (Hamilton Viticulture), Adam Eggins (Taylors Wines), Keith Hayes (Wine Australia), along with Colin Hinze and Peter Morath, is gratefully acknowledged, as is the advice of Mike Trought (New Zealand Plant and Food Research), Richard Hamilton and Peter Clingeleffer (CSIRO) in data analysis and interpretation. Dr André Colaço (CSIRO) kindly commented on an earlier version of this report and also provided valuable assistance to the 2018 fieldwork. We are also grateful to Mrs Trang Shand for assistance with formatting and indexing.

This page intentionally blank

Appendix 1: Communication

No specific communication or extension activities have yet arisen from this project – largely due to the initial yield:quality nexus work (section 3) being somewhat compromised by the demise of the Taylors and Kingston sites, such that only two seasons of data were collected, and also in light of the NIR work being very much 'proof of concept' in nature. However, during the preparation of this report, opportunities for the work conducted during the project to make input to journal publications have arisen. In the event that these are realised, Wine Australia will be provided with copies of drafts.

Pending feedback from Wine Australia on this report, the project team would welcome the opportunity to engage with Wine Australia in producing any articles for industry media or other extension material which Wine Australia thinks may be useful.

The above notwithstanding, preparation of Bramley (2019), an update of Bramley (2010), was undertaken under the aegis of this project.

This page intentionally blank

Appendix 2: Intellectual Property

No intellectual property of an immediately commercialisable nature has been generated during this project. However, it has generated significant know-how which will be important as background IP to any follow-on projects – in particular, in regard to the use of NIR instrumentation on-the-go on harvesters (section 5). Overall however, we expect that the information generated by this project will enter the public domain and be accessible for future reference.

This page intentionally blank

Appendix 3: References

Ben Ghozlen N, Moise N, Latouche G, Martninon V, Mercier L, Besancon E, Cerovic ZG. 2010a. Assessment of grapevine maturity using a new portable sensor: non destructive quantification of anthocyanins. Journal international des Sciences de la Vigne et du Vin 44 1–8.

Ben Ghozlen N, Cerovic ZG, Germain C, Toutain S, Latouche G. 2010b. Non-destructive optical monitoring of grape maturation by proximal sensing. Sensors 10, 10040–10068.

Bindon KA, Schulkin A, Dambergs RG, Solomon M, Barter S, Capone D, Kassara S, Cynkar W, Francis IL, Smith PA. 2017. Objectives measures of grape quality. In: Beames KS, Robinson EMC, Dry PR, Johnson DL (Eds) Proceedings of the 16th Australian Wine Industry Conference, Adelaide, South Australia, 24-28 July, 2016. The Australian Wine Industry Technical Conference Inc. Urrbrae, South Australia. 161-164.

Bramley RGV. 2005. Understanding variability in winegrape production systems. 2. Within vineyard variation in quality over several vintages. Australian Journal of Grape and Wine Research. 11: 33-42.

Bramley, RGV. 2010. Precision Viticulture: Managing vineyard variability for improved quality outcomes. Chapter 12 in: Reynolds, A.G. (Ed) Managing Wine Quality. Volume 1. Viticulture and wine quality. Woodhead Publishing: Cambridge, UK. pp. 445-480.

Bramley R. 2013. Wine sector attitudes to the adoption of Precision Viticulture. Wine and Viticulture Journal 28 (5), 69-73.

Bramley RGV. 2017. Vineyard variability and terroir – Making sense of a sense of place. In: Beames KS, Robinson EMC, Dry PR, Johnson DL (Eds) Proceedings of the 16th Australian Wine Industry Conference, Adelaide, South Australia, 24-28 July, 2016. The Australian Wine Industry Technical Conference Inc. Urrbrae, South Australia. 45-51.

Bramley, RGV. 2019. Precision Viticulture: Managing vineyard variability for improved quality outcomes. Chapter 12 in: Reynolds, A.G. (Ed) Managing Wine Quality. Volume 1. Viticulture and wine quality. 2nd Ed. Elsevier: Cambridge, MA, USA. In press.

Bramley RGV, Hamilton RP. 2004. Understanding variability in winegrape production systems. 1. Within vineyard variation in yield over several vintages. Australian Journal of Grape and Wine Research. 10: 32-45.

Bramley RGV, Hamilton RP. 2007. Terroir and Precision Viticulture: Are they compatible? Journal international des Sciences de la Vigne et du Vin 41 1-8.

Bramley RGV, Williams SK. 2001. A protocol for the construction of yield maps from data collected using commercially available grape yield monitors. Cooperative Research Centre for Viticulture, Adelaide, South Australia.

Bramley RGV, Evans TE, Proffitt APB. 2002. Digital elevation models and EM38 survey – Useful tools in the assessment of constraints to vineyard productivity. In: Blair RJ, Williams PJ, Hoj PB. (eds). Proceedings of the 11th Australian Wine Industry Technical Conference. Winetitles, Adelaide. pp 216.

Bramley R, Gobbett D, Praat J-P. 2007. A proximal canopy sensor – A tool for managing vineyard variability and adding value to viticultural research. Final Report on Project No. CSL06/01 to the Grape and Wine Research and Development Corporation. CSIRO/GWRDC, Adelaide.

Bramley RGV, Jensen TA, Webster AJ, Robson AJ. 2018. Precision Agriculture and sugarcane production – A case study from the Burdekin region of Australia. Chapter 9 in Rott PC (Ed) Achieving sustainable cultivation of sugarcane. Volume 1: Cultivation Techniques, quality and sustainability. Burleigh Dodds Science Publishing: Cambridge, UK. pp.185-202.

Bramley RGV, Le Moigne M, Evain S, Ouzman J, Florin L, Fadaili EM, Hinze CJ, Cerovic ZG. 2011a. On-the-go sensing of grape berry anthocyanins during commercial harvest – Development and prospects. Australian Journal of Grape and Wine Research 17 316-326. DOI: 10.1111/j.1755-0238.2011.00158.x

Bramley RGV, Ouzman J, Boss PK. 2011b. Variation in vine vigour, grape yield and vineyard soils and topography as indicators of variation in the chemical composition of grapes, wine and wine sensory attributes. Australian Journal of Grape and Wine Research 17 217-229.

Bramley RGV, Ouzman J, Thornton C. 2011c. Selective harvesting is a feasible and profitable strategy even when grape and wine production is geared towards large fermentation volumes. Australian Journal of Grape and Wine Research 17 298-305.

Bramley RGV, Proffitt APB, Hinze CJ, Pearse B, Hamilton RP. 2005. Generating benefits from Precision Viticulture through selective harvesting. In: Stafford JV. (Ed) Proceedings of the 5th European Conference on Precision Agriculture. Wageningen Academic Publishers: The Netherlands. 891-898.

Bramley RGV, Trought MCT, Praat J-P. 2011d. Vineyard variability in Marlborough, New Zealand: Characterising variation in vineyard performance and options for the implementation of Precision Viticulture. Australian Journal of Grape and Wine Research 17 72-78.

Bramley RGV, Siebert TE, Herderich MJ, Krstic MP. 2017. Patterns of within-vineyard spatial variation in the 'pepper' compound rotundone are temporally stable from year to year. Australian Journal of Grape and Wine Research 23 42-47.

Cerovic ZG, Moise N, Agati G, Latouche G, Ben Ghozlen N, Meyer S. 2008. New portable optical sensors for the assessment of winegrape phenolic maturity based on berry fluorescence. Journal of Food Composition and Analysis 21 650–654.

Cerovic ZG, Latouche G, Nguyen HK, Fadaili EM, Le Moigne M, Ben Ghozlen N. 2014. CUBA: An internet-based software application for berry anthocyanins units' conversion for viticulturists, oenologists and physiologists. Computers and Electronics in Agriculture 103 122-126.

Chapman DM, Matthews MA, Guinard JX. 2004. Sensory attributes of Cabernet Sauvignon wines made from vines with different crop yields. American Journal of Enology and Viticulture 55 325-334.

Cooley NM, Clingeleffer PR, Walker RR. 2017. Effect of water deficits and season on berry development and composition of Cabernet Sauvignon (*Vitis vinifera* L.) grown in a hot climate. Australian Journal of Grape and Wine Research 23 260-272.

Cozzolino D, Dambergs B, Janik LJ, Cynkar W, Gishen M. 2006. Analysis of grapes and wine by near infrared spectroscopy. Journal of Near Infrared Spectroscopy 14 279-289.

Dambergs R, Gishen M, Cozzolino D. 2014. A review of the state of the art, limitations, and perspectives of infrared spectroscopy for the analysis of wine grapes, must, and grapevine tissue. Applied Spectroscopy Reviews 50 261-278.

Dobrowski SZ, Ustin SL, Wolpert JA. 2003. Grapevine dormant pruning weight prediction using remotely sensed data. Australian Journal of Grape and Wine Research 9 177–182.

Edwards E, Smith J, Walker A, Holzapfel B, Barril C. 2017. Improving industry capacity to manage the yield and wine quality relationship through understanding the influence of vine carbon balance on berry composition. Final report to the Australian Grape and Wine Authority on Project No. CSP1202. CSIRO Agriculture and Food, Glen Osmond, SA / National Wine and Grape Industry Centre, Wagga Wagga, NSW.

Francis IL, Iland PG, Cynkar WU, Kwiatkowski M, Williams PJ, Armstrong H, Botting DC, Gawel R, Ryan C. 1999. Assessing wine quality with the G-G assay. *In*: Blair RJ, Sas AN, Hayes PF, Høj PB. (Eds). Proceedings of the 10th Australian Wine Industry Technical Conference. Australian Wine Industry Technical Conference, Inc.: Adelaide. pp 104-108.

Gishen M, Iland PG, Dambergs RG, Esler MB, Francis IL, Kambouris A, Johnstone RS, Høj PB. 2002. Objective measures of grape and wine quality. *In*: Blair RJ, Williams PJ, Høj PB. (Eds). Proceedings of the 11th Australian Wine Industry Technical Conference. Australian Wine Industry Technical Conference, Inc.: Adelaide. pp. 188-194.

Gray JD, Gibson RJ, Coombe BG, Iland PG, Pattison SJ. 1997. Assessment of winegrape value in the vineyard—Survey of cv. Shiraz from South Australian vineyards in 1992. Australian Journal of Grape and Wine Research 3 253-261.

GWRDC. 2012. Strategic Research, Development and Extension Plan 2012-2017. Grape and Wine Research and Development Corporation: Kent Town, SA. 36pp. www.wfa.org.au/assets/r-and-d/GWRDC-Strategic-Plan.pdf (Accessed August 2018).

GWRDC. 2013. Gaps analyses for 2014-15 investment priorities: Vineyard profitability and process efficiency. Grape and Wine Research and Development Corporation: Kent Town, SA. 4pp.

Iland P, Bruer N, Edwards G, Weeks S, Wilkes E. 2004. Chemical analysis of grapes and wine: techniques and concepts. Patrick Iland Wine Promotions: Campbelltown, SA.

Lamb DW, Weedon MM, Bramley RGV. 2004. Using remote sensing to map grape phenolics and colour in a cabernet sauvignon vineyard - the impact of image resolution and vine phenology. Australian Journal of Grape and Wine Research 10 46-54.

Loonstra EH, van Egmond FM. 2009. On-the-go measurement of soil gamma radiation. In: van Henten EJ, Goense D, Lokhorst C. (Eds.), Precision Agriculture 09. Proceedings of the 7th European Conference on Precision Agriculture, 6–8 July, Wageningen, The Netherlands, pp. 415–422.

Matthews MA. 2016. Terroir and other myths of winegrowing. University of California Press, Oakland, CA, USA. 328 pp.

McCarthy MG. 1999. Weight loss from ripening berries of Shiraz grapevines (*Vitis Vinifera* L. *cv* Shiraz). Australian Journal of Grape and Wine Research 5 10-16.

Minasny B, McBratney AB, Whelan BM. 2005. VESPER version 1.62. (Australian Centre for Precision Agriculture, University of Sydney). www.sydney.edu.au/agriculture/pal/software/vesper.shtml.

Parker AK, De Cortázar-Atauri IG, Van Leeuwen C, Chuine I. 2011. General phenological model to characterise the timing of flowering and veraison of *Vitis vinifera* L. Australian Journal of Grape and Wine Research 17 206-216.

Parker AK, De Cortázar-Ataurie IG, Chuine I, Barbeau G, Bois B, Boursiquot J-M, et al. 2013. Classification of varieties for their timing of flowering and veraison using a modelling approach: A case study for the grapevine species *Vitis vinifera* L. Agricultural and Forest Meteorology 180 249–264.

Parker AK, Hofmann RW, Van Leeuwen C, Mclachlan ARG, Trought MCT. 2014. Leaf area to fruit mass ratio determines the time of veraison in Sauvignon Blanc and Pinot Noir grapevines. Australian Journal of Grape and Wine Research 20, 422–431.

Proffitt T, Bramley R, Lamb D, Winter E. 2006. Precision Viticulture – A new era in vineyard management and wine production. Winetitles: Adelaide, Australia.

Rodrigues FA Jr, Bramley, RGV, Gobbett DL. 2015. Proximal soil sensing for Precision Agriculture: Simultaneous use of electromagnetic induction and gamma radiometrics in contrasting soils. Geoderma 243 183-195.

SAS. 1983. Cubic clustering criterion. SAS Technical Report A-108. SAS Institute: Cary, NC, USA.

Scarlett NJ, Bramley RGV, Siebert TE. 2014. Within-vineyard variation in the 'pepper' compound rotundone is spatially structured and related to variation in the land underlying the vineyard. Australian Journal of Grape and Wine Research 20 214-222.

Sinton TH, Ough CS, Kissler JJ, Kasimatis AN. 1978. Grape juice indicators for prediction of potential wine quality. I. Relationship between crop level, juice and wine composition, and wine sensory ratings and scores. American Journal of Enology and Viticulture 29 267-271.

Taylor JA, McBratney AB, Whelan BM. 2007. Establishing management classes for broadacre agricultural production. Agronomy Journal 99 1366–1376.

Trought, M. 2005. Fruitset – possible implications on wine quality. In: de Garis K, Dundon C, Johnstone R, Partridge S. (Eds) Transforming flowers to fruit. Proceedings of an ASVO seminar, Mildura, 29 July, 2005. Australian Society of Viticulture and Oenology: Adelaide. pp. 27–31.

Trought MCT, Bramley RGV. 2011. Vineyard variability in Marlborough, New Zealand: Characterising spatial and temporal changes in fruit composition and juice quality in the vineyard. Australian Journal of Grape and Wine Research 17 79-89.

Trought MCT, Dixon R, Mills T, Greven M, Agnew R, Mauk JL. Praat J.-P. 2008. The impact of differences in soil texture within a vineyard on vine vigour, vine earliness and juice composition. Journal international des Sciences de la Vigne et du Vin 42 67–72.

Webster R, Oliver MA. 2007. Geostatistics for environmental scientists. Wiley & Sons: Chichester, England.

Zhang P, Barlow S, Krstic M, Herderich M, Fuentes S, Howell K. 2015a. Within-vineyard, within-vine, and within-bunch variability of the rotundone concentration in berries of *Vitis vinifera* L. cv. Shiraz. Journal of Agricultural and Food Chemistry 63 4276–4283.

Zhang P, Howell K, Krstic M, Herderich M, Barlow EWR, Fuentes S. 2015b. Environmental factors and seasonality affect the concentration of rotundone in *Vitis vinifera* L. cv. Shiraz wine. PLoS One 10(7) e0133137. 21pp.

Appendix 4: Staff

The staff that have been engaged on the project are as follows:

Name	Title	Role in project
Dr Rob Bramley	Senior Principal Research Scientist	Project Leader
Ms Jackie Ouzman	Research Technician	Laboratory, statistical and spatial analysis, fieldwork
Mr Damian Mowat	Research Technician	Fieldwork, laboratory analysis, instrumentation design and commissioning
Mr David Gobbett	Senior Experimental Scientist	Instrumentation and programming, fieldwork, spatial analysis.

In addition, field assistance was provided by Dr André Colaço during the 2018 field campaign, although Dr Colaço was not formally allocated to the project.